Product Concept Development and Evaluation Based on Quality Function Deployment, Axiomatic Design and Reinforcement Learning

By

Hamid Reza Fazeli

A Thesis submitted to the Faculty of Graduate Studies of
The University of Manitoba
in partial fulfilment of the requirements of the degree of

DOCTOR OF PHILOSOPHY

Department of Mechanical Engineering
University of Manitoba

Abstract

In the competitive global market, products have to meet high customer satisfactions and low production costs in the short product development cycle. Product concept design plays an important role in searching solutions of the product to meet design requirements based on design constraints and technical measures. In this phase, designers have to explore thousands of possibilities to form a product design concept. However, it is challenging to explore and evaluate all of the possible design concepts efficiently. Also, existing methods of the product concept generation and evaluation rely heavily on experience of designers, which is time-consuming and ineffective. This thesis proposes new methods in five different research tasks to improve the product concept generation and evaluation. These research tasks address existing challenges in satisfying customer requirements, improving efficiency in domain mapping, forming a product concept, evaluating generated design concepts, and automating the design process. Usually, House of Quality is used to translate customer requirements into different product attributes in the conceptual design. However, this tool has some limitations in terms of accuracy and efficiency. A combined method of Decision-making Trial and Evaluation Laboratory and Analytical Network Process is proposed in research task one to model interactions in the correlation matrix of House of Quality. Research task two builds the relationship matrix of House of Quality using an optimization model based on Best-Worst Method and Full Consistency Methods. In research task three, a novel domain mapping approach is proposed to translate customer requirements, functional requirements and design parameters into product attributes for analysis, synthesis and evaluation of design concepts. In addition, a new concept evaluation approach is proposed based on the Multi-Attributive Border Approximation Area to rank generated design concepts. Research task four proposes a multi-agent reinforcement learning technique to enable different agents to work and learn collaboratively in a shared design environment and automate the design process. A scalable intelligent design architecture is proposed to use multi-agent reinforcement learning for adaptable and optimum design decisions based on customer requirements. It is developed to take advantage of parallel design explorations for the collaborative design. This approach improves time-consuming conventional manual design methods. The effectiveness of the proposed methods is evaluated in designing and prototyping a rehabilitation device in research task five. A graphical user interface is developed specifically for hand and finger rehabilitations to assist users track their treatments, record motion data, and support self-assessment of joint motions in rehabilitations. The proposed hand rehabilitation device is fabricated and prototyped. The case studies prove that the proposed research methods can improve solution consistency, reduce data collections, design uncertainties, simultaneously consider different design domains and factors, and automate the design process using intelligent agents.

Acknowledgments

I would like to express my sincere gratitude to whom supported me throughout my doctoral journey. First and foremost, I am deeply grateful to my supervisor, professor Qingjin Peng, for his unwavering support, guidance, and encouragement. His expertise, insights, and constructive criticism have been invaluable to me, and I owe much of my academic success to his mentorship.

I would also like to thank my committee members, professors Ying Chen and Yunhua Luo, for their valuable feedback and suggestions during my research. Their constructive criticism and insightful comments have greatly enhanced the quality of my work. I am also indebted to the staff and faculty of Price Faculty of Engineering, who have provided me with excellent academic resources, research opportunities, and a supportive learning environment. In particular, I would like to thank professor Tony Szturm and professor Igor Telichev for their support and encouragement throughout my doctoral journey.

I would like to express my sincere gratitude to Discovery Grants from the Natural Sciences and Engineering Research Council (NSERC) of Canada, University of Manitoba Graduate Fellowship (UMGF), Lab2Market and Mitacs Programs, and the Graduate Enhancement of Tri-Council Stipends (GETS) from the University of Manitoba for the financial support.

I would also like to express my heartfelt gratitude to my dear friends Yanlin Shi, Rui Li, Vahid Sadrmanesh, Rajiv Kumar Vashisht, Marwan Khalid, Bocheng Xu, Jing Guo, Sumanth Kuntavalli, Fatemeh Younesi Sinaki, and Zohreh Sohrabi. Thank you for always being there for me, listening to my ideas, and offering your feedback.

I am profoundly grateful to my wife Arezoo Abdollahi, who has been my pillar of strength throughout my academic journey. Her love, patience, and unwavering support have been the driving force behind my success.

I would also like to extend my appreciation to my family supported me both emotionally and financially. Their unwavering belief in me and their constant encouragement have been instrumental in helping me to achieve my academic goals.

Thank you all for your support, encouragement, and guidance. I am truly grateful for the opportunity to have pursued my doctoral degree, and I look forward to using the knowledge and skills I have acquired to make a positive impact in my research field.

Table of Contents

Abstract i

Acknowledgments ii

Table of Contents iii

List of Tables vi

List of Figures vii

List of Abbreviations x

Chapter 1 Introduction 1

1.1 Background 1

1.2 Statement of research problems 3

1.3 Identified problems 6

1.4 Research objectives and methods 7

1.5 Contents of the thesis 8

Chapter 2 Literature Review 10

2.1 Generation of design concepts 10

2.2 Evaluation of design concepts 14

2.2.1 Evaluation metrics 14

2.2.2 Evaluation methods 15

2.3 Correlations between TMs 16

2.4 Mapping customer requirements to TMs 18

2.5 Data-driven and reinforcement learning based methods 23

Chapter 3 Design Theories and Methods 30

3.1 Quality function deployment 30

3.2 Extended Axiomatic design 33

3.3 Design structure matrix 35

3.4 Summary 37

Chapter 4 Efficient Extraction of Information from Correlation Matrix using an Integrated QFD-DEMATEL Method............38

4.1 Decision-making trial and evaluation laboratory (DEMATEL)............38

4.2 Analytic network process (ANP)............40

4.3 Case study............43

4.3.1 Design of a hand rehabilitation device............43

4.3.2 TMs importance weights based on different roof shapes............45

4.4 Discussions and results............46

4.5 Summary............50

Chapter 5 Improving Weighting Solution of Design Matrix Using Integrated Approaches............52

5.1 Best-Worst method (BWM)............52

5.2 Full consistency method (FUCOM)............56

5.3 Case study............59

5.4 Results and discussion............62

5.5 Summary............69

Chapter 6 Generation and Evaluation of Product Concepts by Integrating Extended Axiomatic Design, Quality Function Deployment and Design Structure Matrix............71

6.1 Method framework............71

6.1.1 Concept generation and evaluation............71

6.2 Concept ranking............76

6.3 Case study............81

6.3.1 Problem description............81

6.3.1 Generation of design concepts............81

6.3.2 Evaluation of design concepts............85

6.4 Results and discussions............88

6.4.1 Proposed concept 88

6.4.2 Evaluation of the proposed method 90

6.4.3 Typical errors in the design concept generation 92

6.5 Summary 93

Chapter 7 Generative Product Concept Development and Evaluation using Multi-agent Reinforcement Learning 95

7.1 Deep reinforcement learning 95

7.1.1 The environment 99

7.1.2 The proposed algorithm 101

7.2 Case study 105

7.2.1 Implementation 105

7.2.2 Solution search and result 109

7.3 Summary 115

Chapter 8 Implementation of the Proposed Design Concept 117

8.1 Virtual environment and hand motion analysis 117

8.1.1 Data input module 118

8.1.2 Data analysis module 119

8.1.3 User interface module 120

8.2 Hand motion parameters 122

8.3 Discussion 125

8.4 Summary 129

Chapter 9 Conclusion and Future Work 130

9.1 Research summary 130

9.2 Research contributions 131

9.3 Future work 133

Papers published and submitted during this research 135

References 136

List of Tables

Table 4-1 TMs importance weights based on the proposed and traditional methods..50
Table 5-1 Proposed integrated approach to decide importance weights of TMs.........53
Table 5-2 Consistency index (CI) for different aBW values. 56
Table 5-3 Proposed integrated approach to decide importance weights of TMs.........57
Table 5-4 Exoskeleton devices for the hand rehabilitation...61
Table 5-5 Pairwise comparison vectors for the Best and Worst TM. 61
Table 5-6 Comparisons of TMs weights based on AHP-QFD and proposed approaches..64
Table 5-7 Comparison of the proposed approach with AHP-QFD in three different measures..66
Table 6-1 The proposed integrated approach to generate, evaluate, and rank design concepts..73
Table 6-2 Five design candidates developed based on the proposed approach. 84
Table 6-3 Different steps in the ranking process based on the Fuzzy-MABAC approach. 88
Table 6-4 Ranking design concepts. 88
Table 7-1 pseudocode of the Proximal Policy optimization (PPO) algorithm 99
Table 7-2 Action spaces in searching solutions of a hand rehabilitation device 108
Table 7-3 The proposed design solution 113

List of Figures

Figure 1-1 Different stages in the product design process..2
Figure 1-2 Costs and ease of change in different phases of a product lifecycle. 2
Figure 1-3 A typical innovation process funnel...3
Figure 1-4 Mapping different design domains in concept generation. 4
Figure 1-5 Contents of the thesis. 9
Figure 2-1 Comparison between classical and integrated approaches of the relationship matrix in HOQ. (a) Traditional approach (b) Integrated AHP-QFD 23
Figure 3-1 A general form of HOQ in a two-step QFD process.................................30
Figure 3-2 Mapping between different domains in Axiomatic Design. 34
Figure 3-3 DSM forms based on different component configurations. 36
Figure 3-4 DSM framework to represent module relations in a design concept 37
Figure 4-1 Two forms of the correlation matrix in HOQ. 39
Figure 4-2 Proposed Algorithm for calculating influential weights of TMs. 41
Figure 4-3 HOQ based on known customer requirements and TMs of hand rehabilitation devices. 46
Figure 4-4 Normalized square shaped correlation matrix...47
Figure 4-5 DEMATEL prominence-causal relationship of TMs................................48
Figure 4-6 Unweighted super matrix of the device of scenario one. 48
Figure 4-7 Unweighted super matrix of the device of scenario two. 49
Figure 4-8 Different structures formed based on solutions of TM importance weights from (a) the traditional HOQ, (b) triangle-shaped correlation matrix, and (c) proposed square-shaped correlation matrix. 50
Figure 5-1 Comparisons in BWM...54
Figure 5-2 HOQ for mapping customer requirements to TMs for the device. 60
Figure 5-3 Variation of comparison consistency with the preference of the best TM over TM_j a_{Bj}, and the preference of TM_j over the worst TM a_{Wj}. 63
Figure 5-4 Structure of the matrix based pairwise comparison vs vector based pairwise comparison. 65
Figure 5-5 The device developed based on weights of the traditional approach. 68
Figure 5-6 The device developed based on weights of the proposed approach...........68
Figure 6-1 Reduction of the solution space during concept development. 72
Figure 6-2 Proposed approach for generation and evaluation of design concepts. 72

Figure 6-3 Deriving DSM from Design Matrix. 75
Figure 6-4 Different physical solutions lead to different design concepts. 76
Figure 6-5 Weighting design parameters based on relations of different domains. 76
Figure 6-6 Linguistic representation to model relations in the HOQ. 77
Figure 6-7 Border H, upper $H+$, lower $H-$ approximation areas in MABAC. 80
Figure 6-8 Design specifications for hand rehabilitation devices. 82
Figure 6-9 Different approaches for the physical domain in design of a hand rehabilitation device. 83
Figure 6-10 Different exoskeleton finger structures to support hand movements. 83
Figure 6-11 Domain mapping based on the functional decomposition of the hand rehabilitation device. 84
Figure 6-12 HOQ 1 for mapping customer requirements into TMs of the hand rehabilitation device. 86
Figure 6-13 HOQ 2 for mapping TMs into design parameters of the hand rehabilitation device 87
Figure 6-14. (a) The proposed design concept. (b) The structure and actuator support finger movements. (c) The developed virtual environment to analyze and quantify hand motion data. 89
Figure 6-15. (a) Developed design concept based on the QFD process. (b) 91
Figure 6-16 Derived DSM for (a) the proposed design concept, and (b) the soft actuator-driven design concept 92
Figure 6-17 Functional model for design candidate 3. 92
Figure 7-1 A framework of Deep reinforcement learning. 97
Figure 7-2 The concept generation tree for a typical product. 102
Figure 7-3 The proposed multi-agent reinforcement learning system for the design space exploration. 103
Figure 7-4 (a) Handling design variables using a super-agent. (b) A multi-agent framework for design space exploration. 106
Figure 7-5 HOQ 2 for the rehabilitation device design. 107
Figure 7-6. Training results of the proposed algorithm. (a) Single super-agent training and exploration. (b) Centralized multi-agent training and exploration with the centralized execution. 110
Figure 7-7 Examples of hand rehabilitation device concepts in literature. 113

Figure 8-1 (a) Framework and modules of the proposed system. (b) Developed virtual environment of the hand motion analysis. 118
Figure 8-2 Calibration of Leap motion sensor in X,Y, and Z directions. 119
Figure 8-3 De-noised position data of palm in the cartesian space using wavelet transform with different levels. 121
Figure 8-4 Angles between finger bones for a human hand based on captured data. 121
Figure 8-5 Developed user interface to visualize and analyze hand motion parameters. 122
Figure 8-6 Tracking hand palm position in cartesian space and direction vectors of the palm velocity to display and record the details of hand motion. 124
Figure 8-7 Normalized Fist of a user hand based on the angles between fingers and palm to measure the fist hand pose. 125
Figure 8-8 Example of the flexion and extension movements for achieving full range of motion of the wrist. 126
Figure 8-9 Measuring range of motion of hand joints. (a) Variation of finger joint angular data profiles during rotation of the thumb movement, (b) joint angular velocity data profiles during thumb flexion-extension movement for a normal hand. 128
Figure 8-10 A prototype of the proposed device. 128

List of Abbreviations

AHP	Analytic hierarchy process
ANP	Analytic network process
AD	Axiomatic design
BWM	Best-worst method
CNN	Convolutional neural network
CRs	Customer requirements
DEA	Data envelopment analysis
DDPG	Deep deterministic policy gradient
DNNs	Deep neural networks
DQN	Deep Q-networks
DEMATEL	Decision-making trial and evaluation laboratory
DOF	Degree of freedom
DM	Design matrix
DOFs	Degrees of freedom
DPs	Design parameters
DSM	Design structure matrix
FRs	Function requirements
HOQ	House of quality
FUCOM	Full consistency method
GANs	Generative adversarial networks
MABAC	Multi-attributive border approximation area comparison
MDP	Markov decision process
MCP	Metacarpophalangeal
NFRs	Non-functional requirements
PIP	Proximal interphalangeal
PPO	Proximal policy optimization
QFD	Quality function deployment
RL	Reinforcement learning
ROM	Range of motions
SDP	Sequential Decision Process
SVM	Support vector machine
TMs	Technical measures
TD	Total deviation
TOPSIS	Technique to evaluate product performance by similarity to ideal solution
TRIZ	Theory of innovation problem solving
UI	User interface
VE	Virtual environment
VR	Virtual reality
WT	Wavelet transform

Chapter 1 Introduction

1.1 Background

The global competitive market requires product to meet the high customer satisfaction, low production cost and short product development cycle [1]. Figure 1-1 shows different stages of the product design. Conceptual design is the first stage of the product development to generate, evaluate and select design concepts. The conceptual design is also a process of the feasibility study with a high level of creativity and coordination among different factors. It first proposes different ideas to meet design requirements. The design ideas or concepts are then evaluated and refined until the preferred solution is identified. This process typically involves several iterations before the final concept is decided to meet design requirements based on design constraints and technical measures (TMs) [2]. Figure 1-2 shows costs and design changes occurred in different phases of a product lifecycle. The conceptual design phase decides over 50% of the total product lifecycle cost, and over 50% of design changes can be easily made in this stage. Therefore, the concept design is the most important phase in the product development. Embodiment design is a critical phase in the product design process, serving as a primary stage to create an initial design layout. Its main objective is to develop a high-level design that serves as a foundation for the subsequent detailed design phase. Sometimes, embodiment design is also known as preliminary design or system-level design. Embodiment design typically involves generating multiple design concepts and evaluating them against various criteria, such as feasibility, usability, and manufacturability. Figure 1-3 shows a typical innovation process during the product design. Different ideas and suggestions of potential products are analyzed to meet design requirements. The process is iterative and costly as many design possibilities should be evaluated. Therefore, it is important to have an effective method for the concept generation and evaluation.

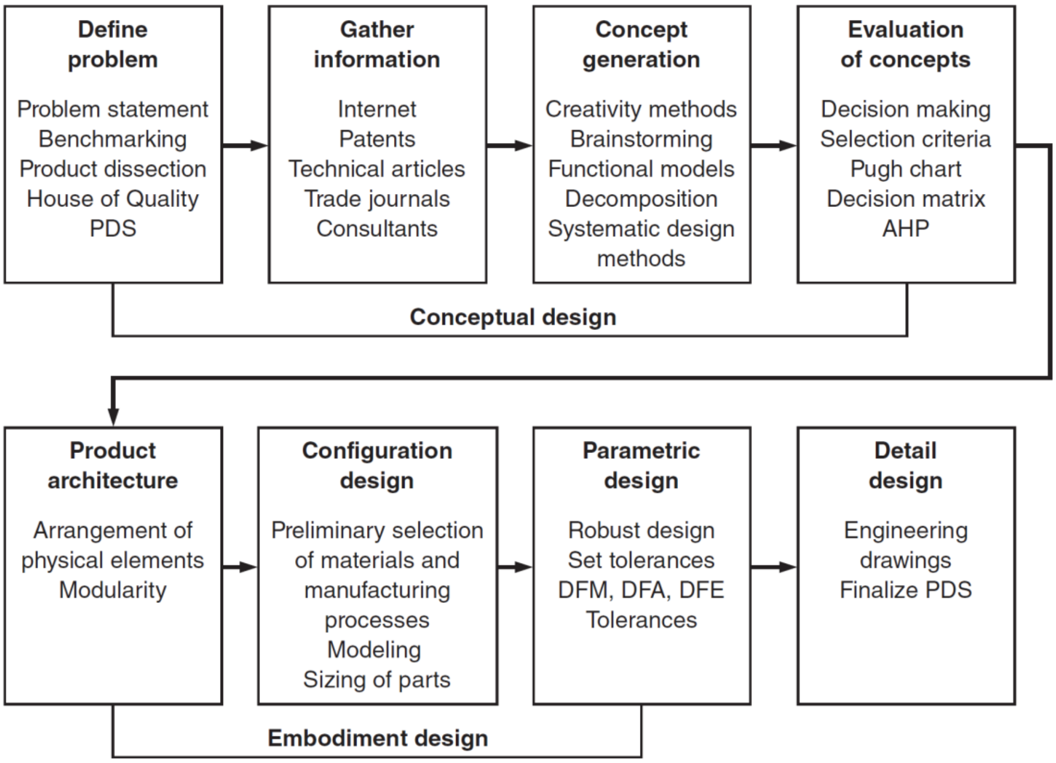

Figure 1-1 Different stages in the product design process [3].

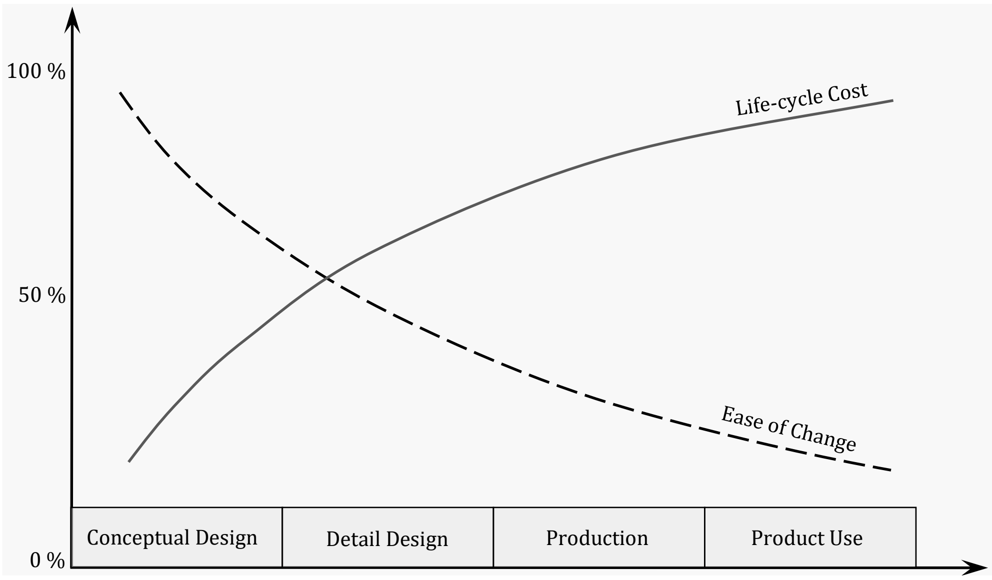

Figure 1-2 Costs and ease of change in different phases of a product lifecycle[4].

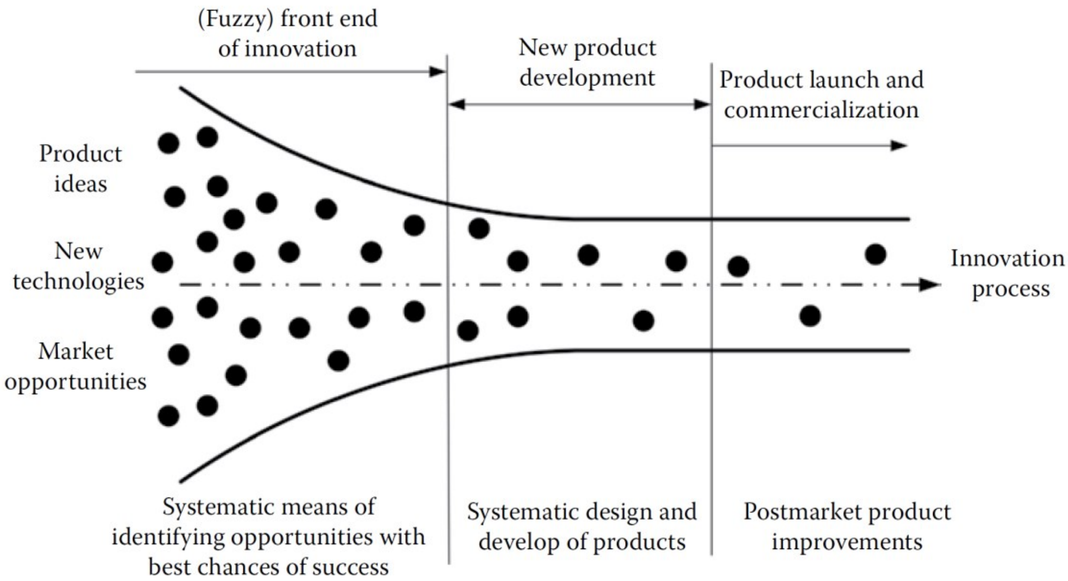

Figure 1-3 A typical innovation process funnel [5]

1.2 Statement of research problems

A variety of design concepts can be proposed using different methods based on design requirements. It is a challenge to generate and evaluate different design concept solutions [6]. A conceptual design starts based on a set of customer requirements (CRs) and their importance ranking. A mapping approach transfers design information in different domains as shown in Figure 1-4. Function requirements (FRs) are proposed to meet customer requirements. Design parameters (DPs) are details of implementing function requirements. Non-Functional requirements (NFRs) define quality attributes of the products such as cost, portability and reliability used in the extended Axiomatic Design (AD) process. TMs are a set of parameters to describe the level of product performance for particular functions based on constraints and specific technologies to satisfy function requirements.

Axiomatic Design is a common method used to map different design domains and generate design concepts. In the classic form of Axiomatic Design, function requirements are directly used as central elements to decide design parameters to form product concepts. Non-functional requirements are not included in domain mapping, which is a limitation for this approach to consider all of product design aspects [7]. For coupling relationships of product functions and components, a special attention is required to map product functions into design solutions [8]. Existing methods usually focus on a specific domain [9, 10].

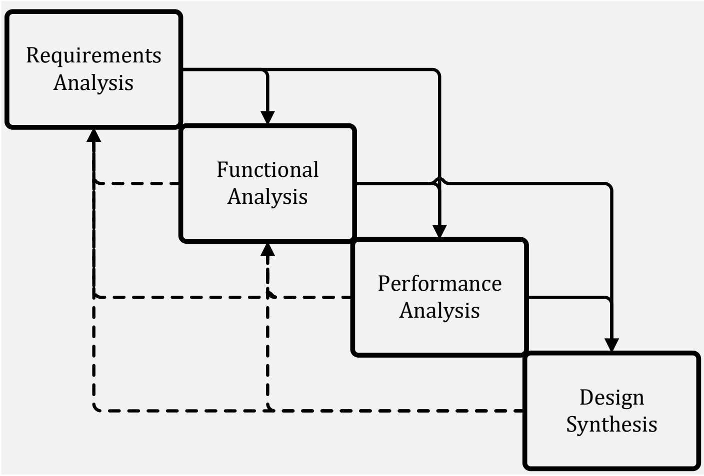

Figure 1-4 Mapping different design domains in concept generation.

Most methods of the product concept generation are based on designers' knowledge to form required functions [11]. As a product can provide different functions, each function may be satisfied by different solutions to form design concepts. The number of possible solutions can be very large [12]. Axiomatic Design method maps function requirements to design parameters of a product based on two design axioms, however, it cannot quantify design concepts to meet customer requirements [13]. Additionally, all function requirements are mapped into design parameters in an equal importance while satisfying Axiomatic Design conditions. But in reality, users may consider different degree of importance for function requirements, which cannot be modeled in Axiomatic Design.

Quality Function Deployment (QFD) is a tool for mapping customer requirements into TMs to form design concepts. It can improve the design quality and reduce product development time [14]. QFD consists of two major processes, extracting voice of customers and transferring customer requirements to TMs [15]. The QFD guides a design process to convert customer requirements into measurable product functions, but it cannot directly form the product structure based on function requirements and TMs.

Concept evaluation is a complex decision-making process which considers different factors to address both voices of designers and customers. Ideally, a concept evaluation method should consider function requirements satisfactions, feasible interactions of different components, and effective product structures. In addition, a concept ranking approach should objectively consider the customer satisfaction. For example, if a product has five functions and each function has 10 solutions, in theory there will be 100000 combinations of design solutions. Although there are different approaches to generate, validate and rank design concepts, they mainly focus on some specific problems. It is necessary to have a comprehensive method of product concept design and evaluation.

House of Quality (HOQ) is an essential mapping tool in QFD for designers to find TMs of customer requirements and their importance weights. Using HOQ, relations of customer requirements and TMs can be identified [16]. Relationship and correlation analyses are two key parts of HOQ. Effects of TMs on each other are represented in a correlation matrix using a triangle-shaped 'roof' of HOQ. As HOQ is applied in a hierarchy structure of QFD, weights of TMs have a big impact on design solutions. Inaccurate data in HOQ can lead to an error propagation into other QFD matrices and undesirable products [17].

The correlation matrix in the roof of HOQ is seldom used by designers as it is difficult to quantify interactions of TMs [18]. Most HOQ approaches focus on mapping customer requirements to TMs and weighting importance by relations between customer requirements and TMs. As some of TMs may not be mutually exclusive in a design solution, it is necessary to model TMs interactions in the design process. Generally, relations in the roof matrix are represented with signs or numbers for the degree of correlations between TMs. However, information based on this representation is not clear enough to provide designers details in considering all of TMs interactions [18]. Some methods, such as the Wasserman normalization for incorporating TMs interactions in determining importance weights, may produce an unacceptable outcome [19]. Another problem in the roof part of HOQ is that the intersection between two TMs shows only their effect degree, we cannot conclude whether they have the same effect on each other. For example, a TM may have a strong effect on another TM, but it doesn't necessarily mean that the reverse is the same.

One of the difficulties in using HOQ is determining appropriate relations of customer requirements and TMs in the relationship matrix. In the classical HOQ, a ranking system (such as 1-3-9) is usually employed to represent the degree of the relation (weak–medium–strong) based on experts' opinions. This is subjective as different experts may provide different solutions based on their different knowledge and experience. Also, there is not a measure in traditional approaches to indicate the consistency in the relationship matrix for TMs to accurately meet customer requirements. Recent research [20] studied normalization approaches in the relationship matrix of HOQ and suggested that classical forms of the relationship matrix may not be accurate and data in the relationship matrix of HOQ should be normalized [21].

The complex relationship between many TMs in HOQ can easily lead to inconsistent solutions to accurately meet customer requirements. For a large scaled HOQ, it is very difficult for designers to complete all of the comparison tasks in a consistent way.

1.3 Identified problems

Although different methods have been proposed for the product concept generation and evaluation, there are some important problems remaining as follows.

1) There is a lack of modeling methods for TMs interactions in mapping different design domains.

2) There is a lack of the systematic analysis of relationships of customer requirements, TMs, function requirements and design parameters. There is no measure in classical approaches for the relationship consistency of TMs to accurately meet customer requirements.

3) There is a lack of a structured approach to generate, evaluate and rank design alternatives based on design criteria and customer requirements simultaneously.

4) The existing methods require the manual data collection and interactive decision making, which is time-consuming for the concept design and evaluation. Also, approaches of the product concept generation are inefficient in considering the design synthesis and feasibility simultaneously.

5) Due to the complex and multidisciplinary nature of medical devices, it is a challenge for the medical device design to identify and evaluate performance of design solutions.

Therefore, an effective method of the concept generation and evaluation is required to accurately and systematically quantify and analyze design concepts and relations of product functions and structures [22].

1.4 Research objectives and methods

Based on the identified problems, this research develops effective methods to generate and evaluate design concepts. Detailed research tasks are as follows.

Task one: Development of an integrated DEMATEL-ANP approach to model TMs interactions in the correlation matrix of HOQ. Outputs of this task are important weights and prominence-causal relationships of TMs for designers to understand the effect of design parameters. This research task addresses current limitations for TMs interactions in HOQ.

Task two: Improvement of design efficiency to reduce the data collection and enhance the weight allocation accuracy and consistency in HOQ using an optimization model. A new approach in modeling relationships between customer requirements and TMs is required to integrate Best-Worst Method (BMW) and Full Consistency Methods (FUCOM) with HOQ.

Task three: Development of a well-structured conceptual design process by technical feasibility evaluations using Design Matrix (DM) and DSM approaches for an efficient design space exploration. A domain mapping approach is also required for translating customer requirements, function requirements and design parameters domains to generate and evaluate design concepts. The holistic design approach should consider both function requirements and non-functional requirements of the product concurrently. Moreover, a concept evaluation approach is required based on the multi-attributive border approximation area comparison (MABAC) to rank generated concepts.

Task four: Development of an automated design process using reinforcement learning to train design agents learning for design. The design agents can learn design rules by interacting an environment formed based on design factors and theories. The previous tasks are prerequisite parts for the environment of a reinforcement learning framework to train the agents for the design concept generation and evaluation.

Task five: Development of a hand rehabilitation device to meet customer requirements in the market and improve the existing systems for the hand motion analysis. The device should be designed to meet customer requirements like the low cost, easy to use, non-contact measurement, and accurate measurements. A virtual environment will be developed using the Unity 3D engine and integrated with the Leap Motion sensor to measure, analyze and display motion parameters.

1.5 Contents of the thesis

Figure 1-5 shows the structure of the thesis and outcomes of each chapter. In Introduction, a general discussion of the product concept generation and evaluation is presented. Chapter 2 reviews existing methods and algorithms in the product concept generation and evaluation. In Chapter 3, related design methods that are used or modified in this thesis are presented. Chapters 4 and 5 present novel approaches to model correlations between TMs and improve the relationship matrix for product concept ranking. In Chapter 6, a new approach is presented to eliminate limitations of existing methods for generating and evaluating product design concepts. Chapters 4-6 are foundations of the learning environment for reinforcement learning agents to develop an automatic concept generation and evaluation approach in Chapter 7. In Chapter 8, the case study of developing a hand rehabilitation device is investigated and verified, followed by the conclusion and future work in Chapter 9.

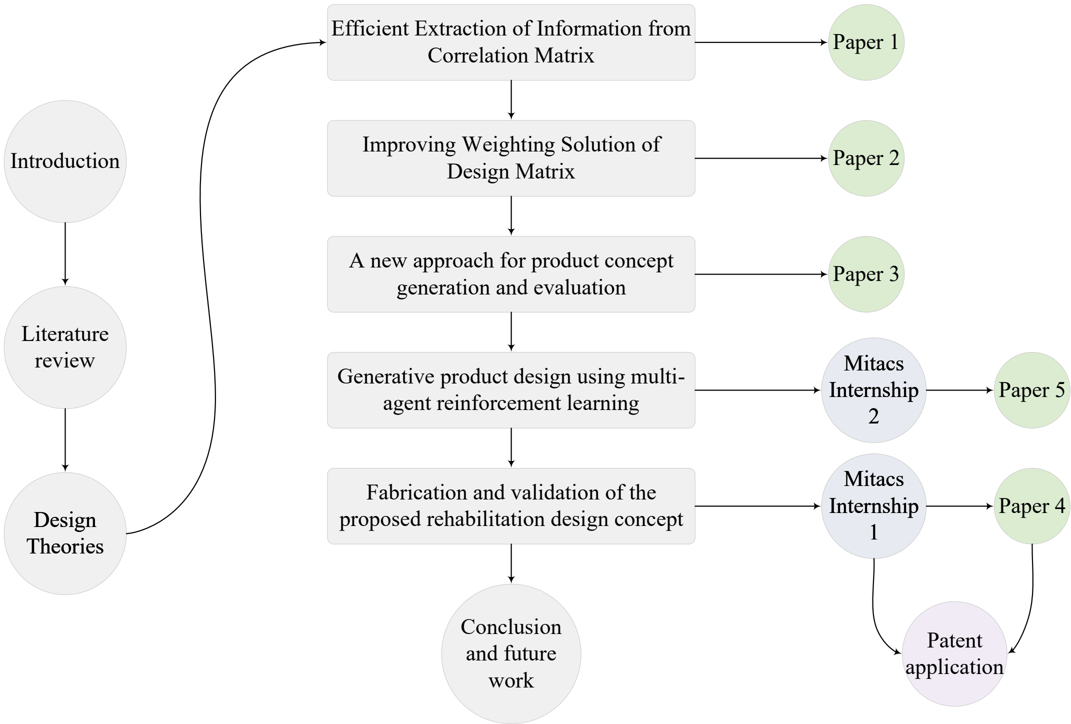

Figure 1-5 Contents of the thesis.

Chapter 2 Literature Review

Product concept generation and evaluation is a broad research area in the engineering design field. Different approaches have been developed by researchers to enhance the performance of conceptual design. This chapter reviews research on product concept generation and evaluation.

2.1 Generation of design concepts

Concept design searches for potential solutions of products to meet design requirements [2]. The domains considered in product design include customer, functional, and physical domains as follows [23].

Customer Requirements (CRs) domain: A set of customer requirements for product attributes, capabilities, and their importance degrees.

Function Requirements (FRs) domain: A collection of statements to describe product behavior and performance to meet customer requirements.

Design Parameters (DPs) or physical domain: It forms product elements, parameters and relationships.

Effective mapping between these domains can lead to creative solutions to meet both customer and designer perspectives. When there are coupling relations between product functions and components, a special attention is required to map product functions into design solutions. It is important to deliver high-quality product solutions in the competitive market, which needs a comprehensive design approach to fully consider customer requirements, function requirements, and design parameters [24]. Formalization, quantification and automation of product solutions are active research areas in product design [25]. It is a challenge to find trade-offs between conflicting design concepts and quantify design alternatives [6]. This research uses the term "concept" to describe a product system, including the product structure and other properties, such as product functions and attributes. Although there are different approaches to address design problems of product concept generation and evaluation, they are inflexible in the solution search. One of the difficulties in product concept development is effectively using data in different design domains. Matching customer needs with design elements and characteristics is a challenging task in product design. The existing research mainly considers customer needs and structural relations between design components. Previous research has proposed specific models for relations between customer needs and design elements. However, it still faces difficulties in the design automation and evaluation [26]. There is only limited work with solutions to generate and validate design concepts to meet customer requirements.

Product concepts are generally formed through the function analysis. Graph grammar-based and matrix-based methods are two main approaches to generating design concepts [27]. In the graph grammar-based approach, relations between function requirements and design parameters are modeled based on the graph theory. The matrix-based methods use different matrix operations to organize and analyze a design process. These matrices are usually operated to characterize and visualize relations of product attributes and functions in the design process [28]. Different matrix-based tools have been used to support the design process. One example of the matrix-based method is HOQ from the QFD method to map customer requirements into function requirements [29]. The input of QFD is the voice of customers being mapped into function requirements and design parameters using HOQ [30]. Moreover, QFD can be combined with other approaches to develop a systematic method for product design. For example, Lee et al. [31] proposed a service design approach to meet customer requirements using the laddering technique. A combined approach of QFD and TRIZ was used to elicit customer requirements, generate functional attributes and evaluate service concepts.

Shvetsova et al. [32] integrated QFD and AHP to evaluate and select the best generated product concept. They applied the approach to an automotive air conditioning design problem. They acknowledged that it could be time-consuming to reach consensus in an AHP decision-making process. Their approach does not consider internal relations between system components in the design evaluation. In a similar study, Karasan et al. [33] proposed a customer-oriented product design method by integrating QFD, AHP, and decision-making trial and evaluation laboratory (DEMATEL) methods. They applied the methods in a case study of the design of a car seat. In another work, Zhai et al. [34] introduced a rough set-based QFD approach to managing uncertain design information. Rough sets were applied in the QFD analysis to handle imprecise design information. It shows that the integrated approach can facilitate decision-making for the bicycle design. However, as their approach focuses on prioritizing engineering characteristics, it does not provide information of components relations and design feasibility. Fan et al. [35] integrated QFD, fuzzy evaluation, and Pareto evolutionary algorithms to address vagueness in data handling and selection of design concepts. The focus of this work was evaluating and ranking design concepts.

Axiomatic Design uses the design matrix to define design correlations of functional and physical domains [36]. It is applied in several studies in the concept design [37]. Independence Axiom and Information Axiom are two important axiomatic design principles. The first one requires independence of function requirements, and the second minimizes information contents of the design concept. Coupling is a term to describe the lack of independence in the design matrix. The design matrix provides valuable information about design elements. In an ideal design, function requirements are independent of each other, and the number of design parameters is equal to the number of function requirements. Additionally, matrix analysis methods can be used to evaluate and alleviate effects of coupling [38]. Xiao et al. [39] applied the Axiomatic Design and conjoint analysis in a case study of designing a cylindrical gear reducer. They used the orthogonal experimental design to generate a set of product combinations and conjoint analysis of customer needs. Lu et al. [40] developed a product concept evaluation model based on Axiomatic Design and Z-numbers. They applied the information axiom to obtain a design combination with the minimum information in an ink pen concept design. Approaches were proposed to extend the Axiomatic Design and consider quality attributes. For example, Mabrok et al. [41] suggested that non-functional requirements can be used in forming design concepts. An AHP was applied in ranking design concepts based on non-functional requirements. Typically, function requirements describe the expected product performance with measurable specifications. Non-functional requirements are quality attributes and constraints of product in the extended Axiomatic Design [41]. A limitation of Axiomatic Design is the exclusion of products' non-functional requirements or quality attributes [41, 42]. Therefore, the Axiomatic Design cannot determine the best solution among generated concepts.

Design Structure Matrix (DSM) represents product elements and interactions [43] to analyze and optimize coupling relationships among functions, subsystems and structures via clustering and decomposition methods. DSM is a well-known representation and analysis tool of the design knowledge, especially for the design decomposition and integration. DSM considers relations of product components in a compact, visual and analytical format using a square matrix with identical rows and columns. Tilstra et al. [44] developed a multi-level DSM to analyze product component relations and evaluate product structures. Although the DSM provides a useful tool for analyzing design interactions, applying it in designing a new product is challenging. The main focus of the DSM is the architectural design [42]. Recently, a few concept generation approaches are proposed based on data-mining methods. For example, Liu et al. [45] developed a function-structure concept network that integrates sentence parsing and word extraction to combine functional and structural information. Although it improves designers' capabilities to explore new design ideas and increase design creativity, it does not consider customer requirements weight during the design process. In a similar work, He et al. [46] proposed a systematic data-mining-based technique for product family design and product configuration. The association rule was used to obtain the configuration knowledge between customer requirements and designers.

Other concept generation approaches include the incidence matrix [47] and function impact matrix [48]. These matrixes are suitable for specific domains or applications of the product conceptual design. Cong et al. [49] developed a design method for the product-service systems based on the information theory. The approach follows Shannon's information theory to develop the best design solution by reducing the design entropy in its closed-loop lifecycle. Additionally, morphological matrices can be applied as a systematic or intuitive combination tool. Morphological thinking explores a complete set of possible relations of a multi-dimensional problem that can be decomposed into constituent sub-problems. Consequently, it becomes difficult to identify compatible solutions with others for their physical combinations during the concept generation. Thus, simply choosing one solution for a FR may not yield a systematic concept if the solution cannot be physically integrated into a working mechanism. Hence, a limitation of using morphological matrices is its difficulty in recognizing compatible solutions to perform a systematic level combination. As morphological charts are constructed without any filtering mechanism, a validation process is required to filter infeasible concepts.

2.2 Evaluation of design concepts

2.2.1 Evaluation metrics

Concept evaluation is an important step in determining the overall utility of design alternatives to meet objectives. Evaluation of design concepts can be divided into process-based and outcome-based methods [50]. The process-based method analyzes an entire process of the design concept generation [51], where the inner mechanism of the cognitive process is unobservable. The outcome-based approach is more feasible than the process-based method. It is a dominant way of the design concept evaluation. Metrics are commonly used in the evaluation of design concepts. There are various metrics used for the concept evaluation. Shan introduced four metrics of novelty, quality, variety and quantity in evaluating design concepts [50]. Novelty means that the degree of a design concept is unfamiliar to others. Quality is the feasibility of concepts for customer requirements and product attributes. Variety measures the degree of difference in design concepts. Quantity is the total number of design concepts. The four metrics are acknowledged and extended by the design community. For example, Kurtoglu introduced a completeness metric to define the design concept of satisfaction for required functions [51].

2.2.2 Evaluation methods

Concept evaluation is a multiple-criteria decision-making process [6]. The graph-based solutions are ranked using a penalty function or historical knowledge in selecting product components. The penalty function-based method requires precise information which is not always available in the early design phase [27]. Genetic and rigorous mathematical programming techniques were introduced as computational analysis tools. Heuristic algorithms can avoid the combinatorial explosion of the analysis by determining a feasible region and reducing the solution space with rules and constraints. The matrix method can map and analyze relations of product functions [2]. Function requirements and their relations with design parameters are represented in the form of vectors and matrices to filter infeasible concepts.

Various methods can be applied [52-54] in multiple-criteria decision-making in the product concept development. Common methods use expert-based approaches based on design knowledge to grade design concepts from different aspects. Based on the expert scores, multiple-criteria decision-making methods such as the Analytic Hierarchy Process (AHP) [52] can be applied in evaluating design concepts. AHP and simulation analysis can be integrated for the design evaluation. Song et al. [55] proposed a hybrid approach to combine the rough number and analytic hierarchy process for evaluating criteria weights of alternatives. Product performance is evaluated by similarity of ideal solutions. The AHP is a time-consuming process when there is a large number of design criteria and alternatives. A large number of criteria results in large pair-wise comparisons and a huge evaluation matrix [56]. It is required to improve the consistency of pair-wise comparison criteria in the analytic hierarchy process [6]. The utility function analysis can only express the evaluation in a quantitative form. It is difficult to represent some intangible design criteria and factors in the quantitative form [6]. The design concepts may have different degrees in meeting different function requirements. Therefore, an efficient approach is required to rank design concepts.

2.3 Correlations between TMs

A variety of design concepts can be proposed for the product functions to meet customer requirements based on design constraints. QFD is an approach for mapping customer requirements to TMs and guiding designers to search product solutions. QFD usually consists of two major processes, extracting voice of customers and transferring TMs to product attributes [15]. The QFD decomposition provides a measurable process of implementation of product functions. Using HOQ, relations of customer requirements and TMs can be identified to analyze their effects [16]. Relation matrix and correlation matrix are two key parts in HOQ templates. The relation matrix of TMs and customer requirements is used to find importance weights of TMs. Moreover, effects of TMs on each other are represented in a correlation matrix which is a triangle-shaped 'roof' of HOQ. As HOQ is applied in a hierarchy structure of QFD, weights of TMs have a big impact on design solutions. Inaccurate data in HOQ can lead to an error propagation into other QFD matrices and undesirable products [17]. A considerable amount of research has been conducted for improving the HOQ template and data analysis. However, most of the existing studies focused on enhancing the relationship matrix in HOQ to find the importance weight of TMs [57]. For example, QFD was integrated with methods of Information Entropy [58], Fuzzy Logic [59, 60], Kano [61], and AHP [62, 63].

A variety of models of data relations in HOQ have been suggested. In most HOQ approaches, designers focus on mapping customer requirements to related TMs and decide importance weights by relations between customer requirements and TMs. However, data in the correlation matrix are not considered during this process. As some of TMs may not be mutually exclusive in a design solution, it is necessary to model TM interactions in the design process. Generally, relations in the roof matrix are represented with signs or numbers for the degree of correlations between TMs. However, information based on this representation is not clear enough to provide designers details in considering all of TMs interactions [18]. Some methods, such as the Wasserman normalization for incorporating TMs interactions in determining importance weights, may produce an unacceptable outcome [19]. Another problem in the roof part of HOQ is that intersections between two TMs show only their effect degrees, we cannot conclude whether they have the same effect on each other. For example, a TM may have a strong effect on another TM, but it doesn't necessarily mean that the reverse is the same.

Most of the existing research on the roof part of HOQ focus on solving conflicts between technical details using methods like the theory of innovation problem solving (TRIZ) [64] and data envelopment analysis (DEA) [65]. A few studies applied effects of the correlation matrix with TMs' weights to select TMs. For example, a weighted average method was used to prioritize and rank TMs [66]. But if TMs have an equal strength of correlations, their weights will remain the same. In another research, a method was introduced to search correlations between TMs for importance weights [67]. In this work, by adding all of correlation values located at each intersection of TMs, the average weight was decided by multiplying weights in the relationship matrix to re-prioritize TMs. But this method decides correlation coefficients at the criterion level, not the sub-criterion level. A recent study proposed an approach for resolving contradictions of customer requirements using TRIZ tools and adjusting TMs' weights in HOQ [68]. A side roof was added in a HOQ template to find contradictions of customer requirements. Information in the roof part of HOQ was used for TMs re-prioritization. Signs were used to show correlations among TMs, but the impact of differences of correlation values was not investigated. Correlation values are suggested to use instead of conventional signs in the roof part of HOQ. Therefore, it is necessary to quantify whether a TM has more effect than others.

Although there are a few studies addressed effects of the correlation matrix of HOQ on the QFD process, none of them provides a systematic method to decide TMs interactions and their influence on each other for design solutions using information of the roof part in HOQ. Moreover, even literature on the prioritization of TMs is vast, a significant gap exists in the efficient extraction of information from the correlation matrix.

2.4 Mapping customer requirements to TMs

QFD can quantify product attributes and deploy solutions for the design quality in subsystems and components. Part deployment can be used to select product components. One of the difficulties in using HOQ is determining appropriate relations of customer requirements and TMs. In the classical HOQ, a ranking system (such as 1-3-9) is usually employed to represent the degree of the relation (weak–medium–strong) based on experts' opinions. This is subjective as different experts may provide different solutions based on their knowledge and experience. Moreover, design information is often limited in this stage. This is particularly true when a new product is developed. Usually, an average of different data is used in the relationship matrix. It is difficult to precisely decide the importance of TMs related to customer requirements. There is no measure in traditional approaches to indicate consistency in the relationship matrix for TMs to accurately meet customer requirements. Recent research has studied normalization approaches in the relationship matrix of HOQ and suggested that classical forms of the relationship matrix may be inaccurate and data in the relationship matrix of HOQ should be normalized [17].

Customer requirements weights, relationship matrix, and correlation matrix are three important parts of HOQ. In order to improve accuracy of HOQ to meet customer requirements, different methods have been proposed such as the combined QFD with weighting methods using AHP [69] and Analytic Network Process (ANP) [70] to improve the CR ranking and relationship matrix of HOQ. However, these methods require a greater number of evaluations than the traditional approach which does not require pairwise comparisons at the same level. In most pairwise comparison-based methods, a consistency index is usually applied to measure reasonableness of ranking results. Most of weighting methods like AHP and ANP use the pairwise comparison approach based on relative priorities of alternatives [71]. In classical methods like AHP, a complete comparison matrix is required to compare all of alternatives. In this form, all alternatives are compared each other. Transitivity is an important feature in the comparison matrix. Typically, it requires an ordered set such as if $i \geq j$, $j \geq k$ then $i \geq k$. For example, there are three TMs namely $TM_A, TM_B, and\ TM_C$ in the relationship matrix. If $TM_B \geq TM_A$ and $TM_A \geq TM_C$, logically, the transitive property should indicate $TM_B \geq TM_C$. If comparison TM_B vs TM_C is transitive, the comparison can be considered as consistent. Conversely, if TM_C is more important than TM_B, this comparison is inconsistent. The complex relationship between many TMs in HOQ can easily lead to inconsistent solutions to meet customer requirements. For a large scaled HOQ, it is very difficult for designers to complete all of comparisons in a consistent way. Moreover, in traditional weighting methods like AHP, after the data collection, the weight of each criterion is usually derived by averaging pairwise comparisons and implementing some matrix operations. However, this weight distribution does not guarantee the accuracy. Some papers have also claimed that there is a low robustness for the variation of values in AHP approaches, and the structure of AHP and ANP methods may cause inconsistent results [72, 73].

For reducing the inconsistency problem, Rezaei (2015) [71] introduced a Best-Worst Method (BWM) to improve efficiency of the weighting process [71]. BWM makes the comparison in a structured way for the easy judgment and understandable. More importantly, it leads to a consistent comparison, hence reliable weights. Comparing with AHP, BWM requires less comparison data to generate more consistent comparisons [74]. For example, if n is the number of TMs, BWM requires (2n-3) comparisons compared to (n(n-1))/2 comparisons required in the AHP method. If there are 9 criteria, 15 pairwise comparisons are required by BWM, while this number is 36 using the AHP method. Similarly, Pamucar et al. [75] introduced Full Consistency Method (FUCOM) as an improved AHP method. FUCOM has three steps to rank criteria from most important to least important, determining the comparative priority between criteria, and calculating weights based on two constraints. The model requires defining two groups of constraints that need to meet the optimal values of weight coefficients. The first type of constraints is mathematical transitivity and the second one is that relations of the weight coefficients of criteria should be equal to comparative priorities of the criteria. As HOQ is applied in a hierarchy structure of QFD, weights of TMs have a big impact on design solutions. Inaccurate data in HOQ can lead to an error propagation into other QFD matrices and undesirable products [76]. In the QFD literature, there are few research publications addressing normalization of the relationship matrix and its efficiency. Although the best-worst method (BWM) and its variations have been used in QFD by other researchers [57, 77], most of their work focus on determining customer requirements and weighting customer requirements in HOQ.

The existing work in the area of decision-making using HOQ can be classified into two groups: 1) Deterministic approaches that focus on improving accuracy of data analysis in different parts of HOQ, and 2) uncertainty-based approaches to consider vagueness in the data collection of HOQ. A lot of improvements for QFD are suggested by researchers. Integrated approaches are usually used to evaluate importance weights of customer requirements [77], TMs, and relations of design factors in the HOQ matrix [77]. Most of the existing research focus on identifying, classifying, and ranking customer requirements. For example, the Kano model is integrated with HOQ to segment potential customers according to their expectations [78]. Avikal et al. [61] integrated a fuzzy Kano model with QFD to examine the customer satisfaction based on aesthetic sentiments in product design. They improved the customer satisfaction in a case study of the sport utility vehicle. Kano models apply a structured survey using pairs of questions for each attribute of a specific product or service [79]. Many studies have evaluated the integration of QFD and Kano models for classifying customer requirements in HOQ [80].

For a multi-criteria decision-making process, there are three approaches to determine weights of design alternatives based on the design criteria that are subjective, objective, and combined subjective and objective methods [81]. Subjective approaches use expert opinions but they are often limited by experts' knowledge and experience. A most commonly used subjective weighting method is AHP. A combination of AHP and QFD can improve a warranty model of products [82]. Ucler (2017) developed an iterative AHP-QFD approach for the production layout in a concurrent engineering environment [83]. In addition to AHP, the ANP method was used to combine with HOQ [84]. It is a generalized version of AHP used in networks of HOQ to enhance the accuracy of TMs ranking.

Objective approaches use mathematical models closely linked to actual data. Objective weights can be decided by the Shannon entropy method [85]. Chen et al. applied the information entropy theory to estimate importance rates of customer requirements in HOQ in a revised design of the human-machine interface of the manned capsule [86]. They used the traditional approach to determine the relationship matrix. Wu and Lin used the information entropy to extract information from competitor data and enhance customer requirements ranking [87]. One of the limitations of objective approaches is that they are vulnerable to extreme values and may cause large false positives [88]. When neither of subjective or objective approaches is appropriate, a combination of them can be applied to take their both advantages. For example, a combination of AHP and Shannon entropy was used to determine the weight of alternatives [89, 90].

Fuzzy numbers are also used to determine final weights of TMs in the relationship matrix [91]. Linguistic-based approaches are combined with AHP [92] and ANP [93] to address vagueness in the QFD process. Fuzzy collective weights and membership functions are used to rank company strategies. Likewise, Tian et al. presented a hybrid approach of fuzzy BWM, MULTIMOORA and QFD in a case study of smart bike-sharing programs [94]. They used the fuzzy BWM approach to decide weights of different customer requirements using linguistic variables. Similarly, membership functions with triangular fuzzy numbers (TFNs) were applied to form the relationship matrix of HOQ. Mi et al. conducted a state-of-the-art survey of BWM for its applications and advantages [95]. Different applications of BWM and ranking methods to solve decision making problems were reviewed. They also presented different formulations of the optimization problem formed by BMW. BWM approaches were extended to different fields such as artificial intelligence and robotics.

In the classical form of a relationship matrix, the way of searching weight results in a distortion of the degree of importance. Olewnik and Lewis claimed that using the traditional scale ("1-3-9") in the relationship matrix may lead to inaccurate solutions [96]. Raharjo suggested an algorithm to normalize the relationship matrix while considering rank reversal [17]. He argued that overlooking normalization in HOQ may result in potentially inaccurate results. Inaccurate weight allocation in the relationship matrix is one of the reasons for this problem [21]. The pencil design problem has been widely studied as an example of the QFD process to check the solution accuracy. Figure 2-1 (a) is a classical form of the relationship matrix of HOQ for the pencil design problem. In this form, designers use a limited range of numbers (e.g., 1 – 3 – 9) to allocate relation weights. This form of representations can lead to a distortion in final weights as some TMs can be overestimated [97]. AHP is commonly used to extract relations of customer requirements and TMs in the relationship matrix of HOQ. Figure 2-1 (b) shows a normalized relationship matrix of HOQ based on integrated AHP-QFD for the pencil design problem. In this form of the representation, designers have more freedom to select a wide range of weights in the relationship matrix. A more reliable result can be generated in the relationship matrix using an integrated AHP-QFD approach with normalized values [97].

General methods of normalizing the relationship matrix use a pairwise comparison to decide weights of TMs. According to the hierarchy structure, a comparative decision can be made for the relative importance of TMs through the pairwise comparison [98] based on a combination of factors like decision makers' intuition, knowledge and experience of the subject. Pairwise comparisons are commonly conducted based on expert opinions for their preferences to provide score estimates with respect to criteria [99]. Inconsistency is a common problem in data obtained by classical approaches due to the lack of concentration in matrix comparisons. One remedy for this problem is to revise the comparison matrix in an iterative process until a consistent matrix is obtained. But it is not effective [100] as inconsistencies of unstructured comparisons. The inconsistency of the pairwise comparison matrix is the relevant weakness of AHP as it may result in inaccurate results. Furthermore, there are a large number of criteria or alternatives in most of HOQs, which may lead to lengthy pairwise comparisons with a reduced consistency [95].

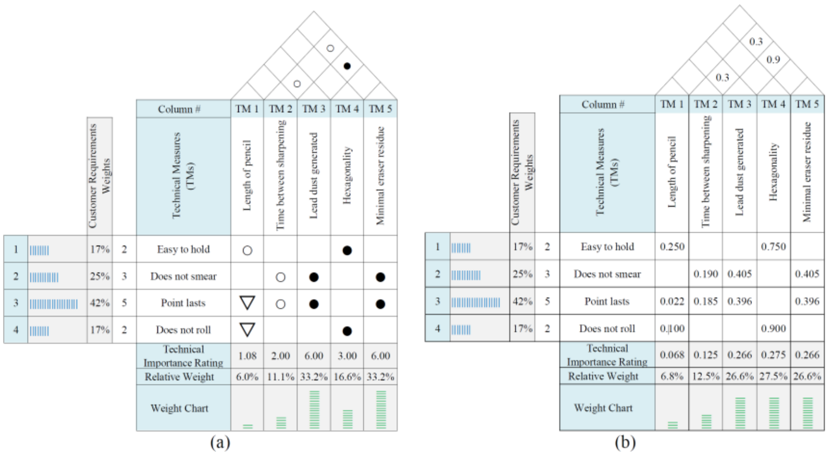

Figure 2-1 Comparison between classical and integrated approaches of the relationship matrix in HOQ. (a) Traditional approach (b) Integrated AHP-QFD

2.5 Data-driven and reinforcement learning based methods

Product concept development is a complex process with collaborative tasks to form the best design solution. In order to obtain a successful product, industry looks for innovative intelligent solutions to improve design processes [101]. As a design process takes different steps that are repetitive and time-consuming, it would be efficient if some routine tasks can be automated [102]. But when the system complexity increases, it becomes an exceptional challenge to consider all of the design interactions based on customer requirements for expected solutions. Therefore, a systematic approach is needed to explore the entire design space.

Product concept development can be viewed as a step-by-step decision-making process, in which designers continuously explore design spaces in an iterative manner. Over time, human designers can learn the design knowledge and process, which is a critical in searching various design domains. The ability to learn sequentially and apply the knowledge to generate design solutions can be simulated using probabilistic models such as a Markov chain (MC) model. There are different approaches to address design automation of complex systems. For example, data-driven modeling methods use solutions of existing designs to learn relations of design elements for new design solutions [103, 104]. High dimensional design problems require large data sets to implement learning models [105], which limits the meta-model accuracy [106-108]. Multidisciplinary design optimization (MDO), concurrent engineering [109] and system engineering methods are commonly used in considering the collaboration of design teams to decompose a complex system into sub-systems or components [110]. As a result, the design process can be modeled as a network of different working tasks to reach an optimal solution. Replacing design processes of human designers by computers is called the design automation, which is an evolutionary stage in the computer-aided design [111]. The design problem is like a multiagent system in which agents collaboratively search separate solutions of elements in the system.

In the early phases of product development, sharing design knowledge across product families and searching various design concepts can lead to a novel product concept [112]. However, this process requires the big data analysis and an automated framework. In the past few years because of recent developments in machine learning, research in Deep Neural Networks (DNNs) and its new applications has been exploded. DNNs can mimic human brains and their setup with the input layer, hidden layers to process information and output layer to produce results. The DNNs setup is reconfigurable and the weight of neurons can be iteratively manipulated to improve the network performance [113].

Each year, over 30000 new products with different functions and specifications are introduced to the market [112]. As a result, the main challenge for designers is not the lack of data, but requirements of growing quantity and diversity. An efficient automatic approach for discovering knowledge in different domains ranging from customer requirements to design parameters is critical in different aspects of engineering design. Imdat et al. studied the applicability of deep learning in architectural decision-making [113]. They used hybrid DNNs to identify design vocabulary and implement a function layout, but they only focused on the generation of concepts in the function-driven conceptual design and didn't consider the quantitative evaluation of the concepts. Kang et al. proposed an automated concept generation approach based on the Bayesian model in analyzing semantic similarities between function requirements and customer requirements [114]. However, the design data acquisition process is required to create a database of different functions. In another study, a deep learning approach was used to predict aesthetic design attributes of product concepts for given customer requirements [115]. A database of different vehicles was used to train the network. The result concludes that the deep learning approach can predict customer perceptions from design concepts. However, this approach requires a large database of design samples to train the network. Li et al. studied the application of Convolutional Neural Network (CNN) in the product design evaluation [116]. They applied CNNs and a Support Vector Machine (SVM) to classify and predict different degrees of product features. However, the approach required a large data set for training CNNs.

Generative Adversarial Networks (GANs) have been developed to produce data samples from a specific domain similarly to the main training set. A GAN architecture contains two interacting DNNs (discriminator and generator) that generally interact in an unsupervised manner by means of an adversarial game [117]. After introducing GANs approach, a lot of applications in computer graphics have been studied. However, very few studies used this approach to generate product concepts based on existing datasets. Burnap et al. introduced a deep generative model to represent a design space from a statistical distribution using a large set of design attributes and images from existing designs [118]. They explored the design space by morphing different design attributes. They only focused on 2D design concepts and claimed that interpretation of the latent space remains a challenge. Andries et al. suggested a neural network variational auto-encoder approach for the automatic generation of object shapes for mapping function-to-form from a dataset of different objects [119]. They used data sets for different chairs and tables to demonstrate the approach and applied affordance tests to evaluate generated concepts. They only focused on simple geometries. Their models didn't include detail information like materials of concepts.

In the context of engineering design, although supervised learning-based design models are data efficient, the quality of design solutions depends on the quality of available data. In order to solve this drawback, Reinforcement learning (RL) based design framework has been formulated in some design applications. For example, the microfluidic device design for flow sculpting has been studied using reinforcement learning with efficient results [120]. A reinforcement learning approach was applied for the learning function in an optimization process of the bulk carrier structure [121].

Reinforcement learning differs from other machine learning approaches mainly through its online adaptability and real-time processing of data. Reinforcement learning focuses on how intelligent agents take actions in an environment to improve the cumulative reward. Most of the existing work in using reinforcement learning for product development is for improving manufacturing process and production operations. Managing the design process is difficult by using only one single agent for a complex system as its exponentially expanding actions and state spaces increase the computational cost [122, 123]. Although reinforcement learning has been applied in different robotics and manufacturing problems, there is a lack of reinforcement learning applications in product design. In general, designing complex systems is a challenge as different parameters, criteria and interactions between subsystems involve in the process.

Designers or subsystems in a complex system are like agents in a multiagent system. Modeling engineering design with Markov-based multiagent systems was addressed to study design interactions between multiple agents and effect of design parameters on the optimal configuration [124]. Hulse et al. proposed an approach based on reinforcement learning and multiagent learning systems to handle distributed design problems with control design variables and shared constraints [110]. They concluded that the learning system provided better-performing designs collaboratively. Also, a reinforcement learning-based approach was proposed for designers to reduce the gap between the problem and solution space in the task-oriented design [125]. In this approach, the 3D design procedure is allocated to an action space in deep reinforcement learning, and the preferred 3D model is computed by training each design action according to the task. Reinforcement learning was also combined with other machine learning methods to improve design efficiency. For example, a combined RL-GANS network was suggested to provide the fast and robust control of GANs network, and convert noisy and partial point cloud data into a high-fidelity completed shape [126].

Recently, there is an evolving concept that treats the conceptual design process as a Sequential Decision Process (SDP). The SDP is a new approach to efficiently explore a large set of design solutions. Some studies considered SDP as a finite Markov Decision Process (MDP) to evaluate sequence of different models [127]. Chhabra et al. suggested that the integration of MDP and reinforcement learning can improve computational cost of the design process [127]. Pandremenos and Chryssolouris developed a clustering approach based on neural network algorithms and DSMs to reorganize components in a cluster and improve their interactions in the concept generation [128]. They only focused on reorganizing the interactions between components in a product concept. Although there are research activities related to applications of reinforcement learning in different areas of engineering, very few studies have focused on applications of reinforcement learning in product design.

Reinforcement learning can use the model-based or model-free approaches. The model-based approaches learn from environments to predict process values or states. Unlike model-based reinforcement learning, model-free methods do not rely on an explicit model of the environment. The goal of the agent is to learn a policy that maximizes the cumulative rewards it receives over time [129]. Value-based, policy-based and hybrid methods are three main model-free approaches of reinforcement learning. In policy-based methods, a continuous action space is considered for mapping a state to an action by forming a representation of the behavior policy. In contrast, value-based approaches such as Deep Q-Networks (DQN) learn from a value function for discrete action spaces to assess each of the potential actions. Hybrid approaches such as Deep deterministic policy gradient (DDPG) apply hybrid actor-critic models to integrate previous approaches advantages [129]. Wang et al. [130] and Naeem et al. [131] conducted a detailed review of algorithmic insights of reinforcement learning. High dimensional problems for the action and state discretization in product design can reduce performances and learning efficiencies of classical reinforcement learning techniques. A combination of deep learning and reinforcement learning can improve this problem [132]. In deep reinforcement learning, a neural network is used as a function approximator to map policy. The advantage of this approach is its capability to process large amounts of raw data.

The design space exploration, evaluation and structural optimization [133, 134] are three main research areas of applications of machine learning in product design [135]. reinforcement learning is also used to perform the active flow control [136] in multi-environment scenarios [137] and various Reynolds numbers [138] in the field of computational fluid dynamics. Comparing with optimization methods, a main advantage of the optimization by deep reinforcement learning techniques is that the reinforcement learning model can generate solutions immediately once the model is trained since it is an end-to-end approach [139]. Hayashi and Ohsaki [140] integrated reinforcement learning and graph embedding for the topology optimization of trusses to minimize the total structural volume under specific design constraints. Ororbia and Warn [135] formulated a structural optimization problem for a Markov decision process using the Q-learning method. They studied the method effectiveness in simplified truss optimization problems. Hulse et al. [110, 124] used multi-agent learning to improve the design optimization. They used epsilon-greedy in a continuous action selection process for a quadrotor design problem. In a similar study, Zurita et al. [141] proposed a cooperative coevolutionary algorithm to design a formula SAE racing car.

Kim et al. [142] used a deep learning-based abstraction process to extract structured function requirements from design specifications and customer requirements. They applied Axiomatic Design in the mapping process of product design. Rauch and Matt [143] suggested that Axiomatic Design can be improved by deep neural networks and natural language processing. The approach starts with an automated clustering of customer feedbacks into meaningful customer needs. The major work in literature focuses on the development of product shapes and sketches using deep reinforcement learning in conceptual design. For example, Pal et al. [113] applied the deep reinforcement learning and graph based method in the evaluation of building designs [113]. Ruiz-Montiel et al. [144] and Mandow et al. [145] used shaped grammars and reinforcement learning in the architectural design. The approach used simple grammar rules to form different layout schemes of single-family housing units.

The reinforcement learning use increases in manufacturing [146-148] to improve or develop different processes or operations [149] such as for the product lifecycle sustainability [150] and assembly sequence planning [151]. Farid et al. [152] applied a multi-agent system in the reconfigurable manufacturing system. Their work applied Axiomatic Design for reconfigurability of shop-floor activities in discrete-part automated manufacturing systems. Zheng et al. [153] developed an industrial knowledge graph-based multi-agent reinforcement learning technique for analyzing Self-X cognitive manufacturing networks. Their approach is based on the extracted empirical knowledge and recognized pattern in the manufacturing process. Brito et al. [154] applied DDPG in combining accuracy of the robot with flexibility of the workforce in a production process to improve productivity and reduce stoppages.

In summary, traditional approaches are limited in data processing and solution searching in the concept generation and evaluation. They mainly explore the entire design space manually in the design process. The research of this thesis will improve above mentioned limitations. Novel approaches will be developed to optimize and automate the design process to meet not only customer requirements, but also the voice of designers and design feasibility.

Chapter 3 Design Theories and Methods

This chapter introduces design theories and methods used or modified in this research to develop and evaluate product concepts. The following sections provide details about customer analysis and design synthesis in the design process.

3.1 Quality function deployment

Quality function deployment (QFD) is a structured approach to transforming qualitative customer requirements into quantitative product characteristics and mapping product functions into design concepts [155]. HOQ provides a tool for QFD applications using matrix formulations to translate the voice of customers into design solutions [156]. A general form of HOQ is shown in Figure 3-1.

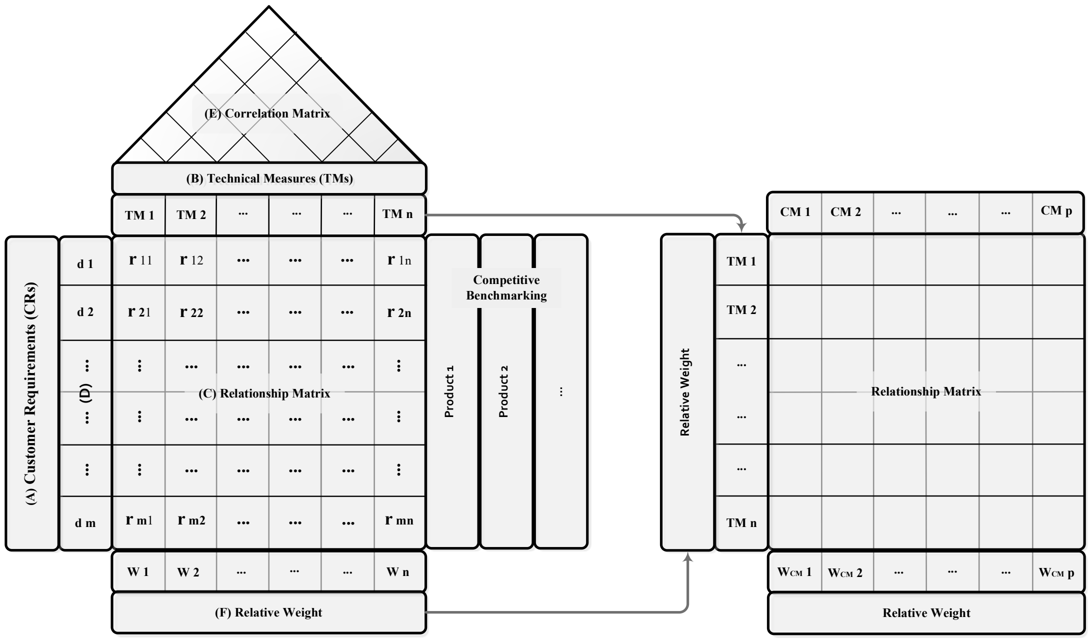

Figure 3-1 A general form of HOQ in a two-step QFD process.

HOQ establishes relationships between customer requirements (Whats) and TMs (Hows) by combinations of matrices: (A) Whats matrix, (B) Hows matrix, (C) Central relationship matrix between WHATs and HOWs, (D) Matrix of relative weights of WHATs, (E) Interrelationship matrix among HOWs, and (F) Matrix of weights of HOWs. Wasserman [157] improves the deployment normalization in HOQ. A modified correlation matrix can improve accuracy of the relationship matrix to obtain a meaningful interpretation of relationships between TMs and customer requirements. Equation (3-1) is Lyman's normalization. Elements of a relationship matrix are determined as follows.

$$r_{i,j}^{norm} = \frac{\sum_{k=1}^{n} r_{i,k} \cdot \gamma_{k,j}}{\sum_{j=1}^{n} \sum_{k=1}^{n} r_{i,j} \cdot \gamma_{j,k}} \tag{3-1}$$

where $r_{i,j}^{norm}$ is the normalized relation value between TM_j and CR_i, m and n are numbers of customer requirements and TMs, respectively. $\gamma_{j,k}$ represents the correlation between TM_j and TM_k. When TMs are independent, we have $\gamma_{j,k} = 1$, if $j = k$, and 0, otherwise. After determining the relationship matrix, weight of each TM can be obtained from the relationship matrix and customer requirements weight as follows.

$$W_j = \sum_{i=1}^{m} d_i . r_{i,j}^{norm} \tag{3-2}$$

where d_i signifies the weight of CR_i and $\sum d_i = 1$; W_j can be normalized for each TM as follows.

$$W_j^n = \frac{W_j}{\sum_{j=1}^{n} W_j} \tag{3-3}$$

Based on W_j^n, the relative technical importance can be used for prioritization of TMs. A two-steps QFD process applies a HOQ to transform customer requirements into TMs and design parameters [158]. In this thesis, TMs are a translation of customer requirements into quality attributes of the product. From a technical viewpoint, non-functional requirements can be used as TMs in HOQ. Once function requirements are determined, non-functional requirements can be derived and mapped from customers and function requirements. The relationship matrix for mapping relations in HOQ is as follows.

$$\begin{bmatrix} CR_1 \\ CR_2 \\ \cdots \\ CR_m \end{bmatrix} = \begin{bmatrix} r_{11} & r_{12} & \cdots & r_{1n} \\ r_{21} & r_{22} & \cdots & r_{2n} \\ \cdots & \cdots & \ddots & \cdots \\ r_{n1} & r_{n2} & \cdots & r_{mn} \end{bmatrix} \begin{bmatrix} TM_1 \\ TM_2 \\ \cdots \\ TM_n \end{bmatrix} \tag{3-4}$$

In the past few years, several mathematical approaches have been proposed for designers to rank design concepts. However, most of them do not include all of the designer preferences to consider uncertainty of the design target [159]. Fuzzy set theory is introduced to include subjective, ambiguous and uncertain factors in design. The fuzzy set theory uses a set of elements with the degree of memberships valued in an interval [0, 1]. The membership function is defined as $\mu_A(x): R \to [0,1]$. A fuzzy knowledge-based model is introduced in this research based on triangular fuzzy numbers characterized by triplets (α, β, γ), where α and γ are the lower and upper bounds of the fuzzy number respectively and β is the element that signifies the closest fit. The membership function of fuzzy number A is defined as follows.

$$\mu_A(x) = \begin{cases} \frac{x-\alpha}{\beta-\alpha} & ,\alpha \le x \le \beta \\ \frac{\gamma-x}{\gamma-\beta} & ,\beta \le x \le \gamma \\ 0 & ,\text{otherwise} \end{cases} \tag{3-5}$$

where α and γ represent lower and upper bounds of fuzzy number A, β is the modal value of A based on membership functions. Correlations between customer requirements and TMs are determined using an average operator of different values assigned by different membership functions as follows.

$$r_{ij} = \frac{1}{k} \otimes \left(r_{ij_1} \oplus r_{ij_2} \oplus \ldots \oplus r_{ij_n}\right) \qquad ,\forall\, i = 1, \ldots, n;\ j = 1, \ldots, m \tag{3-6}$$

where r_{ij} represents the relation of CR_i and TM_j, k is the number of membership functions defined by a group of designers using an adaptive neuro-fuzzy inference system or traditional approaches, m is the number of customer requirements, and n is the number of TMs. Each element r_{ij} in the relationship matrix is a triangular fuzzy number expressed by triplets (α, β, γ). The absolute importance weight of each TM is determined based on the relationship matrix and customer requirements weight as follows.

$$W_j = \frac{1}{n} \otimes \left[\left(r_{j1} \otimes d_1\right) \oplus \ldots \oplus \left(r_{jn} \otimes d_n\right)\right] \qquad ,\forall\, i = 1, \ldots, n \tag{3-7}$$

where d_i signifies the weight of CR_i, and r_{ij} is the relation value between TM_j and CR_i. W_j are triangular fuzzy numbers characterized by triplets (α, β, γ). The effect of correlations between TMs can also be considered using Khoo and Ho's formula [160] to determine the final importance weight of each technical measure as follows.

$$W_j^f = W_j + \frac{1}{n-1}\sum_{i=1, i\neq j}^{n}\left(W_j \otimes C_{ij}\right) \qquad , i, j = 1, \dots, n \tag{3-8}$$

where C_{ij} represents the level of correlation between TM_i and TM_j, $i \neq j$. Based on W_j^f, the relative technical importance is used for the prioritization of TMs. The same approach is used for the component deployment in HOQ 2. The output of HOQ 1 is the importance weights of TMs, which is used as input of HOQ 2 to determine the importance weight of each design parameter. The relationship matrix in the component deployment stage is expressed as follows.

$$\begin{bmatrix} TM_1 \\ TM_2 \\ \cdots \\ TM_n \end{bmatrix} = \begin{bmatrix} p_{11} & p_{12} & \cdots & p_{1k} \\ p_{21} & p_{22} & \cdots & p_{2k} \\ \cdots & \cdots & \ddots & \cdots \\ p_{n1} & p_{n2} & \cdots & p_{nk} \end{bmatrix} \begin{bmatrix} DP_1 \\ DP_2 \\ \cdots \\ DP_k \end{bmatrix} \tag{3-9}$$

where, p_{ij} represents the relation of TM_i and DP_j. Two steps of the HOQ modeling are developed to indirectly link customer requirements weights and design components. In HOQ 2, the relationship matrix represents the degree of satisfaction of TMs (or non-functional requirements) related to design parameters. The matrix is in a fuzzy space.

3.2 Extended Axiomatic design

Axiomatic Design is a mapping tool of different design domains, represented by matrices. Axiomatic Design can analyze relations of elements in domains to decompose function requirements into a set of sub function requirements and derive design solutions for each sub-function requirement in a stepwise zigzag process between domains. A decomposition process is used continuously in functional and physical domains to obtain product concepts for design solutions in details for each sub-functional requirement. Figure 3-2 shows the Axiomatic Design mapping process between different design domains. The design process starts with mapping customer requirements into high-level independent function requirements [161]. Function requirements are then determined by design parameters. Technically, there are many options in customer, functional, and physical domains. An efficient mapping between these domains can lead to creative solutions that satisfy customer and designer perspectives.

In the extended Axiomatic Design, non-functional requirements are introduced as a set of requirements to describe the level of performances for a particular function based on design constraints and specific technologies. In the classic form of Axiomatic Design, function requirements are directly used as central elements to determine design parameters to form product concepts. Non-functional requirements are not included in domain mapping [7]. The limitation of Axiomatic Design is its concentration solely on function requirements. The exclusion of quality attributes of the design process may lead to nonoptimal outcomes. Therefore, it is essential to consider non-functional requirements as the product performance for generating design concepts. In this thesis, non-functional requirements are considered as TMs in the QFD process to quantify and rank the performance of generated concepts based on the MABAC approach. In Axiomatic Design, the relations of function requirements and design parameters are described in design equations. Each FR includes some design parameters as follows.

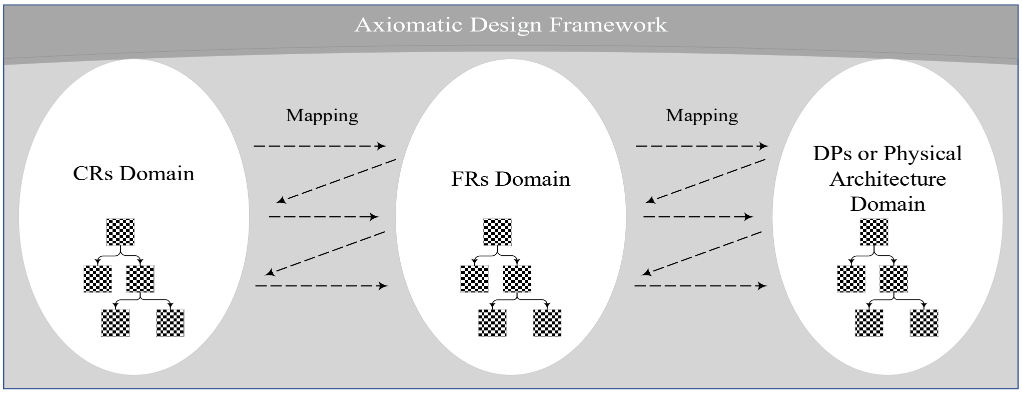

Figure 3-2 Mapping between different domains in Axiomatic Design.

$$\begin{gathered} FR_1 = f_1(DP_1, DP_2, \dots, DP_m) \\ \vdots \\ FR_n = f_n(DP_1, DP_2, \dots, DP_m) \end{gathered} \tag{3-10}$$

or in a vector form:

$$\boldsymbol{FR} = f(\boldsymbol{DP}) \tag{3-11}$$

where f represents a function, a bolded quantity signifies a vector. If we assume function requirements as a vector with n elements, and design parameters as a vector with m elements, a Design Matrix with n rows and m columns is as follows.

$$\begin{bmatrix} FR_1 \\ FR_2 \\ \dots \\ FR_n \end{bmatrix} = \begin{bmatrix} A_{11} & A_{12} & \dots & A_{1m} \\ A_{21} & A_{22} & \dots & A_{2m} \\ \dots & \dots & \ddots & \dots \\ A_{n1} & A_{n2} & \dots & A_{nm} \end{bmatrix} \begin{bmatrix} DP_1 \\ DP_2 \\ \dots \\ DP_m \end{bmatrix} \tag{3-12}$$

function requirements' deferential form is as follows.

$$A_{ij} = \frac{\partial FR_i}{\partial DP_j} \quad \forall\, i \in [1, \dots, n], \forall\, j \in [1, \dots, m] \tag{3-13}$$

The design matrix can be used for the quality assessment of generated concepts. An additional matrix is built to represent relations between design elements and non-functional requirements in the extended Axiomatic Design. Elements of this matrix can be zero, 1 or -1 to show the degree of satisfactions of non-functional requirements. It is suggested that non-functional requirements are considered as TMs in the QFD process. To fully consider weights of customer requirements and other design factors, we integrate the extended Axiomatic Design, QFD and DSM. Relations between non-functional requirements and design parameters are represented by an extended design equation as follows.

$$\begin{bmatrix} NFR_1 \\ NFR_2 \\ \dots \\ NFR_n \end{bmatrix} = \begin{bmatrix} p_{11} & p_{12} & \dots & p_{1k} \\ p_{21} & p_{22} & \dots & p_{2k} \\ \dots & \dots & \ddots & \dots \\ p_{n1} & p_{n2} & \dots & p_{nk} \end{bmatrix} \begin{bmatrix} DP_1 \\ DP_2 \\ \dots \\ DP_k \end{bmatrix} \tag{3-14}$$

where, p_{ij} represents relations of NFR_i and DP_j. Technically, non-functional requirements can be considered as TMs in the QFD process to model performance criteria of a product.

3.3 Design structure matrix

Design structure matrix, or dependency structure matrix, provides a common tool to represent and analyze relations of components in a product. DSM is an equivalent form of N^2 diagram or adjacency matrix in the graph theory. Product functions can be formed by interactions of its components in DSM [162]. Comparing with other system modeling approaches, DSM has two features: a large number of components and their relations can be represented compactly with important data flows such as feedback and feedforward loops, and a lot of matrix operation methods can be used to improve the structure of design concepts. Figure 3-3 shows main DSM forms based on different component configurations. In the parallel configuration, product components are fully independent. In the sequential type, the input of one component is dependent on the output of others. In the coupled configuration, components are mutually dependent.

Figure 3-4 shows a general framework of component relations in a product concept. Crosses above the diagonal represent a feedback information flow, while crosses below the diagonal show a feedforward loop. A DSM is a square matrix representing linkages between system elements. The off-diagonal cells represent linkages between components. Highlighted cells in a DSM indicate a direct connection between two components in design relations or constraints. For a highlighted cell $\{j, k\}$ in the DSM, the output of corresponding components in row j is linked to the input of corresponding components in column k [163]. For example, in Figure 3-3 (b), sign X indicates the output of component C_1 linked to component C_2. Diagonal cells represent component self-iterations (e.g., subsystems or components that may be further decomposed into sub-components). In following chapters, methods developed based on QFD, Axiomatic Design, and DSM described in this chapter are presented.

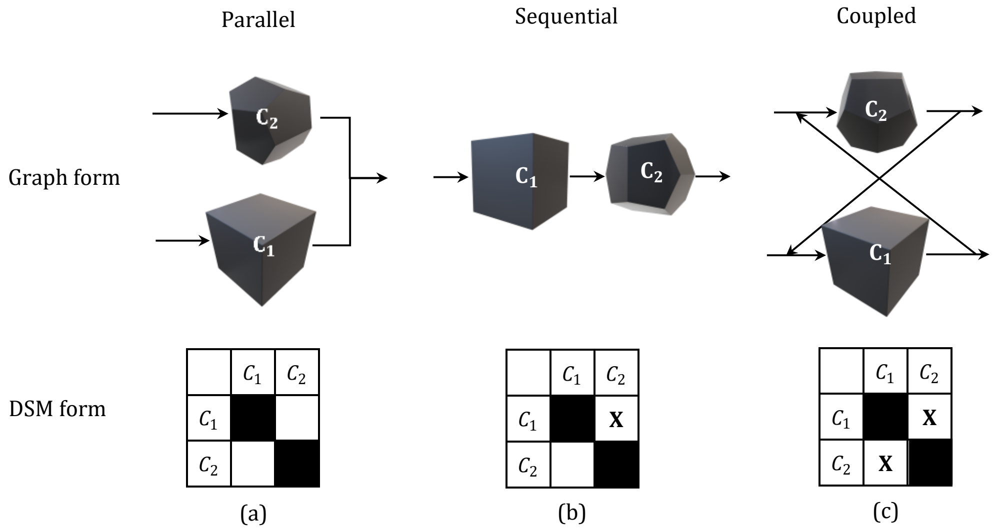

Figure 3-3 DSM forms based on different component configurations.

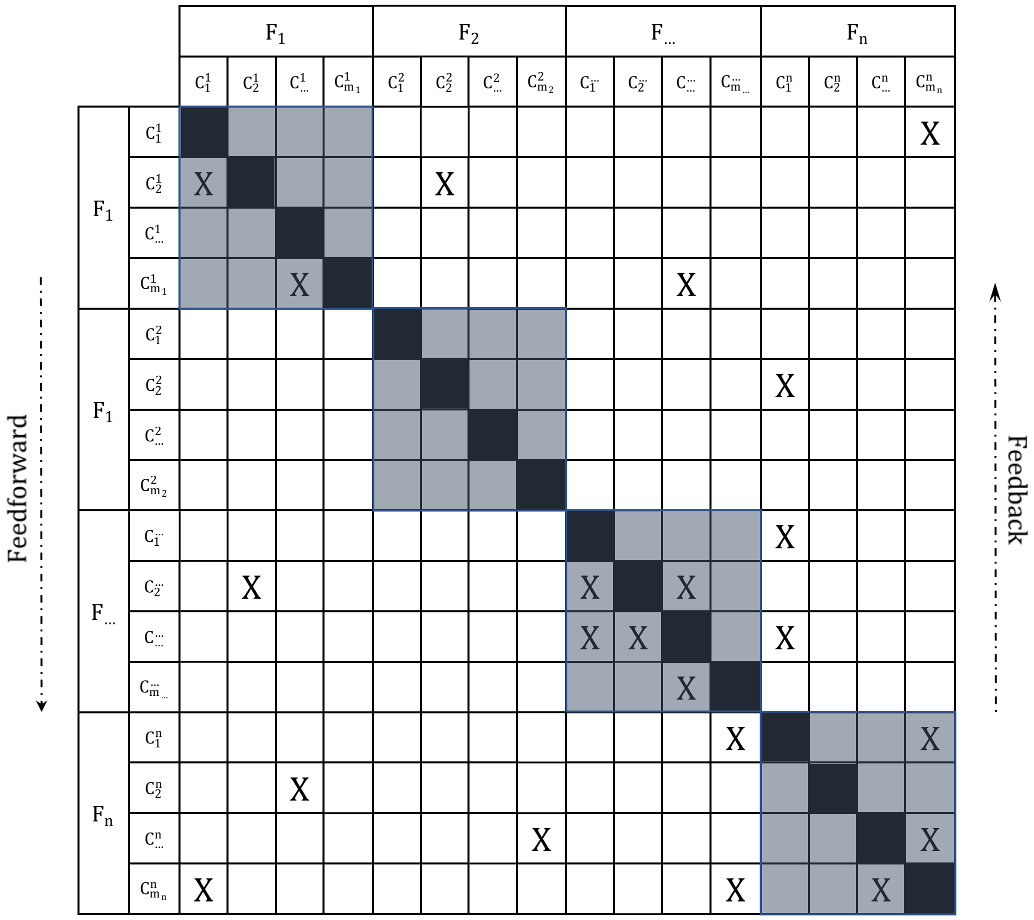

Figure 3-4 DSM framework to represent module relations in a design concept

3.4 Summary

In this chapter, a few fundamental design theories were introduced to address different tasks in the conceptual design process. In the following chapters, the introduced methods will be extended and integrated with approaches to automate the design process.

Chapter 4 Efficient Extraction of Information from Correlation Matrix using an Integrated QFD-DEMATEL Method

In this chapter, a new method for analyzing the roof data of HOQ to extract additional information of correlations between TMs is developed to improve the mentioned limitations about correlations between TMs in a QFD process. The method integrates the decision-making trial and evaluation laboratory (DEMATEL), analytic network process, and QFD to model interrelations of TMs. DEMATEL is used for understanding of the correlation and interdependence of TMs through analysis of TMs in cause-and-effect relations. The final weight is obtained from an ANP super-matrix.

4.1 Decision-making trial and evaluation laboratory (DEMATEL)

DEMATEL provides a comprehensive process to obtain a structural model of casual relationships among criteria in complex decision-making problems [164]. Comparing with other techniques like AHP, it has advantages such as modeling interdependence between factors via the causal diagram, which is ignored in the existing methods [165]. This research applies the DEMATEL technique to evaluate interdependent relationships between TMs in HOQ and divide them into cause-and-effect groups.

Different HOQ templates have been suggested by designers to improve data processing, for example, Shahin [166] developed a C-shaped QFD 3D matrix for service applications. In the classical form of correlation matrix, it is assumed that at each intersection, TMs have the same effect on each other, and their relations is represented with signs that cannot be effectively used by designers. Figure 4-1 shows two forms of the correlation matrix in HOQ. In a common HOQ, it is assumed that TMs have the equal effect in intersections of the correlation matrix, which results in a triangular shape of the roof. However, this simplified assumption affects the TMs selection in design. Therefore, for real-world design problems, a square-shaped form of the roof is suggested for considering unequal mutual interactions. The suggested form is a non-symmetric square matrix that includes design information from both directions of correlations. Data can be collected from users and experts to indicate degrees of the direct effect of TMs on each other in the correlation matrix with a scale range such as from 0 for no effect to 4 for very high effect [167]. They can be obtained in the form of DEMATEL comparison matrix which is available in the literature [168]. An initial matrix A can be formed either by converting the triangular shape correlation matrix into a symmetric square matrix or using a non-symmetric square matrix as follows.

$$A = \begin{bmatrix} a_{11} & \cdots & a_{1j} & \cdots & a_{1n} \\ \vdots & & \vdots & & \vdots \\ a_{i1} & \cdots & a_{ij} & \cdots & a_{in} \\ \vdots & & \vdots & & \vdots \\ a_{n1} & \cdots & a_{nj} & \cdots & a_{nn} \end{bmatrix} \quad (4\text{-}1)$$

In the following equation, N is a normalized initial influence-relation matrix shaped by normalizing average matrix A.

$$N = s \times A, \qquad s > 0 \quad (4\text{-}2)$$

or

$$[N_{ij}]_{n\times n} = s[a_{ij}]_{n\times n}, \qquad s > 0, \quad i, j\epsilon\{1,2,\ldots,n\} \quad (4\text{-}3)$$

where value s can be obtained as follows.

$$s = \frac{1}{max\left(\sum_{j=1}^{n} a_{ij}\,, \sum_{i=1}^{n} a_{ij}\right)} \quad (4\text{-}4)$$

$$\lim_{m\to\infty} N^m = [0]_{n\times n}\,, 0 \le x_{ij} \le 1 \quad (4\text{-}5)$$

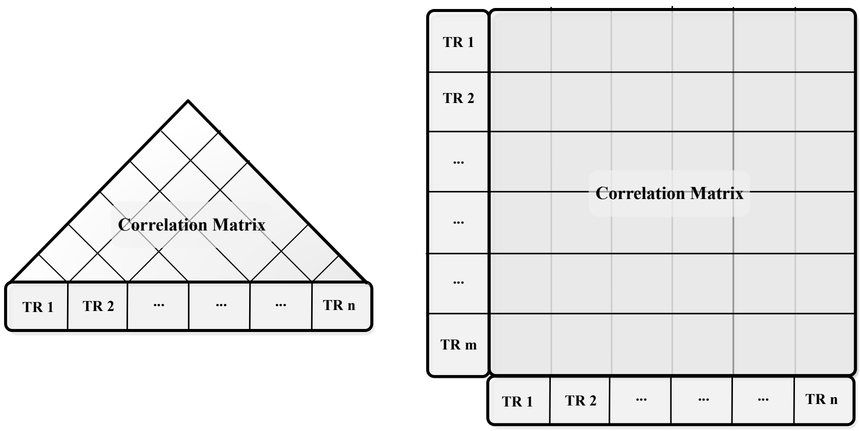

(a) (b)

Figure 4-1 Two forms of the correlation matrix in HOQ.

The total influence matrix T is an n × n matrix as follows.

$$
\begin{aligned}
T &= N + N^2 + \cdots + N^m = N(I + N + N^2 + \cdots + N^{m-1}) \\
&= N(I + N + N^2 + \cdots + N^{m-1})(I - N)(I - N)^{-1} \\
&= N(I - N)^{-1}, \quad When \lim_{m\to\infty} N^m = [0]_{m\times m}
\end{aligned} \tag{4-6}
$$

where I is an $n \times n$ matrix. The sum of columns and rows in total influence matrix T can be characterized as R and C vectors as follows.

$$R = [r_i]_{n\times 1} = \left(\sum_{j=1}^{n} t_{ij}\right)_{n\times 1} \tag{4-7}$$

$$C = [c_j]'_{1\times n} = \left(\sum_{i=1}^{n} t_{ij}\right)'_{1\times n} \tag{4-8}$$

where r_i is a member of vector R, c_j is a member of vector C, and t_{ij} represents each member of total influence matrix T. In the following section, ANP is presented to solve interdependence among TMs by the DEMATEL to form a super matrix.

4.2 Analytic network process (ANP)

ANP is a decision-making technique to systematically model all kinds of dependence among criteria by considering all relations as networks [169]. It is used to analyze the total influence matrix formed by DEMATEL. TMs with same characteristics in a large HOQ can be grouped into small sized clusters based on similar criteria. For example, we can form a cost sub-matrix including manufacturing and operation costs. In small HOQs, each TM can be considered as a separate dimension. Figure 4-2 shows a detail algorithm of the proposed method. The structure of the total-influenced matrix for sub-criterion T_c is shown below.

$$
T_c = \begin{array}{cc} & \\ & c_{11} \\ & \vdots \\ D_1 & c_{1m_1} \\ & \vdots \\ \vdots & c_{i1} \\ & \vdots \\ D_i & c_{im_i} \\ & \vdots \\ \vdots & c_{n1} \\ & \vdots \\ D_n & c_{nm_n} \end{array}
\begin{array}{c}
\begin{array}{ccccc} D_1 & \cdots & D_j & \cdots & D_n \\ c_{11} \ldots c_{1m_1} & \cdots & c_{i1} \ldots c_{im_i} & \cdots & c_{n1} \ldots c_{nm_n} \end{array} \\
\begin{bmatrix}
T_c^{11} & \cdots & T_c^{1j} & \cdots & T_c^{1n} \\
\vdots & & \vdots & & \vdots \\
T_c^{i1} & \cdots & T_c^{ij} & \cdots & T_c^{in} \\
\vdots & & \vdots & & \vdots \\
T_c^{n1} & \cdots & T_c^{nj} & \cdots & T_c^{nn}
\end{bmatrix}
\end{array} \tag{4-9}
$$

Proposed Algorithm

Input: Modified correlation matrix $A_r = [a_{ij}]_{n\times n}, r = 1,2,\ldots,N$ (Number of respondents)

Output: Improved weights of TMs

$A_{sum} = A_1$
for $r = 2\ to\ N$
    $A_{sum}(r) = A_{sum} + A_r$
end for
$A = A_{sum}/N$ //Calculating the initial average matrix
for $j = 1\ to\ n$
    $P(j) = sum(a_{ij})$
end for
for $i = 1\ to\ n$
    $\mathrm{Q}(i) = sum(a_{ij})$
end for
$N = A/\max(P, Q)$ //Calculating normalized initial average matrix
$T_c = N(I - N)^{-1}$ //Calculating the total influence matrix
for $j = 1\ to\ n$
    $D(j) = sum(t_{ij})$
end for
for $i = 1\ to\ n$
    $\mathrm{R}(i) = sum(t_{ij})$
end for
for each $T_c^{ij} \in T_c$
    $e_i = \sum_{j=1}^{m} t_{ij}$
    $T_c^{norm} = \frac{T_c}{e_i}$ //Calculating normalized total influence-relation matrix
end
$Q = (T_c^{norm})'$ //Obtaining unweighted super matrix
for each $T_c^{ij} \in T_c$
    $d_i = \frac{\sum_{i=1}^{m}\sum_{j=1}^{m} t_{ij}}{m\times m}$
end
Construct total influence-relation matrix T_D of criteria
Calculate normalized total influence-relation matrix T_D^{norm}
$W = T_D^{norm} \times Q$ //Calculating weighted super matrix
$While\ \varepsilon < defined\ accuracy$ //Calculating weighted super matrix
    $Q = (T_c^{norm})'$ //Obtaining unweighted super matrix
    $Influential\ weights = \lim_{\alpha\to\infty}(W)^{\alpha}$ //Obtaining unweighted super matrix
end

Figure 4-2 *Proposed Algorithm for calculating influential weights of TMs.*

Where D_n symbolizes the nth criterion; C_{nm} represents the mth sub-criterion in the nth criterion. In order to use this matrix to decide the inner dependency, it should be first normalized and then transposed. Each sub-criterion can be normalized as follows.

$$d_{ci}^{11} = \sum_{j=1}^{m_1} t_{ij}^{11}, \qquad i = 1,2, \dots m_1 \tag{4-10}$$

$$T_c^{norm\,11} = \begin{bmatrix} \frac{t_{c_{11}}^{11}}{d_{c_1}^{11}} & \cdots & \frac{t_{c_{1j}}^{11}}{d_{c_1}^{11}} & \cdots & \frac{t_{c_{1m_1}}^{11}}{d_{c_1}^{11}} \\ \vdots & & \vdots & & \vdots \\ \frac{t_{c_{i1}}^{11}}{d_{c_i}^{11}} & \cdots & \frac{t_{c_{ij}}^{11}}{d_{c_i}^{11}} & \cdots & \frac{t_{c_{im_1}}^{11}}{d_{c_i}^{11}} \\ \vdots & & \vdots & & \vdots \\ \frac{t_{c_{m_1 1}}^{11}}{d_{c_{m_1}}^{11}} & \cdots & \frac{t_{c_{m_1 j}}^{11}}{d_{c_{m_1}}^{11}} & \cdots & \frac{t_{c_{m_1 m_1}}^{11}}{d_{c_{m_1}}^{11}} \end{bmatrix} \tag{4-11}$$

After normalizing matrix T_c, a new matrix is obtained in Equation (4-12).

$$T_c^{norm} = \begin{array}{cc} & \begin{array}{ccccc} D_1 & \cdots & D_j & \cdots & D_n \\ c_{11} \cdots c_{1m_1} & \cdots & c_{i1} \cdots c_{im_i} & \cdots & c_{n1} \cdots c_{nm_n} \end{array} \\ \begin{array}{cc} & c_{11} \\ & \vdots \\ D_1 & c_{1m_1} \\ & \vdots \\ \vdots & c_{i1} \\ & \vdots \\ D_i & c_{im_i} \\ & \vdots \\ \vdots & c_{n1} \\ & \vdots \\ D_n & c_{nm_n} \end{array} & \begin{bmatrix} T_c^{norm\,11} & \cdots & T_c^{norm\,1j} & \cdots & T_c^{norm\,1n} \\ \vdots & & \vdots & & \vdots \\ T_c^{norm\,i1} & \cdots & T_c^{norm\,ij} & \cdots & T_c^{norm\,in} \\ \vdots & & \vdots & & \vdots \\ T_c^{norm\,n1} & \cdots & T_c^{norm\,nj} & \cdots & T_c^{norm\,nn} \end{bmatrix} \end{array} \tag{4-12}$$

Unweighted super matrix Q is a transpose of normalized total influence-relation matrix T_c^{norm}.

$$Q = (T_c^{norm})' \tag{4-13}$$

The weighted super matrix is calculated by multiplying the normalized total influence-relation matrix of dimensions T_D^{norm} and unweighted super matrix as follows.

$$W = T_D^{norm} \times Q \tag{4-14}$$

The weighted super matrix is then limited to a large power α until it converges in a stable super-matrix. Influential weights are then used in HOQ to obtain the final weight of TMs.

$$Influential\ weights = \lim_{\alpha \to \infty} (W)^{\alpha} \tag{4-15}$$

4.3 Case study

4.3.1 Design of a hand rehabilitation device

Hand rehabilitation devices are used for the patient recovery with difficulties in hand motion. As rehabilitation devices have to meet the diverse requirements of different users, various parameters, assumptions and constraints should be considered in the device design. To accommodate the diverse needs of users, these devices require considerations of various parameters, assumptions, and constraints during the design phase. Exoskeleton mechanisms are typically created to replicate the kinematic configuration of the hand through actuator-controlled finger joints, thereby enabling patients to perform a variety of exercises. The use of exoskeleton devices facilitates the repetitive movement of fingers and reinforces neurological pathways to help patient recovery. In order to encourage continued patient motivations during the repetitive treatment process, the devices require the quantifiable feedback on user performances. Although a wide variety of hand rehabilitation devices is available in the market, there are some limitations for improvement in these devices to meet patients' needs. When developing a rehabilitation device, it is important to consider requirements of end users as follows.

Effectiveness: The device should be effective in helping the user achieve their rehabilitation goals. This means that it should be developed with specific exercises or activities that will help users improve their hand function, strength, or range of motion.

Ease of use: The device should be easy for use. It should be intuitive and not require a lot of training or complicated setup. Ideally, the device should be able to fit users' hand comfortably and be easy to put on and take off.

Adjustability: The device should be adjustable to accommodate users' changing needs as they progress through their rehabilitation program, such as adjustable straps, tension settings, or other customizable features.

Comfort: The device should be comfortable for users to wear or use, such as factors of the size and shape of user's hand, materials used in the device, and any padding or support needed for user's comfort.

Safety: The device should be designed with safety, without causing any harm or discomfort to the user, and building with high-quality materials to not break or wear down over time.

Portability: The device should be portable so that the user can use it at home, work, or while traveling, such as a compact design or the ability to easily disassemble and reassemble the device.

Feedback: The device should provide feedback to the user, such as measuring progress and feedback on performance, such as using sensors or other tracking technologies in the device to provide this information.

Affordability: The device should be affordable for the end user, considering the cost of materials and manufacturing of the device.

Repeated treatment tasks need quantified feedback on the user performance for motivation to continue. (There is a large number of hand rehabilitation devices in the market. Advances in wearable rehabilitation systems have enhanced their role as assistive devices. However, their operations still have limitations in meeting user needs. For example, according to findings of user perceptions for existing wearable rehabilitation devices and improvements [170], it is expected to reduce the system assistance in applications. Also, the portability and easiness of operations are essential factors for users. It has been found that setting up process of current rehabilitation systems in the market is time-consuming. The interface of current systems is not user-friendly. Also, the rehabilitation system should be customizable to different hand sizes. In this case study, customer requirements and their weights are collected from literature [171]. Figure 4-3 shows a HOQ of the design problem. Its left column shows customer requirements with their weights. In order to meet these requirements and quantify quality characteristics of design concepts, 13 TMs are identified based on benchmarking products [172, 173]. The relationship matrix in the HOQ provides relations of customer requirements and TMs. Only this matrix is used to decide importance weights of TMs in the traditional HOQ template. However, there may be some TMs with close correlations to affect each other for the design solution. For example, the deriving method has a big impact on the device noise and motion velocity of the structure. It is not enough to decide TMs' weights based on TMs interactions with customer requirements only. It is therefore necessary to find interrelations of TMs using the correlation matrix in the roof of HOQ.

4.3.2 TMs importance weights based on different roof shapes

Two scenarios are investigated to compare with the traditional HOQ method. The first one uses the triangular shape roof of HOQ as shown in Figure 4-3 to form a symmetric initial correlation matrix. The second uses a square asymmetric correlation matrix as shown in Figure 4-4. After normalizing the initial data, total-influenced matrix T_c is formed for both cases. In matrix Tc, D and R are calculated by adding elements of each row and column in the matrix, respectively. Elements of each row (D) are added for each TM to find its effectiveness on other TMs. Elements of each column (R) are added for each TM to find the total effects (both direct and indirect) received from other factors, or effectiveness of variables. These parameters show effects of TMs on each other. Figure 4-5 shows prominence-causal relations of TMs obtained by the total influence-relation matrix Tc for both cases, where the horizontal vector (D+R) is amount of TM interactions. In other words, it shows amount of TM interactions and a central role of each TM. The vertical vector (D-R) indicates the effect power of each TM. Therefore, a positive (D-R) shows the causal parameter, otherwise, the parameter receives influence from other TMs. For the first scenario, as the initial matrix is symmetric, all of D-R values are zero, meaning that TMs have the same effect on each other. The horizontal axis however shows important TMs. For the second scenario, it can be concluded that the structure type has a big impact on other TMs, motion velocities and structure size have effects from other TMs.

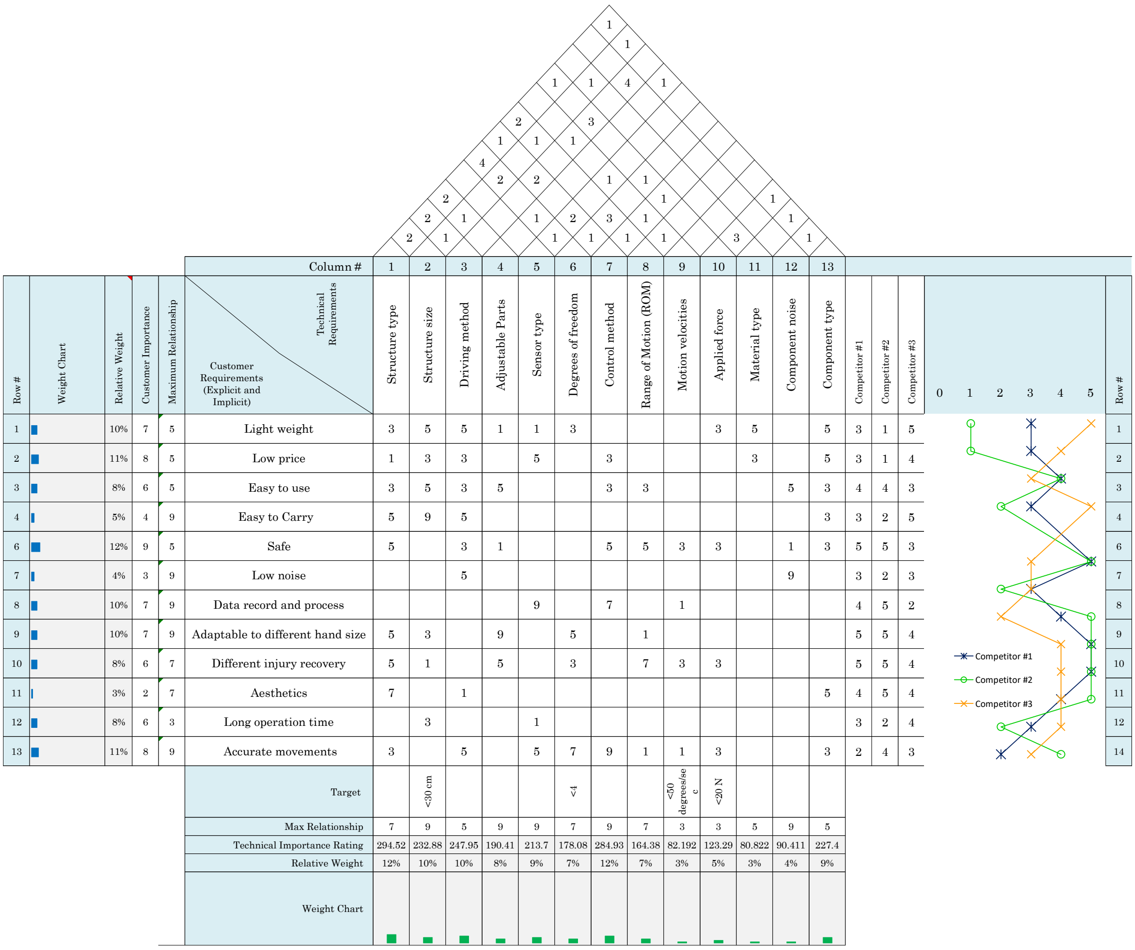

Figure 4-3 HOQ based on known customer requirements and TMs of hand rehabilitation devices.

4.4 Discussions and results

The unweighted super matrix is formed by normalizing and processing total-influenced matrix T_c. Figure 4-6 and Figure *4-7* show the unweighted super matrix for scenarios one and two. The influential weights are converged after four iterations for a stable matrix of TM importance weights. By using the proposed method, we can extract more information from correlations in the roof matrix and re-rank final weights of TMs. Table 4-1 compares TM weights based on the proposed method using the roof and the traditional approach without using the roof information. The result shows that some TMs' weights have changed compared to those generated by the traditional method. Attentions should be paid to these changes in design. For example, in scenario one, the weight of deriving method is increased to indicate its impact on other TMs like motion velocities, and the reduced weight of sensor type shows its weak interactions with other TMs. Although using the triangular shape correlation matrix can improve weighting methods based on the proposed method, the result obtained by the square shape correlation matrix is closer to reality as interactions of TMs correlations can be fully considered in two directions.

	Column #	1	2	3	4	5	6	7	8	9	10	11	12	13
Row #		Structure type	Structure size	Driving method	Adjustable Parts	Sensor type	Degrees of freedom	Control method	Range of Motion (ROM)	Applied velocities	Applied force	Material type	Component noise	Component type
1	Structure type	0	0.15	0.1	0.05	0	0.2	0.05	0.15	0.05	0.05	0	0	0.05
2	Structure size	0	0	0.1	0.05	0.05	0	0	0	0	0	0	0	0
3	Driving method	0.1	0	0	0	0	0	0.15	0.05	0.1	0.15	0.05	0.2	0.1
4	Adjustable Parts	0.15	0.1	0	0	0	0.05	0	0	0	0	0	0	0.05
5	Sensor type	0.1	0.05	0	0	0	0	0.15	0	0	0	0	0	0
6	Degrees of freedon	0.2	0.15	0	0.05	0.1	0	0.05	0.1	0	0.05	0	0	0
7	Control method	0.1	0	0.1	0	0.05	0	0	0.05	0.1	0.1	0	0	0.05
8	nge of Motion (RO	0.15	0.1	0.05	0	0	0.15	0.05	0	0.05	0	0	0	0
9	Applied velocities	0	0	0.05	0	0.05	0	0	0	0	0	0	0.05	0
10	Applied force	0.1	0	0.1	0	0	0.05	0.05	0	0	0	0.15	0	0.05
11	Material type	0	0.1	0	0	0	0	0	0	0	0.05	0	0	0.05
12	Component noise	0	0	0.2	0	0	0	0	0	0	0	0.05	0	0
13	Component type	0.1	0.15	0	0.05	0	0	0.05	0	0	0	0.05	0.05	0

Figure 4-4 Normalized square shaped correlation matrix.

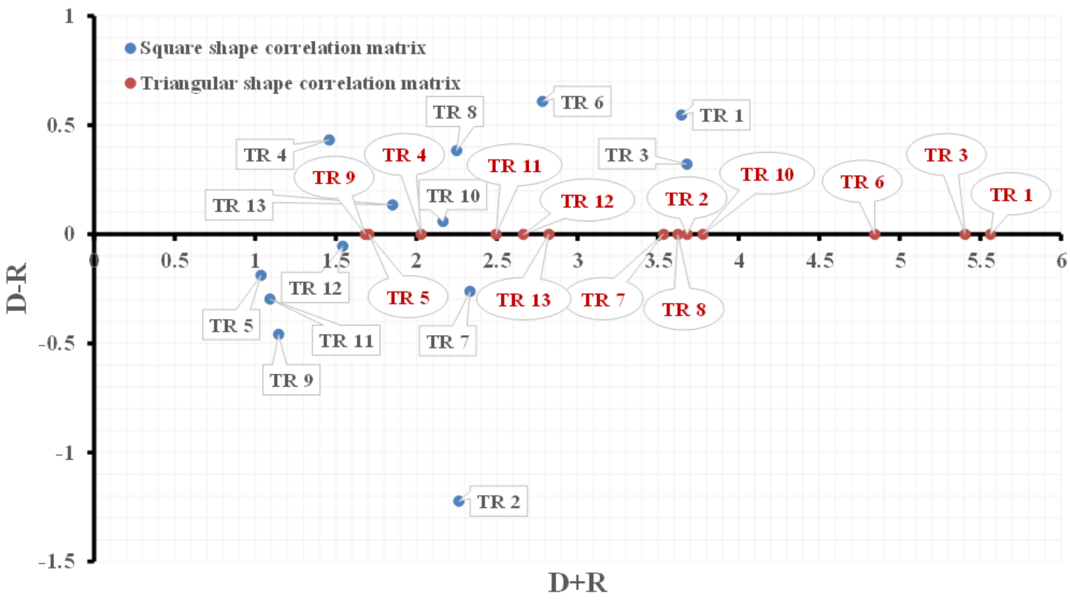

Figure 4-5 DEMATEL prominence-causal relationship of TMs.

	Column #	1	2	3	4	5	6	7	8	9	10	11	12	13
Row #		Structure type	Structure size	Driving method	Adjustable Parts	Sensor type	Degrees of freedom	Control method	Range of Motion (ROM)	Applied velocities	Applied force	Material type	Component noise	Component type
1	Structure type	0.10088	0.2075	0.12884	0.28199	0.20827	0.22451	0.16526	0.23564	0.07896	0.15297	0.07368	0.06312	0.17593
2	Structure size	0.10649	0.05735	0.0659	0.12772	0.1115	0.11933	0.04814	0.09462	0.03424	0.04756	0.10124	0.03502	0.09561
3	Driving method	0.08405	0.08377	0.07375	0.04906	0.05145	0.0502	0.13151	0.08458	0.16074	0.17605	0.14526	0.33131	0.11156
4	Adjustable Parts	0.08879	0.07836	0.02368	0.05082	0.03753	0.07176	0.02979	0.04236	0.01448	0.02803	0.01958	0.0147	0.08263
5	Sensor type	0.06807	0.07101	0.02578	0.03896	0.04469	0.068	0.11229	0.04017	0.12768	0.02602	0.01572	0.01553	0.02908
6	Degrees of freedom	0.13906	0.14402	0.04766	0.14116	0.12885	0.0793	0.09783	0.17936	0.04699	0.08659	0.03825	0.02379	0.05597
7	Control method	0.08106	0.046	0.09889	0.0464	0.16851	0.07747	0.05122	0.08409	0.14667	0.08438	0.0383	0.0476	0.08983
8	Range of Motion (ROM)	0.13021	0.10188	0.07164	0.07433	0.06791	0.16001	0.09473	0.07477	0.13876	0.0498	0.02951	0.03459	0.04931
9	Applied velocities	0.01591	0.01344	0.04965	0.00927	0.07871	0.01529	0.06025	0.0506	0.02951	0.01566	0.0139	0.09246	0.01486
10	Applied force	0.07566	0.04584	0.13349	0.04404	0.03938	0.06915	0.08509	0.04458	0.03844	0.06391	0.25864	0.06683	0.09882
11	Material type	0.02109	0.05648	0.06375	0.01781	0.01377	0.01768	0.02235	0.01529	0.01975	0.1497	0.05153	0.10257	0.07851
12	Component noise	0.01848	0.01997	0.14868	0.01367	0.01391	0.01124	0.02841	0.01833	0.13433	0.03955	0.10488	0.06771	0.07681
13	Component type	0.07024	0.07438	0.06828	0.10478	0.03552	0.03608	0.07312	0.03563	0.02944	0.07977	0.1095	0.10476	0.04107

Figure 4-6 Unweighted super matrix of the device of scenario one.

Row #	Column #	1	2	3	4	5	6	7	8	9	10	11	12	13
		Structure type	Structure size	Driving method	Adjustable Parts	Sensor type	Degrees of freedom	Control method	Range of Motion (ROM)	Applied velocities	Applied force	Material type	Component noise	Component type
1	Structure type	0.10192	0.27207	0.12953	0.2859	0.31041	0.2149	0.17368	0.20878	0.05912	0.1706	0.09049	0.065	0.19899
2	Structure size	0.14196	0.06365	0.04854	0.20918	0.17908	0.15531	0.05239	0.12502	0.02726	0.06495	0.34152	0.03278	0.23931
3	Driving method	0.09819	0.1777	0.06387	0.05238	0.06222	0.05135	0.14929	0.07891	0.2558	0.14276	0.05596	0.42431	0.06089
4	Adjustable Parts	0.05999	0.09079	0.0215	0.03582	0.0303	0.06496	0.02323	0.08967	0.00836	0.02201	0.02817	0.01115	0.08777
5	Sensor type	0.0237	0.07743	0.01181	0.02167	0.02036	0.07825	0.06569	0.02468	0.20456	0.01487	0.01793	0.00619	0.01807
6	Degrees of freedom	0.15325	0.05965	0.04054	0.12731	0.06344	0.06297	0.04624	0.14292	0.01614	0.09069	0.0262	0.02029	0.04395
7	Control method	0.06139	0.03339	0.06153	0.03126	0.14632	0.06607	0.03345	0.08997	0.02796	0.07987	0.02383	0.03035	0.08209
8	Range of Motion (ROM)	0.16426	0.07149	0.1039	0.07454	0.07359	0.17809	0.10307	0.06894	0.03502	0.05877	0.0251	0.05084	0.04899
9	Applied velocities	0.05898	0.03488	0.09217	0.02509	0.03644	0.03358	0.13622	0.09157	0.02903	0.03056	0.01251	0.04483	0.02429
10	Applied force	0.05378	0.03805	0.12171	0.02547	0.02978	0.05235	0.08269	0.02863	0.03739	0.03925	0.16324	0.06322	0.02417
11	Material type	0.01368	0.01491	0.06184	0.00961	0.00798	0.01002	0.02126	0.00863	0.02669	0.17264	0.03043	0.12867	0.07226
12	Component noise	0.02082	0.03247	0.15355	0.01346	0.01302	0.01084	0.03385	0.01798	0.24471	0.02859	0.01684	0.07458	0.07475
13	Component type	0.04805	0.03353	0.0895	0.08833	0.02705	0.02129	0.07895	0.02431	0.02796	0.08444	0.16779	0.04779	0.02446

Figure 4-7 Unweighted super matrix of the device of scenario two.

The modified weights can help designers to choose components and subsystems in a more accurate way in decision-making of the conceptual design. These weights can be used in a sequence of HOQs during the QFD process. For example, for selecting a structure type of the rehabilitation device, designers usually consider factors like the range of motion (ROM), degree of freedom (DOF) and component size. These factors can guide designers to select the right structure according to TMs rankings. Figure 4-8 shows three different structure solutions based on different importance weights using the traditional HOQ, triangle-shaped correlation matrix, and square-shaped correlation matrix, respectively.

In results of using the traditional HOQ, importance weights of the structure type and ROM of finger bones lead to a light finger structure as illustrated in Figure 4-8 (a). In Scenario 1 (Figure 4-8 (b)), the importance weight of ROM is increased for a heavier finger structure with more ROM. As shown in Table 4-1, importance weights of ROM and structure types are highest in Scenario 2, the device structure is improved to meet these requirements (Figure 4-8(c)). Comparing with structures in Figure 4-8 (a) and (b), this finger structure can cover more ROM, however, it increases the importance weight of structure. The finger structure is one of the components in hand rehabilitation devices and there are other components like actuator, motion sensors, etc. to be decided. The selection procedure should be processed similarly using HOQ to map TMs into components and the final concept in a QFD process.

Table 4-1 TMs importance weights based on the proposed and traditional methods.

	TR 1: Structure type	TR 2: Structure size	TR 3: Driving method	TR 4: Adjustable Parts	TR 5: Sensor type	TR 6: Degrees of freedom	TR 7: Control method	TR 8: Range of Motion (ROM)	TR 9: Motion velocities	TR 10: Applied force	TR 11: Material type	TR 12: Component noise	TR 13: Component type
Traditional HOQ	0.12216	0.09659	0.10284	0.07898	0.08864	0.07386	0.11818	0.06818	0.03409	0.05114	0.03352	0.0375	0.09432
Scenario 1 (triangle shape correlation matrix)	0.14642	0.08738	0.11593	0.06194	0.06682	0.08963	0.09439	0.07621	0.03245	0.06224	0.03828	0.04091	0.07601
Scenario 2 (square shape correlation matrix)	0.14757	0.1083	0.11465	0.06406	0.06316	0.07816	0.08517	0.08207	0.04436	0.05576	0.03694	0.04678	0.07302

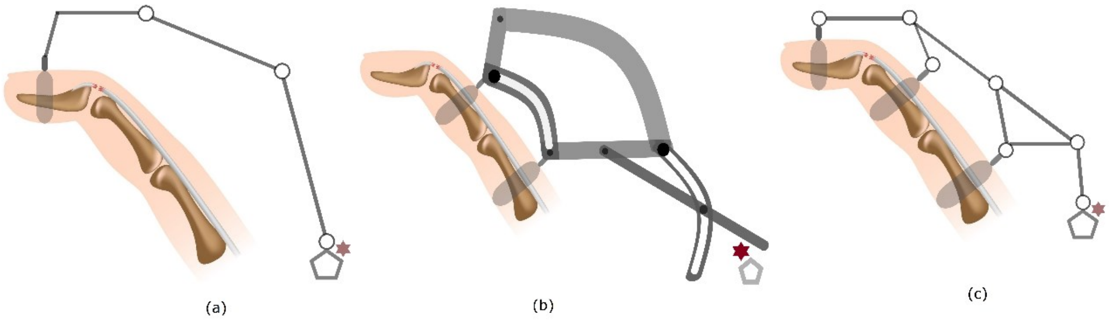

Figure 4-8 Different structures formed based on solutions of TM importance weights from (a) the traditional HOQ, (b) triangle-shaped correlation matrix, and (c) proposed square-shaped correlation matrix.

4.5 Summary

The prioritization of TMs is vital in the QFD process to maximize customer requirements for a competitive product. This chapter introduces an integrated approach of DEMATEL, ANP, and QFD methods for modeling TMs correlations in HOQ to decide TM's weights in product design. The method integrates the decision-making trial and evaluation laboratory (DEMATEL), ANP, and QFD to model interrelations of TMs. DEMATEL is used to understand the correlation and interdependence of TMs through analysis of TMs in cause-and-effect relations. The final weight of TMs is obtained from an ANP super-matrix. The main contribution of this method is the integration of a DEMATEL-based analytic network process with QFD to analyze data in the roof part of HOQ and decide final weights of TMs. It is also novel to literature in handling correlations in HOQ with DEAMETL to evaluate relations between TMs and establishing direct and indirect causal relationships and influence levels. Another contribution of this work is the DEMATEL-based analytic network process to efficiently model interrelations among TMs and remove time-consuming pairwise comparisons. It is identified that TMs interactions cannot be fully considered using the triangular shape correlation matrix in the traditional HOQ. A square roof of the HOQ template is proposed to model the influence and interdependence among TMs, which is neglected in the traditional QFD methods. One advantage of the proposed method is that it doesn't need the lengthy data process of pairwise comparisons. The method provides a systematic tool for analyzing interrelations among TMs via prominence-causal relationships. The case study of design for a hand rehabilitation device verifies the proposed method. It shows that the importance weights of TMs can be updated by considering correlations among the TMs in the roof part of HOQ. The method can be adjusted to solve other design problems for correlations of TMs. In this case study, customer requirements are assumed uncorrelated each other and they are mutually independent. The impact of correlations of customer requirements will be a subject for the future research. It is also recommended to use correlation values instead of conventional signs in HOQ templates.

Chapter 5 Improving Weighting Solution of Design Matrix Using Integrated Approaches

For applying the QFD process, designers need a reliable weighting approach to map different domains. Also, as different levels of HOQs are required to analyze the product life cycle, designers need an efficient method for the data collection and processing. In this chapter, approaches are proposed to improve the accuracy of HOQ in weighting TMs for design problems.

5.1 Best-Worst method (BWM)

One important task in HOQ is to determine relations between TMs and customer requirements. For a large-sized design problem, it can be considered as a multi-criteria decision analysis (MCDA) problem characterized by the following matrix.

$$D = \begin{array}{c} \\ \\ TM_1 \\ TM_2 \\ \vdots \\ TM_n \end{array} \begin{array}{c} \begin{array}{cccc} CR_1 & CR_2 & \dots & CR_m \end{array} \\ \begin{array}{cccc} (d_1 & d_2 & \dots & d_n) \end{array} \\ \begin{bmatrix} r_{11} & r_{12} & \dots & r_{1\mathrm{m}} \\ r_{21} & r_{22} & \dots & r_{2\mathrm{m}} \\ \vdots & \vdots & \ddots & \vdots \\ r_{\mathrm{n}1} & r_{\mathrm{n}2} & \dots & r_{nm} \end{bmatrix} \end{array} \tag{5-1}$$

In this matrix, the top row is a vector of CRs $\{CR_1 \quad CR_2 \quad \dots \quad CR_m\}$ used as criteria to score TMs $\{TM_1 \quad TM_2 \quad \dots \quad TM_n\}$ in the relationship matrix. r_{ij} represents scores of different TMs based on customer requirements. A common method to evaluate different TMs based on customer requirements weights $d_j(d_j \geq 0, \quad \sum_j d_j = 1)$ uses the weight additive function. A number of studies have proposed methods to assign values for r_{ij} in a relationship matrix of HOQ. Most of them use a full pairwise comparison which is a lengthy process and may lead to inconsistency of the comparison to meet customer requirements [174]. However, BWM applies vector-based comparisons to reduce the mentioned difficulties as shown in Figure 5-1. The proposed method in this research contains seven steps as shown in Table 5-1 to determine TM weights. Inputs are customer requirements to search TMs, and outputs are final weights of TMs. Details are as follows.

Step 1: Determining a set of TMs. A set of TMs that have the most effect on customer requirements and product performance is defined based on benchmarking of existing designs or designers' knowledge.

Step 2: Forming HOQ 1. This step maps CRs to TMs in a QFD process.

Step 3: Determining the best (most important) and worst (least important) TMs with respect to each CR.

Table 5-1 Proposed integrated approach to decide importance weights of TMs.

Algorithm 5-1

Input: Vector of CRs $CR = [CR_1, CR_2, \ldots, CR_m]_{1\times m}$, m is number of customer requirements.

Output: Final weights of TMs

Step 1: Determining a vector of TMs $TM = [TM_1, TM_2, \ldots, TM_n]_{1\times n}$ for each CR.

Step 2: Forming HOQ 1. //The same approach can be used for next HOQ

foreach $CR_1 \in CR$

Step 3: Determining the best and worst TM with respect to each CR.

Step 4: Specifying preference of the best TM over the other TMs.

$A_B = (a_{B1}, a_{B2}, \ldots, a_{Bn})$ //Calculate Best-to-Others vector

Step 5: Specifying the preference of all TMs over the worst TM.

$A_W = (a_{W1}, a_{W2}, \ldots, a_{Wn})$ //Calculate Others-to-Worst vector

Step 6: Finding the optimal r value in the relation matrix for CR_i.

$$\min \xi$$

$$s.t.$$

$$\left|\frac{r_B}{r_j} - a_{Bj}\right| \le \xi,\ for\ all\ j$$ //An optimization problem is formed

$$\left|\frac{r_j}{r_W} - a_{Wj}\right| \le \xi,\ for\ all\ j$$

$$\sum_j r_j = 1$$

$$r_j \ge 0 \quad for\ all\ j$$

Step 7: Checking $consistency\ ratio \le 0.1$ //Acceptable values are less than 0.1

end

Calculation of the importance weight of each TM

$$W_j = \sum_{i=1}^{m} d_i . r_{ij}$$

Normalizing importance weights.

$$W_j^n = \frac{W_j}{\sum_{j=1}^{n} W_j}$$

Step 4: Specifying preference of the best TM over the other TMs. The preference of the most important TM over all of the other TMs is indicated using a number of ranges from 1 to 9. In this scaling system, 1 means an equal degree of importance, while 9 indicates the best TM that is much more important compared to the TM in the comparison. The output of this step is a Best-to-Others vector:

$$A_B = (a_{B1}, a_{B2}, a_{Bj} \dots, a_{Bn}) \tag{5-2}$$

where a_{Bj} represents the preference of the best TM over TM_j.

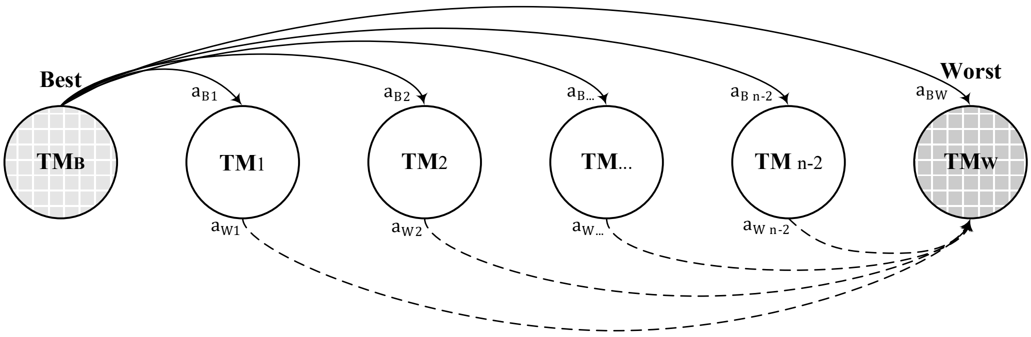

Figure 5-1 Comparisons in BWM.

Step 5: Specifying the preference of all TMs over the worst TM using a number of ranges from 1 to 9. Where 1 specifies an equal importance and 9 means that TM in the comparison is a lot more important than the least important TM. The output of this step is an Others-to-Worst vector:

$$A_W = (a_{W1}, a_{W2}, \dots, a_{Wn}) \tag{5-3}$$

Step 6: Finding the optimal r value in the relation matrix for CR_i. For each CR, a set of related TMs is identified. Relations between TMs and customer requirements are determined by using data available from Best-to-Others and Others-to-Worst vectors. Considering relations between CR_i and best TM, worst TM, and TM_j as r_B, r_W and r_j respectively, optimal r values for each TM can be obtained when $\frac{r_B}{r_j} = a_{Bj}$ and $\frac{r_j}{r_W} = a_{Wj}$ for each pair of $\frac{r_B}{r_j}$ and $\frac{r_j}{r_W}$. In order to satisfy this constraint, an optimization problem is defined where the maximum absolute difference of $\left|\frac{r_B}{r_j} - a_{Bj}\right|$ and $\left|\frac{r_j}{r_W} - a_{Wj}\right|$ for all TM_j is minimized. Considering the non-negativity and sum condition for the relation matrix in HOQ, following optimization problem can be formulated.

$$\min \max \left\{ \left| \frac{r_B}{r_j} - a_{Bj} \right|, \quad \left| \frac{r_j}{r_W} - a_{Wj} \right| \right\}$$
$$\text{subject to} \sum_j r_j = 1 \qquad (5\text{-}4)$$
$$r_j \geq 0 \quad for\ all\ j$$

Equation (5-4) can be changed into the following problem.

$$\min \xi$$
$$\text{subject to}$$
$$\left| \frac{r_B}{r_j} - a_{Bj} \right| \leq \xi, \qquad for\ all\ j$$
$$\left| \frac{r_j}{r_W} - a_{Wj} \right| \leq \xi, \qquad for\ all\ j \qquad (5\text{-}5)$$
$$\sum_j r_j = 1$$
$$r_j \geq 0 \quad for\ all\ j$$

Step 7: By solving the optimization problem in Equation (5-5), optimal values of the relation matrix in HOQ and ξ^* can be obtained. To determine relationship matrix values, for each CR (each row in relationship matrix), a weighting sub-problem as shown in Equation (5-5) is formed. In the proposed approach, only one pair of vectors is required for comparing TMs according to customer requirements.

Definition: A comparison is fully consistent when $a_{Bj} \times a_{Wj} = a_{BW}$, where $a_{Bj}, a_{Wj}\ and\ a_{BW}$ are preference of the best TM over the TM_j, preference of the TM_j over the worst TM, and preference of the best TM over the worst TM, respectively.

When $a_{Bj} \times a_{Wj}$ is lower or higher than a_{BW}, the consistency is decreased. In the case of inequality, ξ is defined as a parameter that should be added to a_{BW} and subtracted from a_{Wj} and a_{Bj} as follows.

$$(a_{Bj} - \xi) \times (a_{Wj} - \xi) = (a_{BW} + \xi) \qquad (5\text{-}6)$$

The minimum consistency occurs when a_{Bj}, a_{Wj} and a_{BW} have the same values. By considering this condition and solving Equation (5-5) for different a_{BW} values, the possible value of ξ can be obtained. Table 5-2 shows the possible Consistency Index (CI) values for different situations. Finally, the consistency ratio can be obtained by Equation (5-7) that shows the analysis accuracy. The value of consistency ratio closed to zero represents a minimal inconsistency of the analysis.

$$Consistency\ Ratio = \frac{\xi^*}{CI} \tag{5-7}$$

The consistency ratio is an index to determine whether the pairwise comparisons can generate close results or not to meet customer requirements. This factor uses Best-to-Others, Others-to-Worst and output weights vectors to check the solution being neither unreliable nor random in the pairwise comparisons. If this measure is lower than 0.10, the comparison is reliable. However, values higher than 0.10 represent a sign that the applied model is unable to generate reliable results. Furthermore, this index can be directly linked to the accuracy and effectiveness of the decision-making problem. A less consistency index value results in more accurate weights. The algorithm presented in Table 5-1 provides the BWM-QFD approach to complete the relationship matrix of HOQ. When a group of data is used, a normalized average value with a consistency index less than 0.1 can be applied.

Table 5-2 Consistency index (CI) for different a_{BW} values.

a_{BW}	1	2	3	4	5	6	7	8	9
Consistency Index (CI)	0.00	0.44	1.00	1.63	2.30	3.00	3.73	4.47	5.23

5.2 Full consistency method (FUCOM)

FUCOM like BWM forms an optimization model to decide optimal weight values while reducing inconsistency. FUCOM provides a measure to check and validate weights by determining deviations from the full consistency and error value. Comparing with BWM which considers one pair of comparison vectors, the FUCOM framework doesn't have this feature. Table 5-3 shows the proposed FUCOM method to determine the relationship matrix in following steps.

Step 1: $TMs = \{TM_1, TM_2, \dots, TM_n\}$ are ranked based on related customer requirements. The ranking starts from TM with the highest effect on CR to the least effect. The output of this step is a ranked TMs vector.

$$TM_{i\,(1)} > TM_{i\,(2)} > \cdots > TM_{i\,(k)} \quad , i = 1, \dots, m \tag{5-8}$$

where m is the number of customer requirements, and k is the rank of the observed TM.

Step 2: Forming HOQ 1. This step maps CRs to TMs in a QFD process.

Step 3: $\mathrm{TMs} = \{\mathrm{TM}_1, \mathrm{TM}_2, \dots, \mathrm{TM}_n\}$ are ranked based on related CR.

Step 4: The vector of the comparative priorities is formed as follows.

$$\beta = \left(\beta_{1/2}, \beta_{2/3}, \dots, \beta_{k/(k+1)}\right) \tag{5-9}$$

Table 5-3 Proposed integrated approach to decide importance weights of TMs.

Algorithm 5-2

Input: Vector of CRs $CR = [CR_1, CR_2, \dots, CR_m]_{1\times m}$, m is number of customer requirements.
Output: Final weights of TMs
1: Step 1: Determining a vector of TMs $TM = [TM_1, TM_2, \dots, TM_n]_{1\times n}$ for each CR.
2: Step 2: Forming HOQ 1. //The same approach can be used for next HOQ
3: foreach $CR_j \in CR$
4: Step 3: $TMs = \{TM_1, TM_2, \dots, TM_n\}$ are ranked based on related CR.
5: Step 4: vector of the comparative priorities is formed.
6: $\beta = \left(\beta_{1/2}, \beta_{2/3}, \dots, \beta_{k/(k+1)}\right)$ //a pairwise comparison of the TMs is determined
7: Step 5: forming an optimization problem to find TM weights related to CR.
8:

$$\begin{aligned} &\min \varphi \\ &\text{subject to} \\ &\left|\frac{r_{j(k)}}{r_{j(k+1)}} - \beta_{k/(k+1)}\right| \le \varphi \end{aligned}$$

//An optimization problem is formed

$$\begin{aligned} &\left|\frac{r_{j(k)}}{r_{j(k+2)}} - \beta_{k/(k+1)} \times \beta_{(k+1)/(k+2)}\right| \le \varphi \\ &\sum r_j = 1 \\ &r_j \ge 0 \quad for\ all\ j \end{aligned}$$

9: Step 6: Checking $deviation\ from\ full\ consistency\ \varphi \le 0.1$
10: end
11: Calculating importance weight of each TM

$$W_j = \sum_{i=1}^{m} d_i . r_{ij}$$

12: Normalizing importance weights.

$$W_j^n = \frac{W_j}{\sum_{j=1}^{n} W_j}$$

where k represents the rank of observed TMs. In the vector of the comparative priorities, $\beta_{k/(k+1)}$ is preference of TM_k compared to TM_{k+1}. Moreover, like BWM, TMs can be compared based on the most important TM. For example, in a design problem with five TMs ranked as $TM_4 > TM_1 > TM_5 > TM_2 > TM_3$ based on the designer preference, following priorities of TMs are determined.

$$\omega_{TM_4} = 1\,, \omega_{TM_1} = 2\,, \omega_{TM_5} = 4\,, \omega_{TM_2} = 5\,, \omega_{TM_3} = 7 \tag{5-10}$$

Since the first-ranked TM is compared with itself (its score is $\omega_{TM_4} = 1$). A vector of the comparative priorities can be calculated as $\beta_{TM_4/TM_1} = \frac{2}{1} = 2$, $\beta_{TM_1/TM_5} = \frac{4}{2} = 2$, $\beta_{TM_5/TM_2} = \frac{5}{4} = 1.25, and\ \beta_{TM_2/TM_3} = \frac{7}{5} = 1.4$.

Step 5: Forming an optimization problem to find TM weights related to CR. For the formed optimization problem, final values of TM weights are decided based on customer requirements in the relationship matrix. The optimization problem should satisfy following two constraints:

1) The ratio of weight coefficients is equal to the competitive priority among TMs as follows.

$$\frac{r_k}{r_{k+1}} = \beta_{k/(k+1)} \tag{5-11}$$

2) Like BWM, values of TM weights should satisfy the condition of the mathematical transitivity.

$$\beta_{k/(k+1)} \times \beta_{(k+1)/(k+2)} = \beta_{k/(k+2)} \tag{5-12}$$

As $\beta_{k/(k+1)} = \frac{r_k}{r_{k+1}}$ and $\beta_{(k+1)/(k+2)} = \frac{r_{k+1}}{r_{k+2}}$, then:

$$\frac{r_k}{r_{k+2}} = \beta_{k/(k+1)} \times \beta_{(k+1)/(k+2)} \tag{5-13}$$

Step 6: Checking deviation from full consistency $\varphi \leq 0.1$

The full consistency is achieved only if conditions one and two are satisfied and transitivity is fully respected. Based on the defined constraints, an optimization problem is formed as follows to find the optimal TMs weights while reducing deviations from full consistency φ.

$$\begin{aligned} &\min \varphi \\ &\text{subject to} \\ &\left|\frac{r_{j_{(k)}}}{r_{j_{(k+1)}}} - \beta_{k/(k+1)}\right| \leq \varphi \\ &\left|\frac{r_{j_{(k)}}}{r_{j_{(k+2)}}} - \beta_{k/(k+1)} \times \beta_{(k+1)/(k+2)}\right| \leq \varphi \\ &\sum r_j = 1 \\ &r_j \geq 0 \quad for\ all\ j \end{aligned} \tag{5-14}$$

where $j = 1, \dots, m$ represent desired customer requirements in forming the optimization problem. The above optimization problem should be solved for all customer requirements to form the relationship matrix.

5.3 Case study

The case study used in Chapter 4 is further investigated. Methods presented in Table 5-1 and Table *5-3* are used in the process. Its first step determines the vector of TMs. Table *5-4* shows important features of existing hand rehabilitation devices. Reported devices of the hand rehabilitation vary widely in terms of the number of active degrees of freedom (DOF), range of motion of joints, actuation, sensing method, output force/ torque, etc. These parameters are generally used as TMs to address customer requirements in QFD. In order to meet customer requirements and quantify quality characteristics of design concepts, 15 TMs are identified based on benchmarking of existing products.

In order to form design concepts of the device, multiple integrated HOQs are required to map customer requirements to component levels. HOQ 1 starts with mapping customer requirements to TMs for performance parameters of the device. HOQ 2 is used for decision-making of suitable components of the device based on TMs weights. In this case study, HOQ 1 is focused, however the same approach can be extended to the entire QFD process. customer requirements are then mapped to TMs via HOQ as shown in Figure 5-2, where the left column shows customer requirements with their weights and the top row lists related TMs. A relationship matrix is used to map customer requirements to TMs. To compare the proposed method with the existing methods, it is assumed that customer requirements and their weights are identical. The objective is to assign accurate normalized values in the relationship matrix to decide TMs weights. In order to conduct comparison studies, TMs weights are decided based on BWM, FUCOM and AHP methods.

In the next step, for each CR, a group of effective TMs including the most important (Best) and least important (Worst) is identified. Each CR is related to some TMs in HOQ. Benchmarks of existing devices and available data in literature are used to select the most important and least important TMs for each CR. In Steps 4 and 5, Best-to-Others and Others-to-Worst vectors are determined for each CR. For example, Lightweight is one of the customer requirements affected by the structure, adjustable parts, degrees of freedom, applied force, material properties, power energy density, and number of components.

Table *5-5* shows the vector-based pairwise comparison for related TMs for Lightweight as a CR.

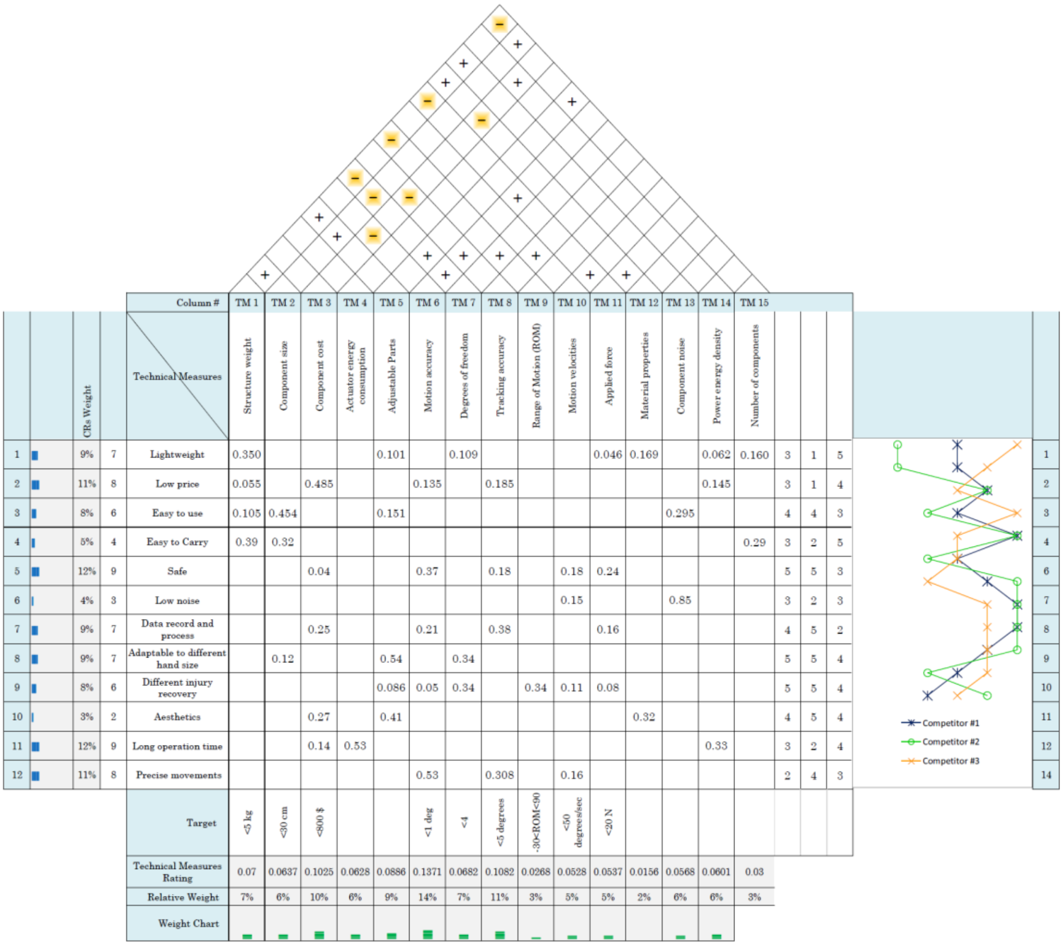

Figure 5-2 HOQ for mapping customer requirements to TMs for the device.

Best-to-Others and Others-to-Worst vectors are then used in Step 6 as inputs to find optimal values of the relationship matrix as outputs of the process. The objective of the optimization problem is improving accuracy of TMs importance weight ranking. The optimization process not only normalizes the relationship matrix, but also decides the best ranking of TMs. As an example, the optimization problem for data in

Table *5-5* is formed based on Equation (5-5) as follows.

$$
\begin{aligned}
&\min \xi \\
&\text{subject to} \\
&\left|\frac{r_B}{r_{TM5}} - 4\right| \leq \xi \qquad && \left|\frac{r_{TM1}}{r_W} - 9\right| \leq \xi \\
&\left|\frac{r_B}{r_{TM7}} - 4\right| \leq \xi && \left|\frac{r_{TM5}}{r_W} - 2\right| \leq \xi \\
&\left|\frac{r_B}{r_{TM11}} - 9\right| \leq \xi && \left|\frac{r_{TM7}}{r_W} - 2\right| \leq \xi \\
&\left|\frac{r_B}{r_{TM12}} - 3\right| \leq \xi && \left|\frac{r_{TM12}}{r_W} - 3\right| \leq \xi \\
&\left|\frac{r_B}{r_{TM14}} - 6\right| \leq \xi && \left|\frac{r_{TM14}}{r_W} - 2\right| \leq \xi \\
&\left|\frac{r_B}{r_{TM15}} - 3\right| \leq \xi && \left|\frac{r_{TM15}}{r_W} - 3\right| \leq \xi \\
&\sum_j r_j = 1 \\
&r_j \geq 0 \quad for\ all\ j
\end{aligned}
\tag{5-15}
$$

Table 5-4 Exoskeleton devices for the hand rehabilitation.

No.	System	Active DOF	Transmission	Actuation	Weight	Output force/ torque	Sensing method
1	HandSOME	1	Linkage	Passive	220 g	0–4 N m	-
2	CyberGrasp	4	Cable/linkage	Servo motor	450 g	12 N	Flex Sensor
3	HEXORR	2	Linkage	AC motor		22.6 N m	-
4	Hand of Hope	5	Cable /linkage	DC linear motors	700 g	-	EMG
5	HANDEXOS	5	Cable-crank slider	DC motor	270 g		-
6	Gloreha	5	Cable	DC motor	250 g	20 N	-
7	iHandRehab	8	Cable	DC motor	250 g	-	Force sensor
8	WaveFlex	1	Cable	DC motor	-	42 N	-
9	HWARD	3	Linkage	Pneumatic	-	15 N	-
10	Rutgers Master II	4	Linkage	Pneumatic	80 g	16.4 N	Hall effect

Table 5-5 Pairwise comparison vectors for the Best and Worst TM.

	TM 1	TM 5	TM 7	TM 11	TM 12	TM 14	TM 15
Best criterion: TM 1	1	4	4	9	3	6	3
Worst criterion: TM 11	9	2	2	1	3	2	3

The above optimization problem can be easily solved using conventional solvers like the simplex algorithm in linear programming or Sequential Quadratic Programming (SQP) in constrained nonlinear programing. The same procedure can be used for all customer requirements to complete the relationship matrix.

5.4 Results and discussion

After collecting required data and solving optimization problem in Equation (5-15), results generate $r_{TM1} = 0.35, r_{TM5} = 0.101$, $r_{TM7} = 0.109$, $r_{TM11} = 0.046, r_{TM12} = 0.169, r_{TM14} = 0.062$, and $r_{TM15} = 0.16$ as correlation values in the relationship matrix for Lightweight. As $a_{BW} = 9$, the consistency index of this TM can be obtained from Table 5-2 as 5.2. The consistency ratio is calculated as $\frac{0.046}{5.2} = 0.008$ which shows the accuracy in comparisons. In addition to the consistency ratio, the comparison approach of BWM and consistency relation $a_{Bj} \times a_{Wj} = a_{BW}$ are applied to measure the consistency of the comparisons and detect the possible source of low consistencies. Figure 5-3 shows variations of the consistency ratio with respect to different values of a_{Bj} and a_{Wj} ranging from 1 to 9 for one TM. In this figure, a_{Bj} represents the preference of the best TM over TM_j, and a_{Wj} is the preference of TM_j over the worst TM. As shown in Figure 5-3, changing values of a_{Bj} and a_{Wj} results in a relative change in ξ. The maximum value of ξ is recognized when both a_{Bj} and a_{Wj} are assigned the maximum value. However, the minimum value of ξ (shown with blue color) occurs when $a_{Bj} \times a_{Wj}$ is close to a_{BW} which is 9 in this example. Acceptable values of ξ are near optimal region under 0.1 in Figure 5-3. The structure of this comparison provides decision makers an easy approach to assign comparison values.

In addition, the above TMs ranking problem is implemented by the FUCOM approach. The final weights are obtained by solving the optimization problem. The output of this integrated approach is the importance weight of TMs. After completing

TMs comparison, Equation (5-5) or (5-14) can be solved for each CR. Calculated relation values are used in the relationship matrix of HOQ to rank the TMs. This problem is also studied using the integration of AHP and QFD. Table *5-6* shows the comparison of TMs weights based on the proposed approaches and classical method. The final weights are slightly different each other. Three measures, namely the number of pairwise comparisons, consistency ratio, and Total deviation (TD), are used to evaluate the performance of studied approaches as follows.

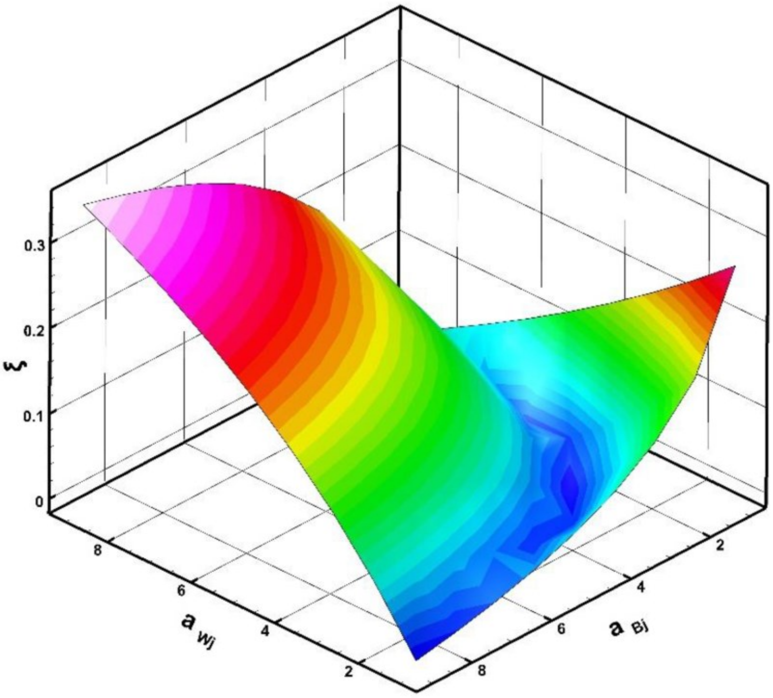

Figure 5-3 Variation of comparison consistency with the preference of the best TM over TM_j (a_{Bj}), and the preference of TM_j over the worst TM (a_{Wj}).

1) The number of required pairwise comparisons. For each CR, comparisons are required for related TMs. Similarly, TMs are mapped to selected components in the next step. Figure 5-4 compares a structure of the pairwise comparison for BWM and AHP approaches. Highlighted areas represent required data collections. If n is the number of related TMs for each CR, the number of required comparisons for each HOQ can be obtained based on the structure of different weighting methods as follows.

Table 5-6 Comparisons of TMs weights based on AHP-QFD and proposed approaches.

Column #	TM 1	TM 2	TM 3	TM 4	TM 5	TM 6	TM 7	TM 8	TM 9	TM 10	TM 11	TM 12	TM 13	TM 14	TM 15
TMs	Structure weight	Component size	Component cost	Actuator energy consumption	Adjustable Parts	Motion accuracy	Degrees of freedom	Tracking accuracy	Range of Motion (ROM)	Motion velocities	Applied force	Material properties	Component noise	Power energy density	Number of components
AHP	6.9 %	5.6 %	12.8 %	9.2 %	6.5 %	15.1 %	5.3 %	9.5 %	2.1 %	4.9 %	5.1 %	3.2 %	6.2 %	4.4 %	3.4 %
FUCOM	6.1 %	5.7 %	11.2 %	6.1 %	8.10 %	14.4 %	7.3 %	10.6 %	3.8 %	5.8 %	5.2 %	2.2 %	4.4 %	5.6 %	3.5 %
BWM	5.7 %	5.4 %	10.3 %	6.3 %	9.9 %	13.8 %	7.9 %	10.9 %	3.7 %	5.3 %	5.4 %	1.6 %	4.7 %	6.0 %	3.0 %

$$N_{BWM} = \sum_{i=1}^{CR_m} (2n-3)_{CR_i}, i = 1, \ldots, m \quad (5\text{-}16)$$

$$N_{FUCOM} = \sum_{i=1}^{CR_m} (n-1)_{CR_i}, i = 1, \ldots, m \quad (5\text{-}17)$$

$$N_{AHP} = \sum_{i=1}^{CR_m} (n\frac{n-1}{2})_{CR_i}, i = 1, \ldots, m \quad (5\text{-}18)$$

For each CR in HOQ, a separate weight allocation problem should be formed. In Equations (5-16) - (5-18), the number of pairwise comparisons can be calculated by summation of comparisons based on the structure of different weighting methods for m different customer requirements. As shown in Equation (5-18), in the AHP approach, N_{AHP} follows a nonlinear term which increases the number of comparisons exponentially. In this case study, while BWM requires 60 vector-based comparisons, FUCOM requires 36 comparisons, compared to 89 matrix-based comparisons in the AHP-QFD method. This is only for one HOQ completed for one expert ranking. The process for a large sized HOQ in real world problems can lead to an exponential increase in the number of required pairwise comparisons in the AHP-QFD approach.

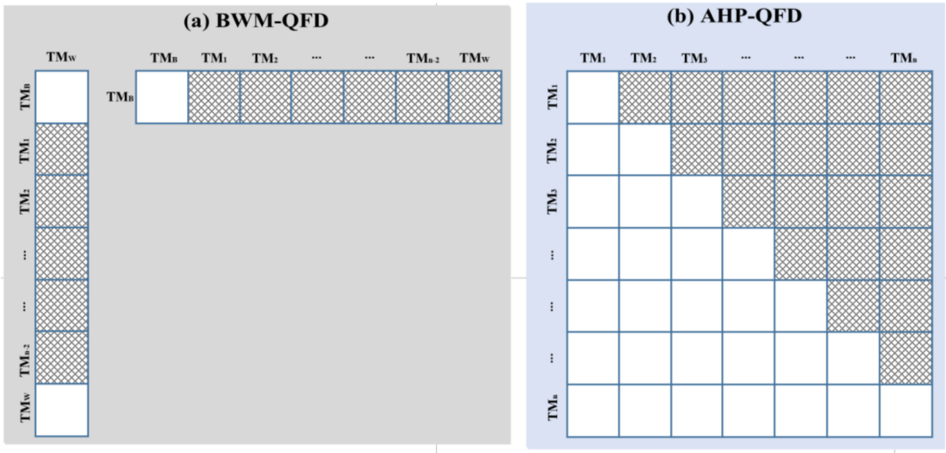

Figure 5-4 Structure of the matrix based pairwise comparison vs vector based pairwise comparison.

2) The consistency ratio of comparisons. As mentioned earlier, a consistency ratio is used to measure the accuracy of results to meet customer requirements. This factor shows the reliable evaluation. In all methods, numbers of customer requirements and TMs are the same. However, in determining relationship matrix values, for each CR (each row in the relationship matrix), a weighting sub-problem is formed. While in FUCOM and BWM approaches, one and two comparison vectors are required respectively to form the optimization problem, however, in the AHP-QFD approach, one square matrix is required for comparing TMs, which necessitates more comparisons that lead to more data collections. Comparing with the proposed approach, the matrix structure of pairwise comparisons in AHP may result in inconsistent outputs to meet customer requirements. In this matrix form, in order to find importance weights, TMs should be compared against each other in the order as depicted in the highlighted area in Figure 5-4 (b). Values in the diagonal area are equal to one. For example, if TM A compared to TM B has a numerical score of 4 and if TM B related to TM C has a numerical rating of 2, the perfect consistency of TM A compared to TM C would have a numerical rating of 8. If the A to C numerical rating allocated by the designer is higher or lower than 8, some inconsistency would happen in the comparison matrix. This common problem can be more challenging when designers have to deal with design problems with a large number of TMs where they

have to compare a group of TMs related to each other. However, in the proposed approach to form the relationship matrix, only one or two vectors of comparisons are required, which can increase accuracy of the process and reduce inconsistency in comparisons. Table 5-7 shows average values of the consistency ratio for different TMs in a HOQ based on studied approaches. The average value of the proposed approaches for BWM and FUCOM is 0.021 and 0.012, respectively, compared to 0.034 for the AHP-QFD approach. The less Consistency Ratio means the more accurate calculation. By applying the vector-based comparison of the proposed approaches, designers can determine relation values in complex situations of HOQs.

Table 5-7 Comparison of the proposed approach with AHP-QFD in three different measures.

	AHP-QFD	FUCOM -QFD	BWM -QFD
Number of pairwise caparisons	89	36	60
Consistency Ratio	0.034	0.012	0.021
Total Deviation (TD)	0.378	0.252	0.215

3) Performance of the total deviation. In order to measure the performance of the methods further, the total deviation is used. Obviously, the smaller the value of total deviation is, the better consensus is in decision-making. As shows in Equation (5-19), total deviation is the actual Euclidean distance between the calculated weight ratios $\frac{w_i}{w_j}$ and their related pairwise comparison value a_{ij}.

$$TD = \sum_i \sum_j \left(a_{ij} - \frac{W_i}{W_j} \right)^2 \tag{5-19}$$

The smaller total deviation values represent the closer weight ratios as a result the more accurate solutions. Table 5-7 compares the average value of total deviation for different customer requirements in a HOQ based on the proposed approaches and AHP-QFD. It shows that the total deviation value of the BWM-QFD is 0.215 compared to 0.252 and 0.378 for the FUCOM and AHP approaches, which illustrates the more accurate solution by the proposed approaches than AHP-QFD. The results show that the final weights of TMs are comparatively different from each other. The calculated weights can be used in the next step of a design process for selecting suitable components to satisfy function requirements. To achieve this goal, another HOQ can be formed in the QFD process to use TM's weights as criteria in decision-making and mapping process. The selection procedure should be processed similarly using HOQ to map TMs into component levels and the final concept in a QFD process. In the component selection stage, a near optimal configuration of the system can be formed. The configuration consists of different components for each function of the device. Different TMs weights can lead to different design solutions. For example, for selecting a structure type of the rehabilitation device, designers usually consider factors like the range of motion (ROM), degree of freedom (DOF), compatibility with different hand size, etc. These factors can guide the selection of the right structure according to TMs weights. Table *5-6* shows the comparison of TMs weights based on the AHP-QFD and proposed approaches. It shows that weights of degrees of freedom and adjustable parts are much higher in the result of the proposed approach. After weighting TMs, a ranking approach like MABAC (Multi-Attributive Border Approximation Area Comparison) is used to rank decisions. Figure 5-5 and 5-6 display two different design solutions based on different importance weights using the AHP-QFD and BWM-QFD approaches, respectively. The importance weights play a key role in the part deployment for the QFD process. The resulted design concepts indicate the effect of TMs importance weights in the component selection phase of a QFD process.

In the result of the proposed approaches, high weights of adjustable parts and degrees of freedom, and the low weight of actuator energy consumption lead to a design solution with five degrees of freedom and the adjustable mechanism for different hand sizes. It uses five small linear actuators to provide independent movements for each finger. However, the more energy consumption of the device can lead to lower operation time. On the other hand, in the result of AHP-QFD, as weights of energy consumption and structure mass are higher, and the degree of freedom is lower, the generated concept uses two linear actuators with two independent degrees of freedom with longer operation time. The presented approach improves accuracy of the relationship matrix. The importance weighting method in the relationship matrix of HOQ can be used for TMs ranking and part deployment in the QFD process.

The Shannon information entropy describes the degree of disorder and system information. The entropy weight characterizes the relative intensity of coefficients in the competitive sense. Shannon entropy is mostly used for determining objective weights of customer requirements. But it may be difficult to form the relationship matrix of HOQ as limited data available for the entropy approach. However, in some design studies when enough data are available, objective and subjective weights can be combined. If we suppose the weight decided by the proposed approach and entropy as $W_s = w_1^s, w_2^s, \dots, w_n^s$ and $W_o = w_1^o, w_2^o, \dots, w_n^o$, respectively, the final weights of TMs can be obtained as follows.

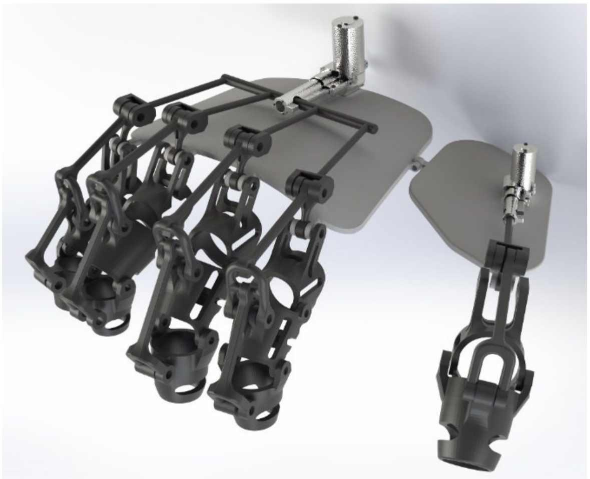

Figure 5-5 The device developed based on weights of the traditional approach.

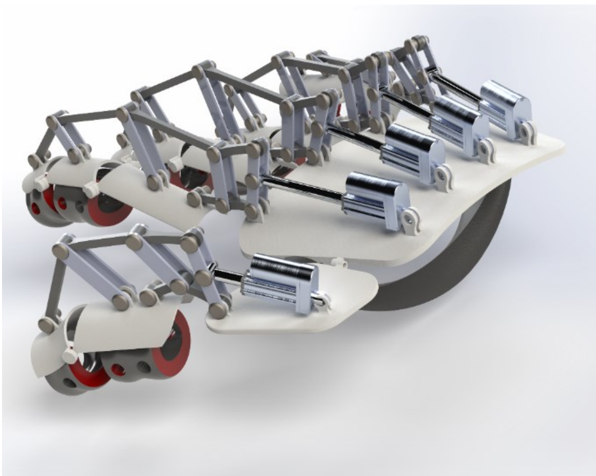

Figure 5-6 The device developed based on weights of the proposed approach.

$$W_j = \frac{w_j^s\, w_j^o}{\sum_{j=1}^{n} w_j^s\, w_j^o} \tag{5-20}$$

Equation (5-20) is useful in design studies where objective and subjective weight allocations are required.

5.5 Summary

In this chapter, two different approaches, BWM-QFD and FUCOM-QFD are proposed to model the relationship matrix of HOQ and improve its accuracy in weighting TMs for design problems where reliable and efficient data processing is required. The proposed approaches use pairwise comparison vectors to form optimization models for normalized relationship matrix values and consistency measures. The model performance and feasibility are demonstrated. The proposed methods not only reduce the data collection, but also improve inconsistency problems. They can be used to solve the relationship matrix weighting problem in HOQ. BWM searches relations between customer requirements and TMs based on a modified pairwise comparison of TMs with respect to the best and worst ones. The consistency ratio is used to measure the accuracy of the derived weights. Technically, FUCOM like BWM uses a vector based pairwise comparison and applies the mathematical transitivity to form an optimization model. The case study of designing the hand rehabilitation device shows advantages of the proposed method. Although both approaches work efficiently to reduce inconsistency issues in the relationship matrix of HOQ, they have some differences. BWM requires pairwise comparison vectors in the data collection, compared to FUCOM which only requires one vector that leads to a reduction in the number of comparisons. FUCOM provides a measure to check and validate weights by determining deviations from the full consistency and error value. Therefore, the BWM-QFD method is more suitable for design problems where the reliable weight allocation is important. On the other hand, FUCOM-QFD can be applied for the efficient weight allocation for large scaled HOQs as it requires less pairwise comparisons. Results of the proposed methods are compared with AHP-QFD considering the number of pairwise comparisons, which shows that the comparison tasks using the proposed methods are significantly less than the AHP-QFD method. The proposed model can obtain reliable TMs ranking in an efficient way that contributes to the decision-making in product design. Therefore, the proposed BWM-QFD and FUCOM-QFD approaches have following beneficial features.

- The vector-based approach requires less comparisons compared to matrix-based methods like AHP-QFD which requires a full pairwise comparison.
- The structure of the proposed approaches ensures the solution consistency to meet customer requirements in product design.

Like other subjective models to determine the weight of TMs, there is a subjective influence of designers' preference on values of TMs weights. However, results obtained by the proposed approaches have significantly less variations and inconsistencies. Although the input of HOQ is mostly based on human's subjective decision, there are some measures to prevent this issue during a decision-making process. The subjective problem is common in traditional approaches of product design. BWM-QFD and FUCOM-QFD approaches are proposed with the consistency ratio and total deviation measures to reduce this issue in decision-making.

Chapter 6 Generation and Evaluation of Product Concepts by Integrating Extended Axiomatic Design, Quality Function Deployment and Design Structure Matrix

A comprehensive method for the concept generation and evaluation is proposed based on benchmarks of existing solutions for different FRs to help designers work effectively in different design domains and rank generated design concepts. This chapter introduces the integrated customer-centric and domain mapping design approach to bridge gaps in existing methods in product concept development for customer satisfaction and design validation.

6.1 Method framework

6.1.1 Concept generation and evaluation

At the beginning of a design process, the FR domain is derived from the CR domain. The space of physical solutions has a wide dimension in mapping function requirements to design parameters. However, design constraints limit feasible solutions. Figure 6-1 shows the reduction of the solution space during the product development. The proposed integrated algorithm to generate, evaluate, and rank design concepts is shown in Figure 6-2 and Table 6-1, which provides guidelines to meet customer requirements and product performance attributes. Working steps shown in Figure 6-2 are as follows.

Step 1: This step translates customer requirements into a set of independent function requirements to satisfy the product function needs. The input is a set of customer requirements and their associated weights. Extended Axiomatic Design maps customer requirements domain to function requirements domain as follows.

$$\exists FR_i \subset \Omega: \rightarrow \lambda_{satisfy}\left(FR_i, CR_j\right) \tag{6-1}$$

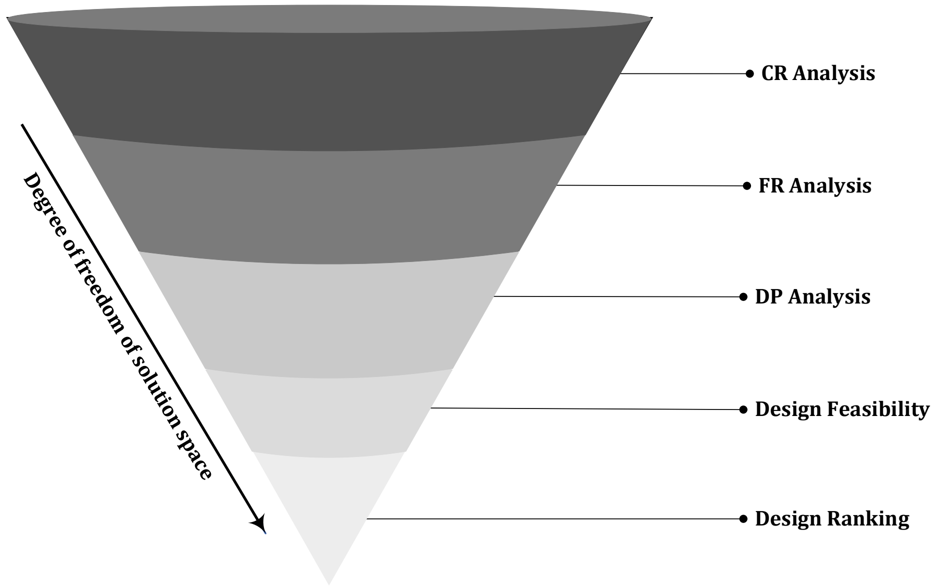

Figure 6-1 Reduction of the solution space during concept development.

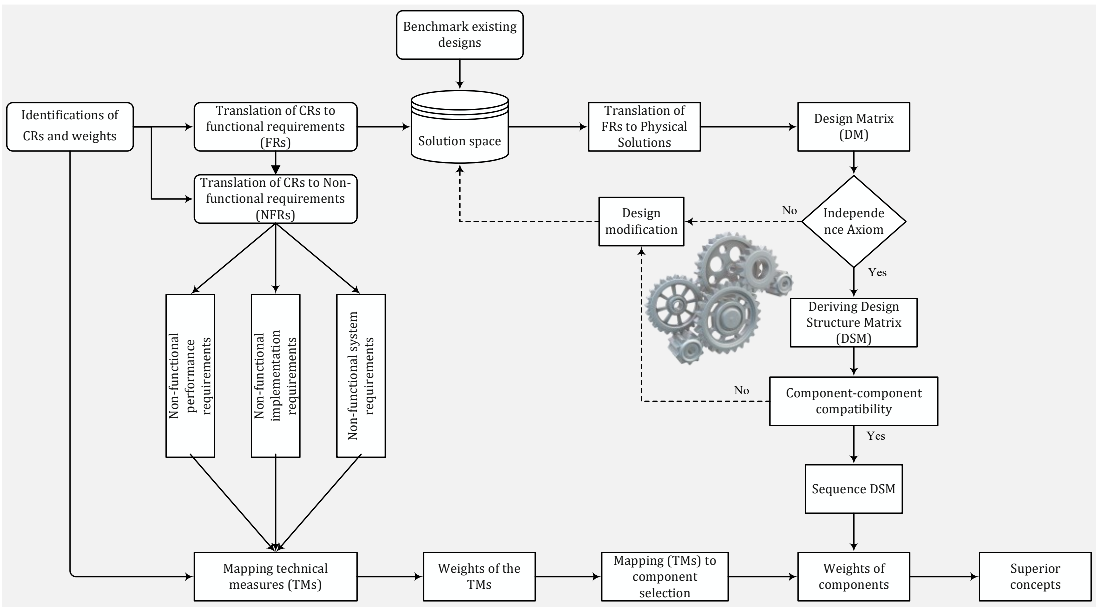

Figure 6-2 Proposed approach for generation and evaluation of design concepts.

where Ω is the function domain and $\lambda_{satisfy}$ specifies that FR_i can satisfy CR_j. Design requirements are classified into function requirements and non-functional requirements under design constraints. To fully satisfy customer requirements, the function decomposition may be needed. Non-functional requirements define nonbehavioral aspects of a product for attributes and constraints such as affordability and reliability under which the product works. Non-functional requirements can be classified into three groups [41]: Nonfunctional performance requirements to describe the level of performance of a specific function, nonfunctional system requirements to consider system or sub-system constraints, and nonfunctional implementation requirements associated with a specific solution to build a particular part of the product. In this step, a set of non-functional requirements is derived and considered as TMs in HOQ 1 to quantify and rank product attributes.

Table 6-1 The proposed integrated approach to generate, evaluate, and rank design concepts.

Algorithm 6-1

Input: Vector of CRs $CR = [CR_1, CR_2, \dots, CR_m]_{1\times m}$, m is number of customer requirements.

Output: Final ranking of feasible design concepts

Step 1: Mapping customer requirements into a set of independent function requirements.

$$\exists FR_i \subset \Omega: \rightarrow \lambda_{satisfy}(FR_i, CR_j)$$

Step 2: A solution space for each FR is completed based on benchmarking existing systems.

foreach design candidate $\in$ $design\ space$

Step 3: Mapping function requirements into physical solutions (DPs).

$$\exists DP_i \subset \Phi: \rightarrow \lambda_{satisfy}(DP_i, FR_j)$$

Step 4: Design matrix is formed to check independence axiom.

Step 5: DSM is derived from information available in design matrix.

$$T: DM \rightarrow DSM \quad or \quad DSM = T(DM)$$

Step 6: The derived DSM is evaluated.

$$DSM_{ij} = \frac{DP_i}{DP_j} \quad \forall\, i, j \in [1, 2, \dots, n]$$

Step 7: Forming HOQ 1.

Step 8: Forming HOQ 2, mapping TMs to DPs and development the vector of design attributes.

$$E_l = (\varepsilon_{l1}, \varepsilon_{l2}, \dots, \varepsilon_{ln})$$

Step 9: Development of the initial decision matrix (E).

Step 10: Normalizing the initial decision matrix (E).

$$E^n = \begin{array}{c} \\ E_1^n \\ E_2^n \\ \dots \\ E_q^n \end{array} \begin{array}{c} \begin{array}{cccc} TM_1 & TM_2 & \dots & TM_n \end{array} \\ \begin{bmatrix} \varepsilon_{11}^n & \varepsilon_{12}^n & \dots & \varepsilon_{1n}^n \\ \varepsilon_{21}^n & \varepsilon_{22}^n & \dots & \varepsilon_{2n}^n \\ \dots & \dots & \dots & \dots \\ \varepsilon_{q1}^n & \varepsilon_{q2}^n & \dots & \varepsilon_{qn}^n \end{bmatrix} \end{array}$$

Step 11: Calculating the weighted matrix (V).

$$v_{ij} = w_i^f \,.\, (\varepsilon_{ij}^n + 1)$$

Step 12: The Border Approximation Area vector H is formed.

$$h_i = \left(\prod_{j=1}^{q} v_{ij}\right)^{\frac{1}{q}}$$

Step 13: The distance of design solutions from the border approximation area is obtained.

$$D = V - H$$

Step 14: The final values for TMs functions are calculated.

$$\tilde{T}_i = \sum_{j=1}^{n} d_{ij}\,, \quad j = 1, 2, \dots, n\,, \quad i = 1, 2, \dots, q$$

end

Step 15: Final ranking of design solutions is determined using a defuzzification process for TMs functions.

Step 2: Existing systems are evaluated and decomposed to find a set of physical solutions for each functional requirement. Benchmarking is used to assess the competitiveness of existing products. A solution space for each function requirement is the output of this step.

Step 3: This step maps the set of function requirements into physical solutions. The input is a vector of function requirements, and the output is the design equation which shows the relations of function requirements and design parameters. It is a zigzag process to decompose the product in detail with physical solutions for each sub-function. Design matrix $[A]_{m\times n}$ for relations between product functions and physical solutions is formed using Equation (3-12) in Chapter 3. The mapping process is as follows.

$$\exists DP_i \subset \Phi\colon \rightarrow \lambda_{satisfy}\left(DP_i, FR_j\right) \tag{6-2}$$

where Φ represents the design parameters domain, $\lambda_{satisfy}$ specifies that DP_i can satisfy FR_j.

Step 4: Design matrix, Equation (3-12), is used to check the independence condition of the extended axiomatic design. This condition may not be applicable in some cases, especially for complex products with coupled sub-functions. However, a design solution with an independence axiom is easy to implement. Solutions with less coupled relations are more desirable in design. Design solutions can be modified to reduce dependencies. The output of Step 3 is a design matrix for evaluating the design quality to meet the independence axiom; however, it cannot guarantee the design feasibility from the DP requirement. For example, in the design of a vacuum machine, the function of circulating air can be met by using an electrical pump. However, the function model cannot show the way to link the electric pump to other components to meet the designed function. The next step forms a DSM from the design matrix to check the technical feasibility.

Step 5: As interactive relations between design parameters are unknown yet, it is difficult to directly form a DSM. This step forms a DSM based on the design matrix generated in Step 3. The DSM can be derived from information available in the design matrix by the following operation [42, 175].

$$T: DM \rightarrow DSM \quad or \quad DSM = T(DM) \tag{6-3}$$

where T is a conversion operator working as follows. (I) For each row of Design Matrix, it selects the dominant design parameter (X_0 in Design Matrix); (II) A composite matrix is constructed to describe relations between X_0 and related elements; (III) DSM is derived by transferring dominant design parameters on the diagonal and permuting the matrix. A hypothetical example of the design matrix with four function requirements and design parameters is shown in Figure 6-3. When the DSM is derived, the physical structure can be evaluated to check design feasibility and component compatibility.

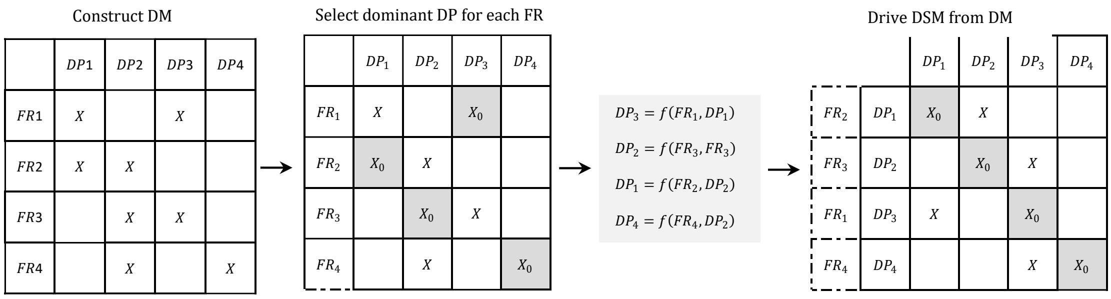

Figure 6-3 Deriving DSM from Design Matrix.

Step 6: The derived DSM is evaluated through the technical feasibility check. A design is technically feasible when a set of design parameters can satisfy all function requirements while their interactions do not violate laws of physics, their properties and constraints. The interaction between design parameters is as follows.

$$DSM_{ij} = \frac{DP_i}{DP_j} \quad \forall\, i, j \in [1,2, \dots, n] \tag{6-4}$$

After evaluation of the DSM and technical feasibility, the design concept is passed to the next stage for ranking feasible concepts. Otherwise, the solution is revised for a new design matrix and DSM. Figure 6-4 depicts different physical solutions that can lead to different design concepts. If there are m_1 possible design parameters for FR_1, m_2 design parameters for FR_2 and so on, there will be a total of $N = m_1 \times m_2 \times \dots \times m_n$ possible concept combinations. If there are many components and functions, the number of possible concept combinations is enormous.

Nevertheless, only a limited number of design solutions can satisfy function requirements and component-component compatibility. The evaluating design matrix and DSM can filter many infeasible concepts to reduce the solution search space.

6.2 Concept ranking

One of the requirements of multiple-criteria decision-making is the weight of design alternatives based on design criteria. The proposed approach uses two HOQs to determine design parameters weights based on their connections with customer requirements and TMs. Figure 6-5 shows the weighting process of design parameters based on relations of different domains. Based on obtained TMs weights from the output of HOQ 1, design alternatives can be ranked with respect to TMs in HOQ 2.

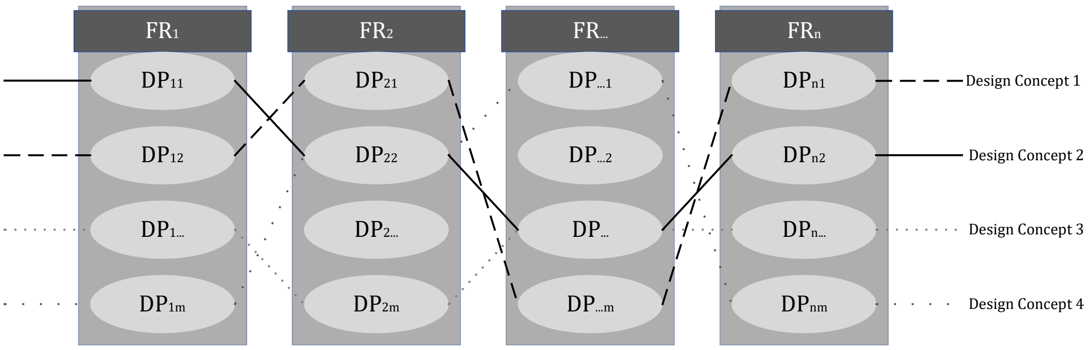

Figure 6-4 Different physical solutions lead to different design concepts.

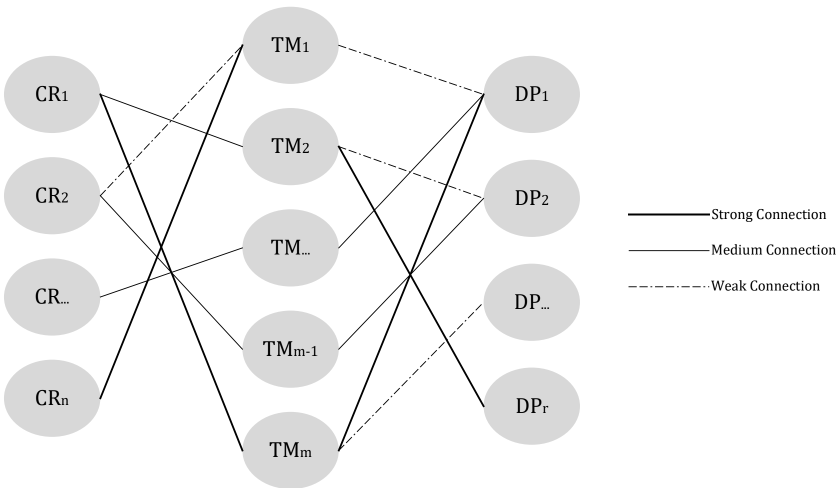

Figure 6-5 Weighting design parameters based on relations of different domains.

One of the requirements of the multiple-criteria decision-making approach is weighting matrix for criteria and alternatives. The proposed approach uses a HOQ to form a weighting matrix for design criteria and alternatives. However, classical forms of the relationship matrix are not accurate. Although the combination of QFD with weighting methods like AHP [69] and ANP can improve the relationship matrix, these methods need a great number of pair-wise comparisons to assign values for r_{ij} in a relationship matrix of HOQ [174]. The approach applies the QFD process in a fuzzy environment for uncertain decision variables.

Step 7: HOQ 1 is formed to map customer requirements into TMs. The inputs are customer requirements and their associated weights, and outputs are important weights of TMs. The linguistic variables shown in Figure 6-6 are used to model importance levels in the relationship matrix of HOQ 1.

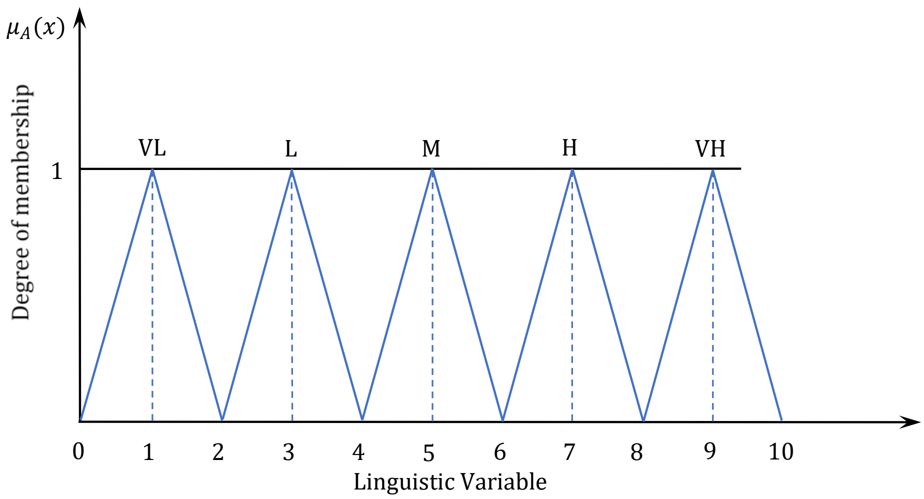

Figure 6-6 Linguistic representation to model relations in the HOQ.

Step 8: This step forms HOQ 2 to map TMs into design parameters. The same procedure in the previous step can be used to determine the weight of each design parameter based on TMs. The output of this step is relations between design parameters and TMs to rank product concepts. The relationship matrix in HOQ 2 is considered as the extended design equation to represent relations between non-functional requirements (TMs in HOQ) and design parameters. The score of each design concept related to TM_i is calculated using correlations between design parameters and TM_i by the following operation.

$$x_i = p_{i1} \oplus p_{i2} \oplus \ldots \oplus p_{ik} \tag{6-5}$$

The same approach is used for all TMs to form the vector of design attributes for design concept l.

$$E_l = (\varepsilon_{l1}, \varepsilon_{l2}, \ldots, \varepsilon_{ln}) \tag{6-6}$$

MABAC [176] is a method of the multiple-criteria decision-making. The basic assumption of this approach is the distance definition for alternatives from the border approximation area, which signifies the average value for all alternatives. In the proposed approach, the MABAC method is integrated with the QFD process to rank generated design alternatives in the fuzzy environment. Implementation of the fuzzy MABAC method is described in following steps.

Step 9. The input of this step is the vector of design attributes for each design concept, and the output is the development of the initial decision matrix (E) based on the evaluation of q design solutions according to n TMs (design criteria). The weighting vector of each design solution is obtained from the relationship matrix of HOQ 2. The initial decision matrix for q design candidates is formed as follows.

$$E = \begin{array}{c} \\ E_1 \\ E_2 \\ \dots \\ E_q \end{array} \begin{array}{c} \begin{array}{cccc} TM_1 & TM_2 & \dots & TM_n \end{array} \\ \begin{bmatrix} \varepsilon_{11} & \varepsilon_{12} & \dots & \varepsilon_{1n} \\ \varepsilon_{21} & \varepsilon_{22} & \dots & \varepsilon_{2n} \\ \dots & \dots & \dots & \dots \\ \varepsilon_{q1} & \varepsilon_{q2} & \dots & \varepsilon_{qn} \end{bmatrix} \end{array} \tag{6-7}$$

where ε_{ij} is the weight of design solution i with respect to criteria j represented by triangular fuzzy numbers, q specifies the number of the design solutions, and n is the number of TMs.

Step 10. This step normalizes the initial decision matrix (E) as follows.

$$\varepsilon_{ij}^{n} = \frac{\varepsilon_{ij} - \varepsilon_i^-}{\varepsilon_i^+ - \varepsilon_i^-} \tag{6-8}$$

where ε_{ij} is an element of the initial decision matrix (E). ε_i^+ and ε_i^- are as follows.

$\varepsilon_i^+ = max\left(\varepsilon_{1i_r}, \varepsilon_{2i_r}, \dots, \varepsilon_{qi_r}\right)$ is the highest weight of the right distribution of fuzzy numbers for TM_i in the initial decision matrix.

$\varepsilon_i^- = min\left(\varepsilon_{1i_l}, \varepsilon_{2i_l}, \dots, \varepsilon_{qi_l}\right)$ is the lowest weight of the left distribution of fuzzy numbers for TM_i in the initial decision matrix.

Elements of normalized initial decision matrix E^n are characterized as follows.

$$E^n = \begin{array}{c c} & \begin{array}{cccc} TM_1 & TM_2 & \dots & TM_n \end{array} \\ \begin{array}{c} E_1^n \\ E_2^n \\ \dots \\ E_q^n \end{array} & \begin{bmatrix} \varepsilon_{11}^n & \varepsilon_{12}^n & \dots & \varepsilon_{1n}^n \\ \varepsilon_{21}^n & \varepsilon_{22}^n & \dots & \varepsilon_{2n}^n \\ \dots & \dots & \dots & \dots \\ \varepsilon_{q1}^n & \varepsilon_{q2}^n & \dots & \varepsilon_{qn}^n \end{bmatrix} \end{array} \tag{6-9}$$

Step 11. The weighted matrix (V) is determined based on the normalized initial decision matrix E^n and weight coefficients of TMs obtained from HOQ 1. Members of the weighted matrix are as follows.

$$v_{ij} = w_i^f . (\varepsilon_{ij}^n + 1) \tag{6-10}$$

$$V = \begin{bmatrix} v_{11} & v_{12} & \dots & v_{1n} \\ v_{21} & v_{22} & \dots & v_{2n} \\ \dots & \dots & \dots & \dots \\ v_{q1} & v_{q2} & \dots & v_{qn} \end{bmatrix} = \begin{bmatrix} w_1^f . (\varepsilon_{11}^n + 1) & w_2^f . (\varepsilon_{12}^n + 1) & \dots & w_n^f . (\varepsilon_{1n}^n + 1) \\ w_1^f . (\varepsilon_{21}^n + 1) & w_2^f . (\varepsilon_{22}^n + 1) & \dots & w_n^f . (\varepsilon_{2n}^n + 1) \\ \dots & \dots & \dots & \dots \\ w_1^f . (\varepsilon_{q1}^n + 1) & w_2^f . (\varepsilon_{q2}^n + 1) & \dots & w_n^f . (\varepsilon_{qn}^n + 1) \end{bmatrix} \tag{6-11}$$

where w_n^f is an element of the final importance weight calculated in Chapter 3, q is the number of design solutions and n is the number of TMs.

Step 12. Elements of border approximation area vector H are calculated for each technical measure based on the weighted matrix (V) as follows.

$$h_i = \left(\prod_{j=1}^{q} v_{ij} \right)^{\frac{1}{q}} \tag{6-12}$$

where v_{ij} is an element of weighted matrix V, and q is the number of design solutions. If a design solution is above the border approximation area, its value will be positive and vice versa.

$$H = \begin{array}{cccc} TM_1 & TM_2 & \dots & TM_n \\ [h_1 & h_2 & \dots & h_n] \end{array} \tag{6-13}$$

Step 13. The distance of design solutions from the border approximation area is calculated as the difference between V and H. Distance d_{ij} of alternatives from H is determined as the difference between elements in V and values of H as follows.

$$D = V - H = \begin{bmatrix} v_{11} & v_{12} & \dots & v_{1n} \\ v_{21} & v_{22} & \dots & v_{2n} \\ \dots & \dots & \dots & \dots \\ v_{q1} & v_{q2} & \dots & v_{qn} \end{bmatrix} - \begin{bmatrix} h_1 & h_2 & \dots & h_n \\ h_1 & h_2 & \dots & h_n \\ \dots & \dots & \dots & \dots \\ h_1 & h_2 & \dots & h_n \end{bmatrix} = \begin{bmatrix} d_{11} & d_{12} & \dots & d_{1n} \\ d_{21} & d_{22} & \dots & d_{2n} \\ \dots & \dots & \dots & \dots \\ d_{q1} & d_{q2} & \dots & d_{qn} \end{bmatrix} \tag{6-14}$$

Each design solution S_i can be located in an upper approximation area H^+, lower approximation area H^-, or H based on its distance. The H^+ area contains more desirable solutions, while the H^- area includes less desirable solutions.

$$S_i \in \begin{cases} H^+ & if \quad d_{ij} > 0 \\ H & if \quad d_{ij} = 0 \\ H^- & if \quad d_{ij} < 0 \end{cases} \tag{6-15}$$

Comparing with other design candidates, a good design solution has much more TMs in the upper approximation area H^+.

Step 14. This step ranks design solutions based on the distance of each design solution from the border approximation area. Figure 6-7 shows different design solutions located in border approximation area regions. For each design solution, the value of TMs functions is determined as the sum of the distance of design solutions from border approximation areas. The final values for TMs functions T are calculated as a sum of elements of matrix D by rows.

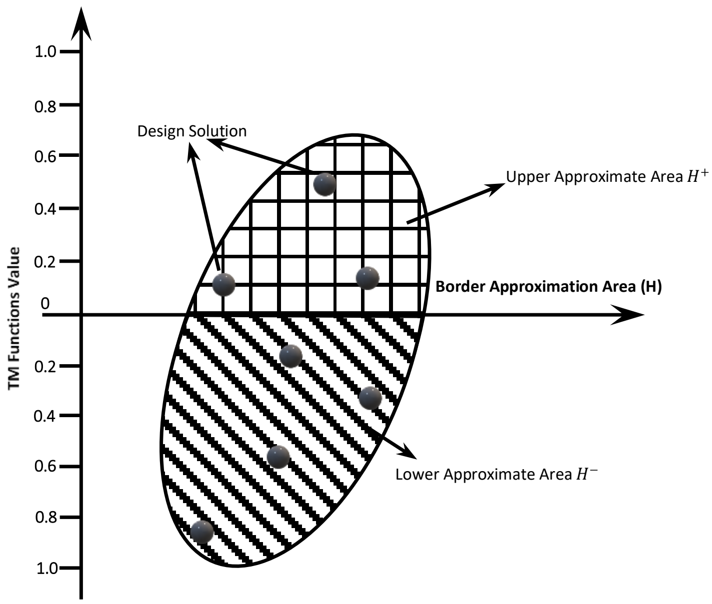

Figure 6-7 Border H, upper H^+, lower H^- approximation areas in MABAC.

$$\tilde{T}_i = \sum_{j=1}^{n} d_{ij}\,, \quad j = 1,2,\dots,n\,, \quad i = 1,2,\dots,q \tag{6-16}$$

where n is the number of TMs, q is the number of design solutions.

Step 15. The final ranking of design solutions is determined using a defuzzification process for obtained values of $\tilde{T}_i$. For a final operational step, it is essential to perform the defuzzification process of the fuzzy number to determine a crisp value. Equation (6-17) or (6-18) is used for the defuzzification.

$$\mathrm{T}_i = \frac{\alpha_i + 4\beta_i + \gamma_i}{6} \tag{6-17}$$

$$\mathrm{T}_i = \frac{[(\gamma_i - \alpha_i) + (\beta_i - \alpha_i)]}{3} + \alpha_i \tag{6-18}$$

where α_i and γ_i represent lower and upper bounds of fuzzy number $\tilde{T}_i$ respectively, and β_i is the modal value of $\tilde{T}_i$. The best design solution is the one that has the highest value.

6.3 Case study

The proposed method is applied in the concept generation and evaluation of a hand rehabilitation device design problem introduced in previous sections.

6.3.1 Problem description

While the overall functions of the current devices are favorable, as new haptic and sensing technologies emerge in shifting the market to digital rehabilitation, a new design is required for improving current devices in the sensing approach, data processing, and support structure. Figure 6-8 shows different design specifications for exoskeletons available in the market. A wide range of design parameters such as degrees of freedom, actuator type, number of actuators, type of mechanism, and materials properties should be considered when designing a hand rehabilitation device. The range of these specifications can be obtained by the benchmark analysis of existing devices and available data in the literature for hand exoskeleton devices.

6.3.1 Generation of design concepts

This case study collects customer requirements and their weights from literature [170-173, 177-182]. The method presented in Figure 6-2 is applied in the design process. The first step determines function requirements and a set of different TMs based on related customer requirements. Benchmarking products help to determine functional and physical domains for hand rehabilitation systems. Figure 6-9 shows different approaches and solutions for the physical domain in the design of a hand rehabilitation device. The hand rehabilitation device consists of mechanical, computer and electrical components. The mechanical components include the structure mechanism to support the hand for motion trajectories. The computer components include hardware and software to display, visualize and report treatment data. The electrical components provide energy to the system, sense motion data and control signal to actuators. Biofeedback sensors (e.g., electromyography, brain monitoring, pain sensors) can be used in conjunction with the exoskeleton to monitor the performance of treatments. Structure requirements define a kinematic chain of the mechanism. The number of DOFs, nature of motion, and driving approach are the most important parameters of the structure mechanism [172]. Figure 6-10 shows different exoskeleton finger structures to support hand movements. The torque and force are transmitted to the exoskeleton structure through the mechanical linkage, cable and crank slider.

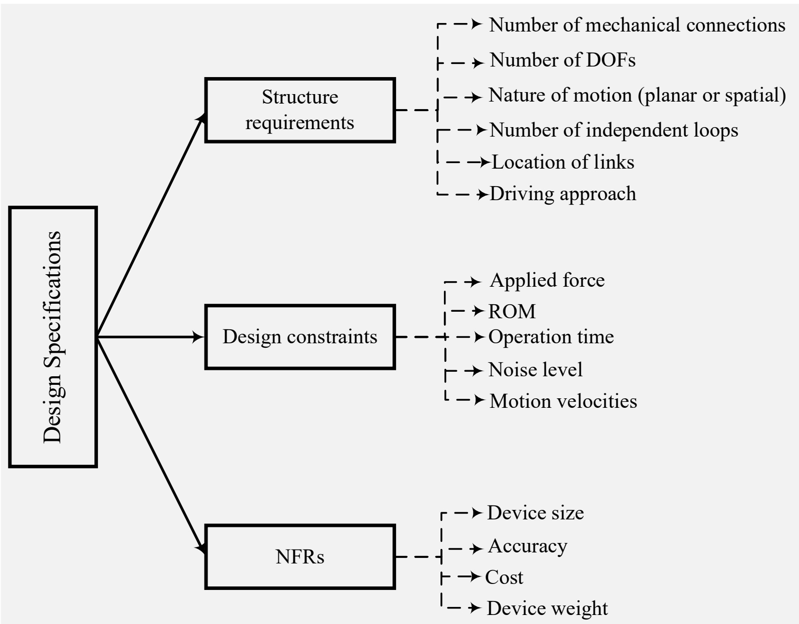

Figure 6-8 Design specifications for hand rehabilitation devices.

The proposed approach in Figure 6-2 is used to generate and evaluate rehabilitation device design concepts. The first step applies the extended Axiomatic Design to form the main function requirements level and establish a high-level mapping between function requirements and design parameters spaces. Step 2 forms the solution space, as shown in Figure 6-9, for each FR based on benchmarking. In Step 3, a set of function requirements is mapped to corresponding design parameters at each level of the design hierarchy. Each satisfying function requirement is decomposed into a set of sub function requirements at the next level of the design hierarchy. This process is repeated in a zigzag approach until all function requirements for the hand rehabilitation device are decomposed and satisfied, as shown in Figure 6-11.

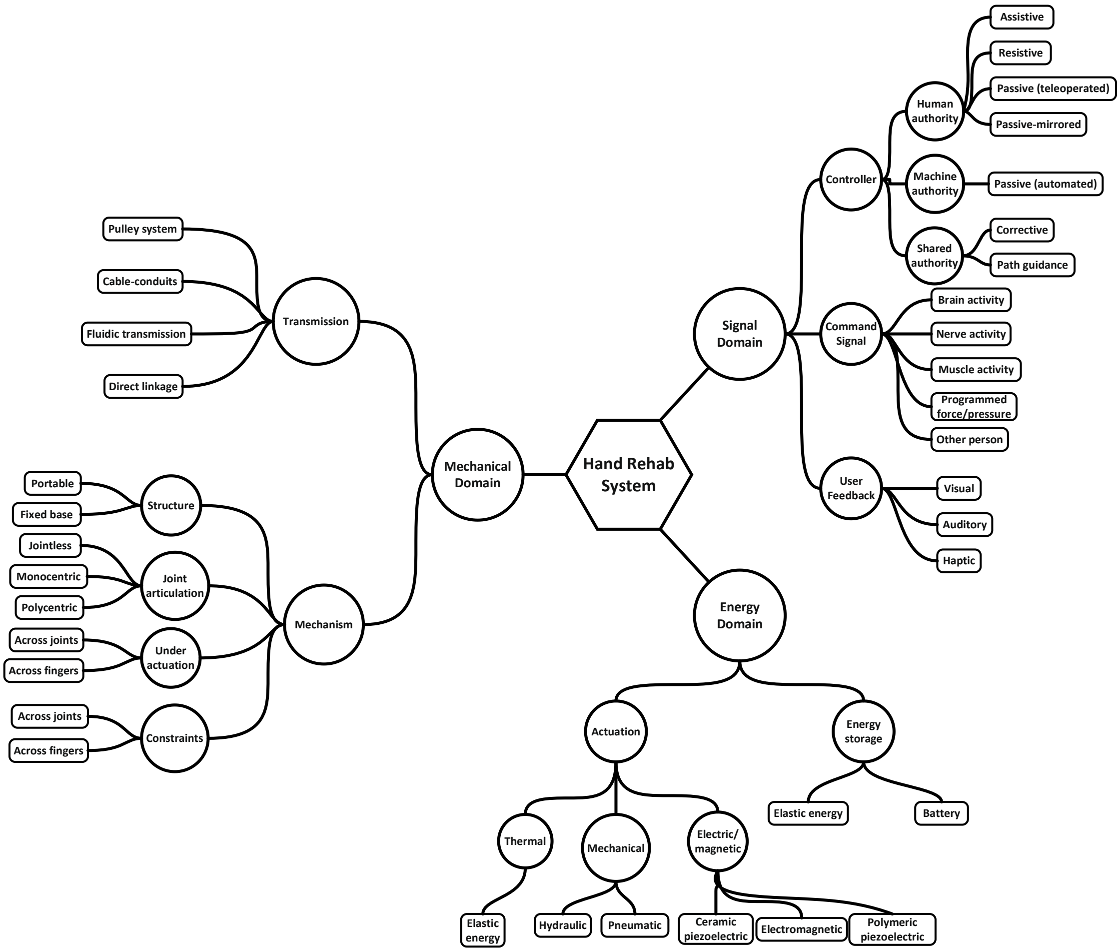

Figure 6-9 Different approaches for the physical domain in design of a hand rehabilitation device.

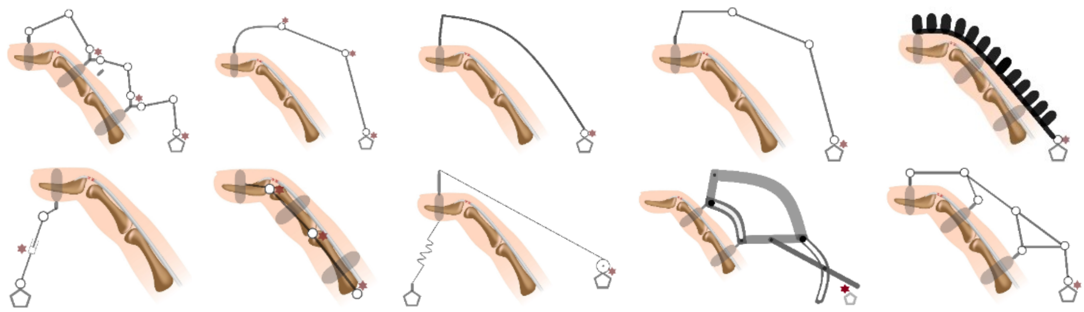

Figure 6-10 Different exoskeleton finger structures to support hand movements.

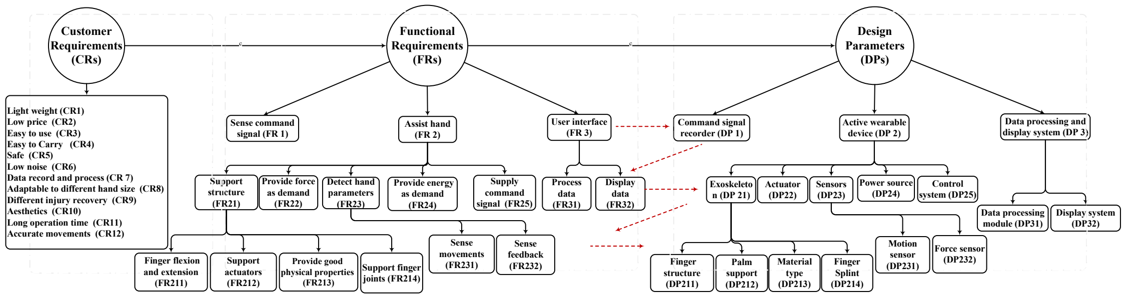

Figure 6-11 Domain mapping based on the functional decomposition of the hand rehabilitation device.

Based on the solution tree presented in Figure 6-9, different combinations of design parameters for function requirements can lead to different possible product concepts. From the possible 15000 design concepts, five different design concepts are selected based on the similarity of the available products in the market, as shown in Table 6-2. The selected design concepts are evaluated in detail for the concept ranking.

Table 6-2 Five design candidates developed based on the proposed approach.

	Candidate 1	**Candidate 2**	**Candidate 3**	**Candidate 4**	**Candidate 5**
DP 1	EMG sensor	Brain monitoring sensor	EMG sensor	EMG sensor	Brain monitoring sensor
DP211	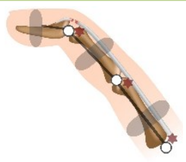	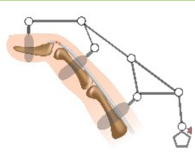	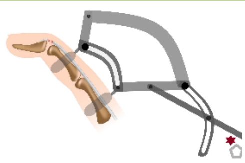		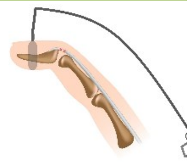
DP212	Palm support	Palm support	Palm support	Palm support	Palm support
DP213	Carbon fiber	Aluminum alloy	Polycarbonate	PLA	Aluminum alloy
DP22	Lithium polymer battery	Lithium-ion battery	Lithium-polymer battery	Lithium-polymer battery	Lithium-ion battery
DP23	Assistive-resistive	PID	Assistive-resistive	PID	PID
DP24	Electromagnetic	Pneumatic	Electromagnetic	Electromagnetic	Hydraulic
DP251	Flex sensor	Flex sensor	Vision sensor	Gyro sensor	Vision sensor
DP252	Capacitive load	Inductive load	Piezoelectric	Inductive load	Capacitive load
DP31	Data processing and user interface	Data processing and user interface	Data processing and user interface	Data processing and user interface	Data processing and user interface
DP32	VR module	AR module	VR module	2D display	2D display

6.3.2 Evaluation of design concepts

Different combinations of DPs can lead to potential design concepts. However, the challenging parts are feasibility study and ranking of the generated concepts. Concept validation can be performed by extended Axiomatic Design and Design Structure Matrix theories. Concept ranking is done according to the weight of DPs based on CRs weights calculated in a two steps QFD process. Therefore, changing CRs weights as inputs of the design method can lead to different weights for DPs and different design ranking results. In the case study of the rehabilitation device design, the structure of concepts can be formed by combining existing solutions for satisfying different FRs. In Step 4, solutions are searched to meet Axiom 1 and coupling relations based on hierarchies mapping relationships between function requirements and design parameters. For instance, relationships between function requirements and design parameters for design candidate 3 in Table 6-2 are as follows.

$$\begin{bmatrix} FR_1 \\ FR_{2_{1_1}} \\ FR_{2_{1_2}} \\ FR_{2_{1_3}} \\ FR_{2_{1_4}} \\ FR_{2_2} \\ FR_{2_3} \\ FR_{2_4} \\ FR_{2_{5_1}} \\ FR_{2_{5_2}} \\ FR_{3_1} \\ FR_{3_2} \end{bmatrix} = \begin{bmatrix} X & & & & & & & & & & & \\ & X & & & & & & & & & & \\ & & X & & & & & & & & & \\ & X & X & X & & & & & & & & \\ & & & & X & & & & & & & \\ & X & & & & X & & & & & & \\ & X & & & & & X & & & & & \\ & X & & & & & & X & & & & \\ X & & & & & X & X & X & X & & & \\ X & & & & & X & X & X & X & X & & \\ & & & & & & & & & X & X & \\ & & & & & & & & & & X & X \end{bmatrix} \begin{bmatrix} DP_1 \\ DP_{2_{1_1}} \\ DP_{2_{1_2}} \\ DP_{2_{1_3}} \\ DP_{2_{1_4}} \\ DP_{2_2} \\ DP_{2_{3_1}} \\ DP_{2_{3_2}} \\ DP_{2_4} \\ DP_{2_5} \\ DP_{3_1} \\ DP_{3_2} \end{bmatrix} \tag{6-19}$$

The next step uses the approach presented in Step 5 to derive a DSM based on information available in the design matrix for the generated design concepts. Deriving a DSM provides a useful tool to check component-component compatibility and relations between different sub-systems in a design concept. Infeasible design concepts can be filtered in Step 6. After generating a set of feasible concepts, the QFD process is applied to rank design alternatives based on design specifications and customer requirements. In Step 7, to meet customer requirements and quantify characteristics of design concepts, HOQ 1 is formed, and 15 TMs are identified based on benchmarking of existing products [172, 173, 177-181]. The linguistic variables and triangular fuzzy numbers shown in Figure 6-6 are used to model importance levels in the relationship matrix of HOQ 1. Figure 6-12 shows HOQ 1 for mapping customer requirements into TMs of the hand rehabilitation device. Different linguistic variables, such as very low, low, medium, high, and very high (VL, L, M, H, VH), represent correlations between customer requirements and TMs in the relationship matrix. After the importance weights of different TMs are determined, according to Step 8, HOQ 2 is formed to map TMs into different components (DPs) of the device. Each DP should satisfy the corresponding FR in the set of generated feasible concepts. However, to measure design quality with respect to different customer requirements, HOQ 2 is formed to indirectly map customer and physical domains. Figure 6-13 shows HOQ 2 for mapping TMs into DPs of the hand rehabilitation device.

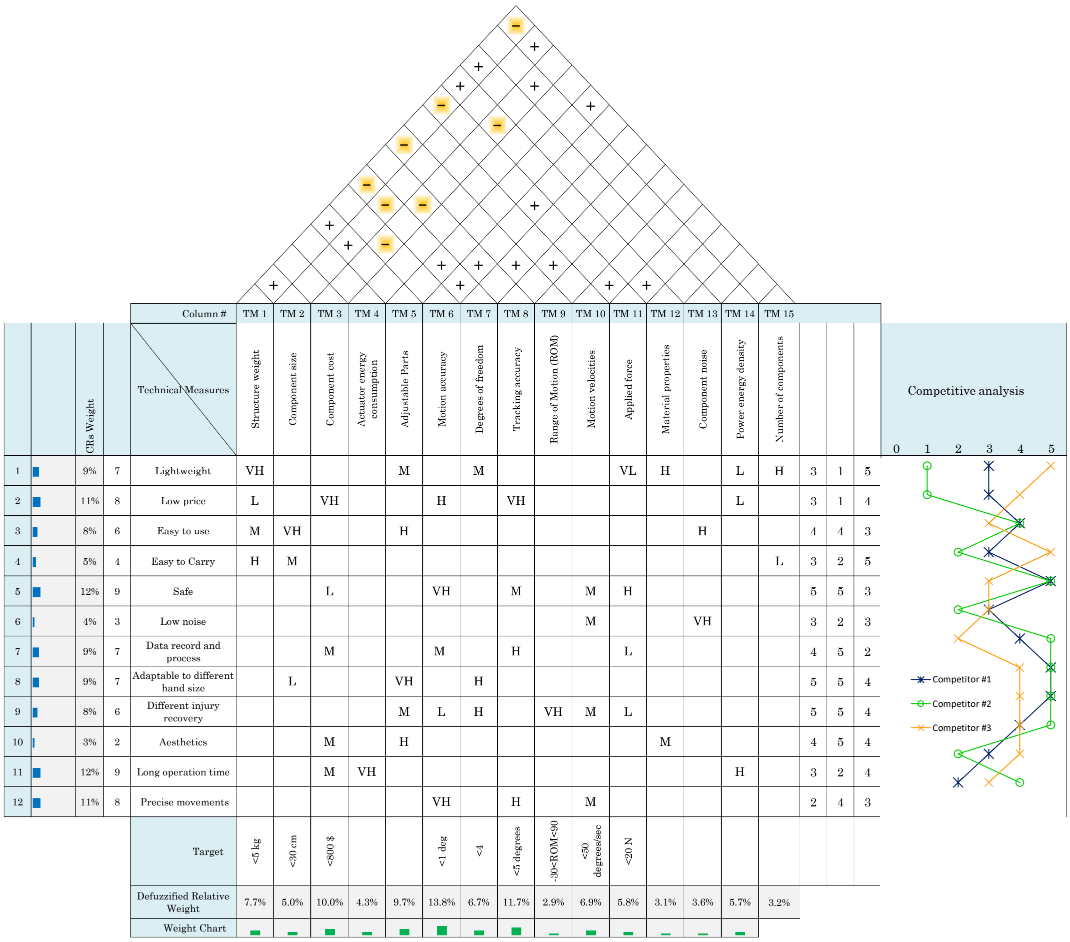

Figure 6-12 HOQ 1 for mapping customer requirements into TMs of the hand rehabilitation device.

TMs’ importance weights are obtained from HOQ 1 as triangular fuzzy numbers. Fuzzy membership functions are implemented to model relations between design parameters and each technical measure. Equation (6-5) is used to determine the score of each design concept related to TM_i. A vector of design attributes for design concepts is formed using Equation (6-6). The proposed fuzzy-QFD approach is used to form an initial decision matrix X for each design concept in Step 9. The initial decision matrix is formed based on Equation (6-7), as represented in Step 9 in Table 6-3. The next step normalizes the initial decision matrix X based on Equation (6-8), as shown in Step 10. Weighted matrix V is formed for each design candidate, as shown in Step 11 in Table 6-3. After obtaining V, the proposed Fuzzy-MABAC is used to rank design alternatives. Equation (6-12) forms border approximation area vector H in Step 12. In Step 13, the distance of design candidates from the border approximation area is determined and represented as Step 13 in Table 6-3.

					Column #	1	2	3	4	5	6	7	8	9	10	11	12	13
		Relative Weight				Design parameters (DPs)												
Row #	Weight Chart	α	β	γ	Technical Measures	Brain Activity	Finger Structure 3	Palm support	Aluminum Alloy	Finger Splint	Lithium-Ion Battery	PID	Hydraulic Actuator	Leap Motion	Capacitive load	Data processing module	Display Monitor	
1		6.3%	7.7%	9.0%	Structure weight	L	H	L	L	VL	VL		VL	L				
2		4.1%	5.0%	5.9%	Component size	VL	M				M		L				VL	
3		8.1%	10.0%	11.8%	Component cost	L	M		VL		L		M	L	L	M	M	
4		3.8%	4.3%	4.8%	Actuator energy consumption							L	VL					
5		8.2%	9.7%	11.2%	Adjustable Parts		VL	M		L								
6		11.8%	13.8%	15.8%	Motion accuracy	VL	VL					H	H					
7		5.6%	6.7%	7.7%	Degrees of freedom		L											
8		10.0%	11.7%	13.4%	Tracking accuracy									H	M			
9		2.5%	2.9%	3.2%	Range of Motion (ROM)		VL									M		
10		5.5%	6.9%	8.2%	Motion velocities							M				H		
11		4.2%	5.8%	7.3%	Applied force								VH		L	M		
12		2.6%	3.1%	3.6%	Material properties				M									
13		3.2%	3.6%	4.1%	Component noise								M					
14		4.4%	5.7%	7.0%	Power energy density						M							
15		2.6%	3.2%	3.8%	Number of components	L	VH						M	VH		M	L	

Figure 6-13 HOQ 2 for mapping TMs into design parameters of the hand rehabilitation device

Table 6-3 Different steps in the ranking process based on the Fuzzy-MABAC approach.

Step 9 - Development of the initial decision matrix (X)

	TM 1			TM 2			TM 3			TM 4			TM 5			TM 6			TM 7			TM 8		
Design candidate 1	1.01	1.84	2.87	0.74	1.15	1.66	2.28	3.69	5.44	0.38	0.51	0.67	0.49	0.87	1.34	2.84	3.87	5.07	0.34	0.47	0.62	0.8	1.17	1.61
Design candidate 2	0.76	1.53	2.51	0.66	1.05	1.54	2.44	3.89	5.68	0.15	0.26	0.38	0.99	1.46	2.01	1.89	2.77	3.8	0.34	0.47	0.62	0.8	1.17	1.61
Design candidate 3	1.27	2.14	3.23	0.82	1.25	1.77	2.6	4.09	5.91	0.38	0.51	0.67	1.15	1.65	2.24	3.07	4.15	5.39	0.34	0.47	0.62	1.2	1.64	2.15
Design candidate 4	1.27	2.14	3.23	0.66	1.05	1.54	2.44	3.89	5.68	0.3	0.43	0.57	0.49	0.87	1.34	2.13	3.04	4.12	0.22	0.33	0.46	0.4	0.7	1.07
Design candidate 5	0.89	1.68	2.69	0.41	0.75	1.18	1.95	3.29	4.97	0.08	0.17	0.29	0.49	0.87	1.34	1.42	2.21	3.17	0.11	0.2	0.31	1	1.41	1.88

	TM 9			TM 10			TM 11			TM 12			TM 13			TM 14			TM 15		
Design candidate 1	0.25	0.34	0.44	0.55	0.82	1.15	0.42	0.75	1.17	0.21	0.28	0.36	0.25	0.33	0.41	0.27	0.4	0.56	0.58	0.9	1.29
Design candidate 2	0.25	0.34	0.44	0.55	0.82	1.15	0.76	1.21	1.75	0.11	0.16	0.22	0.13	0.18	0.25	0.18	0.29	0.42	0.48	0.77	1.14
Design candidate 3	0.3	0.4	0.51	0.55	0.82	1.15	0.51	0.86	1.31	0.11	0.16	0.22	0.25	0.33	0.41	0.27	0.4	0.56	0.79	1.16	1.6
Design candidate 4	0.25	0.34	0.44	0.55	0.82	1.15	0.59	0.98	1.46	0.16	0.22	0.29	0.25	0.33	0.41	0.27	0.4	0.56	0.58	0.9	1.29
Design candidate 5	0.1	0.17	0.25	0.55	0.82	1.15	0.59	0.98	1.46	0.11	0.16	0.22	0.13	0.18	0.25	0.18	0.29	0.42	0.74	1.1	1.52

Step 10 - Normalized initial decision matrix

	TM 1			TM 2			TM 3			TM 4			TM 5			TM 6			TM 7			TM 8		
Design candidate 1	0.10	0.44	0.85	0.24	0.54	0.91	0.08	0.44	0.88	0.52	0.74	1.00	0.00	0.22	0.49	0.36	0.62	0.92	0.44	0.70	1.00	0.23	0.44	0.69
Design candidate 2	0.00	0.31	0.71	0.18	0.47	0.83	0.12	0.49	0.94	0.13	0.31	0.52	0.28	0.55	0.87	0.12	0.34	0.60	0.44	0.70	1.00	0.23	0.44	0.69
Design candidate 3	0.21	0.56	1.00	0.30	0.62	1.00	0.16	0.54	1.00	0.52	0.74	1.00	0.38	0.66	1.00	0.42	0.69	1.00	0.44	0.70	1.00	0.46	0.71	1.00
Design candidate 4	0.21	0.56	1.00	0.18	0.47	0.83	0.12	0.49	0.94	0.39	0.60	0.84	0.00	0.22	0.49	0.18	0.41	0.68	0.22	0.44	0.69	0.00	0.17	0.38
Design candidate 5	0.05	0.37	0.78	0.00	0.25	0.57	0.00	0.34	0.76	0.00	0.16	0.35	0.00	0.22	0.49	0.00	0.20	0.44	0.00	0.17	0.39	0.35	0.58	0.85
W		0.0766			0.0502			0.0998			0.0428			0.0971			0.1383			0.0665			0.1172	

	TM 9			TM 10			TM 11			TM 12			TM 13			TM 14			TM 15		
Design candidate 1	0.38	0.59	0.84	0.00	0.45	1.00	0.00	0.25	0.56	0.42	0.69	1.00	0.44	0.71	1.00	0.23	0.58	1.00	0.09	0.38	0.73
Design candidate 2	0.38	0.59	0.84	0.00	0.45	1.00	0.25	0.59	1.00	0.00	0.20	0.43	0.00	0.19	0.42	0.00	0.28	0.63	0.00	0.27	0.59
Design candidate 3	0.50	0.73	1.00	0.00	0.45	1.00	0.06	0.33	0.67	0.00	0.20	0.43	0.44	0.71	1.00	0.23	0.58	1.00	0.28	0.61	1.00
Design candidate 4	0.38	0.59	0.84	0.00	0.45	1.00	0.13	0.42	0.78	0.21	0.44	0.72	0.44	0.71	1.00	0.23	0.58	1.00	0.09	0.38	0.73
Design candidate 5	0.00	0.17	0.38	0.00	0.45	1.00	0.13	0.42	0.78	0.00	0.20	0.43	0.00	0.19	0.42	0.00	0.28	0.63	0.24	0.55	0.93
W		0.0285			0.0686			0.0576			0.0312			0.0364			0.0570			0.0322	

Step 11 - Weighted Normalized Matrix

	TM 1			TM 2			TM 3			TM 4			TM 5			TM 6			TM 7			TM 8		
Design candidate 1	0.084	0.110	0.142	0.062	0.077	0.096	0.108	0.144	0.188	0.065	0.074	0.086	0.097	0.118	0.144	0.188	0.224	0.266	0.096	0.113	0.133	0.144	0.169	0.198
Design candidate 2	0.077	0.100	0.131	0.059	0.074	0.092	0.112	0.149	0.194	0.048	0.056	0.065	0.125	0.151	0.182	0.155	0.185	0.221	0.096	0.113	0.133	0.144	0.169	0.198
Design candidate 3	0.092	0.119	0.153	0.065	0.081	0.100	0.116	0.154	0.200	0.065	0.074	0.086	0.134	0.162	0.194	0.196	0.234	0.277	0.096	0.113	0.133	0.171	0.201	0.234
Design candidate 4	0.092	0.119	0.153	0.059	0.074	0.092	0.112	0.149	0.194	0.059	0.068	0.079	0.097	0.118	0.144	0.163	0.195	0.232	0.081	0.096	0.113	0.117	0.138	0.162
Design candidate 5	0.080	0.105	0.136	0.050	0.063	0.079	0.100	0.134	0.176	0.043	0.050	0.058	0.097	0.118	0.144	0.138	0.166	0.199	0.067	0.078	0.092	0.158	0.185	0.216
Geometric Mean	0.08	0.11	0.14	0.06	0.07	0.09	0.11	0.15	0.19	0.06	0.06	0.07	0.11	0.13	0.16	0.17	0.2	0.24	0.09	0.1	0.12	0.15	0.17	0.2

	TM 9			TM 10			TM 11			TM 12			TM 13			TM 14			TM 15		
Design candidate 1	0.039	0.045	0.053	0.069	0.100	0.137	0.058	0.072	0.090	0.044	0.053	0.062	0.053	0.062	0.073	0.070	0.090	0.114	0.035	0.044	0.056
Design candidate 2	0.039	0.045	0.053	0.069	0.100	0.137	0.072	0.092	0.115	0.031	0.037	0.045	0.036	0.044	0.052	0.057	0.073	0.093	0.032	0.041	0.051
Design candidate 3	0.043	0.049	0.057	0.069	0.100	0.137	0.061	0.077	0.096	0.031	0.037	0.045	0.053	0.062	0.073	0.070	0.090	0.114	0.041	0.052	0.064
Design candidate 4	0.039	0.045	0.053	0.069	0.100	0.137	0.065	0.082	0.102	0.038	0.045	0.053	0.053	0.062	0.073	0.070	0.090	0.114	0.035	0.044	0.056
Design candidate 5	0.029	0.033	0.039	0.069	0.100	0.137	0.065	0.082	0.102	0.031	0.037	0.045	0.036	0.044	0.052	0.057	0.073	0.093	0.040	0.050	0.062
Geometric Mean	0.04	0.04	0.05	0.07	0.1	0.14	0.06	0.08	0.1	0.03	0.04	0.05	0.05	0.05	0.06	0.06	0.08	0.11	0.04	0.05	0.06

Step 13 - Distance from the Border Approximate Area (Q)

	TM 1			TM 2			TM 3			TM 4			TM 5			TM 6			TM 7			TM 8		
Design candidate 1	-0.058	-0.001	0.057	-0.029	0.004	0.037	-0.082	-0.002	0.078	-0.009	0.011	0.030	-0.063	-0.014	0.036	-0.050	0.025	0.099	-0.024	0.012	0.047	-0.056	-0.002	0.053
Design candidate 2	-0.066	-0.010	0.046	-0.032	0.000	0.033	-0.078	0.003	0.084	-0.025	-0.008	0.010	-0.036	0.019	0.073	-0.083	-0.014	0.055	-0.024	0.012	0.047	-0.056	-0.002	0.053
Design candidate 3	-0.051	0.009	0.068	-0.026	0.008	0.041	-0.074	0.008	0.090	-0.009	0.011	0.030	-0.027	0.029	0.085	-0.041	0.034	0.110	-0.024	0.012	0.047	-0.029	0.030	0.089
Design candidate 4	-0.051	0.009	0.068	-0.032	0.000	0.033	-0.078	0.003	0.084	-0.014	0.005	0.023	-0.063	-0.014	0.036	-0.074	-0.004	0.066	-0.038	-0.006	0.026	-0.083	-0.033	0.017
Design candidate 5	-0.062	-0.005	0.051	-0.041	-0.011	0.020	-0.090	-0.012	0.066	-0.031	-0.014	0.003	-0.063	-0.014	0.036	-0.099	-0.033	0.033	-0.053	-0.024	0.006	-0.043	0.014	0.071

	TM 9			TM 10			TM 11			TM 12			TM 13			TM 14			TM 15		
Design candidate 1	-0.011	0.002	0.015	-0.069	0.000	0.069	-0.043	-0.009	0.026	-0.005	0.011	0.028	-0.011	0.008	0.027	-0.035	0.007	0.049	-0.022	-0.002	0.019
Design candidate 2	-0.011	0.002	0.015	-0.069	0.000	0.069	-0.029	0.011	0.051	-0.018	-0.004	0.010	-0.027	-0.010	0.006	-0.048	-0.010	0.028	-0.025	-0.005	0.015
Design candidate 3	-0.008	0.006	0.020	-0.069	0.000	0.069	-0.040	-0.004	0.032	-0.018	-0.004	0.010	-0.011	0.008	0.027	-0.035	0.007	0.049	-0.016	0.006	0.028
Design candidate 4	-0.011	0.002	0.015	-0.069	0.000	0.069	-0.036	0.001	0.038	-0.012	0.003	0.019	-0.011	0.008	0.027	-0.035	0.007	0.049	-0.022	-0.002	0.019
Design candidate 5	-0.022	-0.010	0.002	-0.069	0.000	0.069	-0.036	0.001	0.038	-0.018	-0.004	0.010	-0.027	-0.010	0.006	-0.048	-0.010	0.028	-0.018	0.004	0.026

Step 14 uses Equation (6-16) to rank design candidates. For each design solution, the value of TMs functions is determined as the sum of the distance of design solutions from border approximation areas. In Step 15, the final ranking of design solutions is determined using a defuzzification process for obtained values of $\tilde{T}_i$. Equation (6-18) is used for defuzzification of TMs. Table 6-4 shows the ranking of design candidates based on the proposed approach. As shown in the table, design candidate 3 has the highest distance from the border approximation area, which shows its superiority over other design candidates.

Table 6-4 Ranking design concepts.

	Fuzzy Si			Si	Rank
Design candidate 1	-0.568	0.051	0.669	0.051	2
Design candidate 2	-0.627	-0.017	0.594	-0.02	3
Design candidate 3	-0.476	0.160	0.796	0.16	1
Design candidate 4	-0.630	-0.020	0.590	-0.02	4
Design candidate 5	-0.721	-0.128	0.464	-0.13	5

6.4 Results and discussions

6.4.1 Proposed concept

Concept 3 shown in Figure 6-14 (a) is selected as one of the optimal design candidates based on the evaluation of design concepts. Figure 6-14 (b) and (c) show the finger structure and user interface modules. The human hand has a complex structure with over 20 DOFs. To simplify the complexity and reduce the system weight, the finger structure uses mechanical coupling within finger joints driven by linkages. This approach offers increased functionality and adaptability to follow finger joints' ROM. The proposed concept is an example to verify the developed method for main components of the device. Mapping of the functional requirement and design parameter is implemented in the extended Axiomatic Design to narrow the design concept for the design of sub-systems such as software and electrical components.

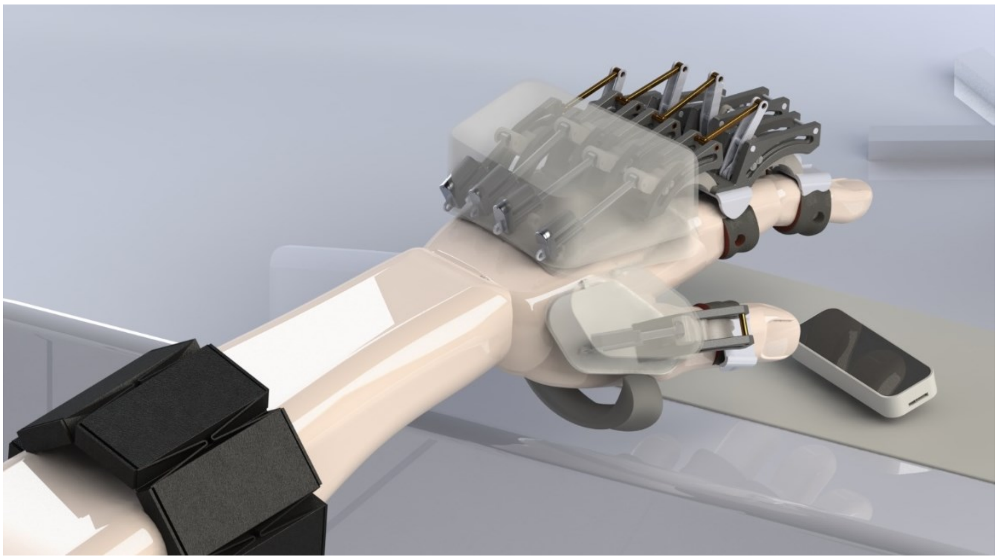

(a)

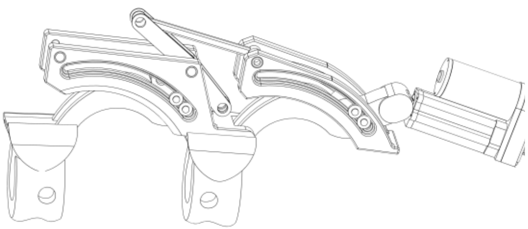

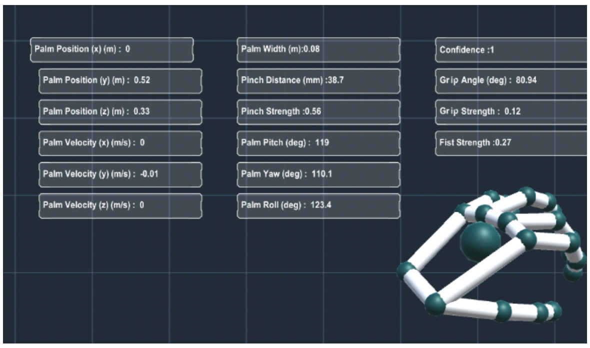

(b) (c)

Figure 6-14. (a) The proposed design concept. (b) The structure and actuator support finger movements. (c) The developed virtual environment to analyze and quantify hand motion data.

6.4.2 Evaluation of the proposed method

To verify the proposed approach, the design concept is compared with a design solution based on the QFD approach and one of the existing designs in the market. Figure 6-15 (a) and (b) show design concepts by the QFD approach and a cable-driven design concept of the hand rehabilitation device in the market. The first design concept uses pneumatic actuators with soft fiber-reinforced joints. The ROM of finger joints is controlled by pressurized reinforced joints regulated by control valves. The system uses bend sensors to measure hand motion parameters. Although the system provides ROM for the hand functionality, the additional system components reduce the device's portability. For example, the external pressurization system can increase system weight and size, reducing portability. Figure 6-15 (b) shows a cable-driven design concept that is popular in the rehabilitation device market. Although the system can mimic the ROM of the human hand, it cannot completely follow flexion/extension movements of fingers. Moreover, additional contact-based sensors are needed to track motion parameters of joints. *Figure 6-16* compares the derived DSM for the proposed design and soft actuator-driven design based on the QFD that shows dependency with feedback loops between system components. As shown in *Figure 6-16* (b), the derived DSM for the soft actuator-driven design includes feedback loops between DP211–DP22 and DP211–DP231. However, following Axiom 1 in the extended Axiomatic Design theory, as the proposed design uses the linkage-driven mechanism with vision-based sensors, these feedback loops are removed, leading to reduced design complexity and cost.

Moreover, comparing with gyro and bend sensors used in existing designs, the proposed design uses a non-contact vision-based sensor to track joint motions. This new tracking approach reduces not only the number of components in the system but also the manufacturing cost of the system to improve the convenience of maintenance. The functional model of the proposed design is shown in Figure 6-17. It represents mechanical, electrical and signal interactions between system components. The signal flow shown with the black dash line transfers captured joint motion data by a non-contact vision-based sensor to the controller. This non-contact approach removes wiring connections associated with most existing designs.

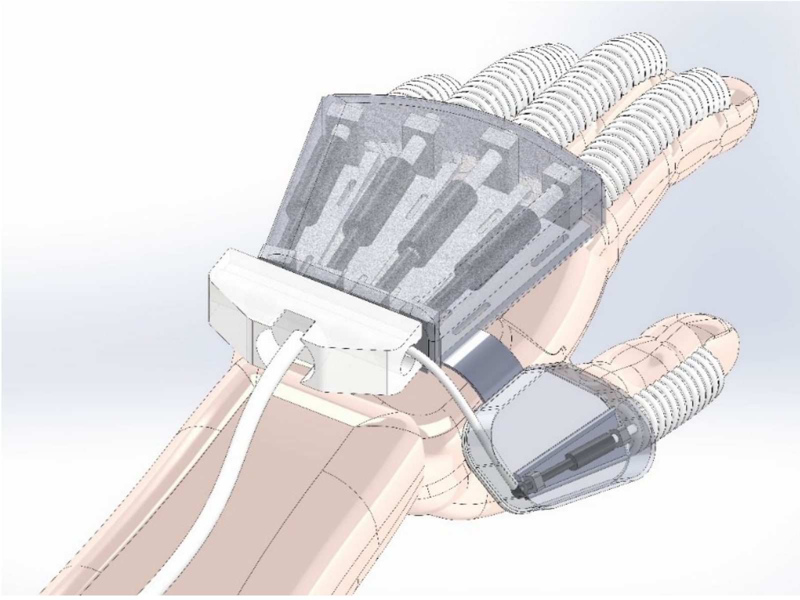

(a)

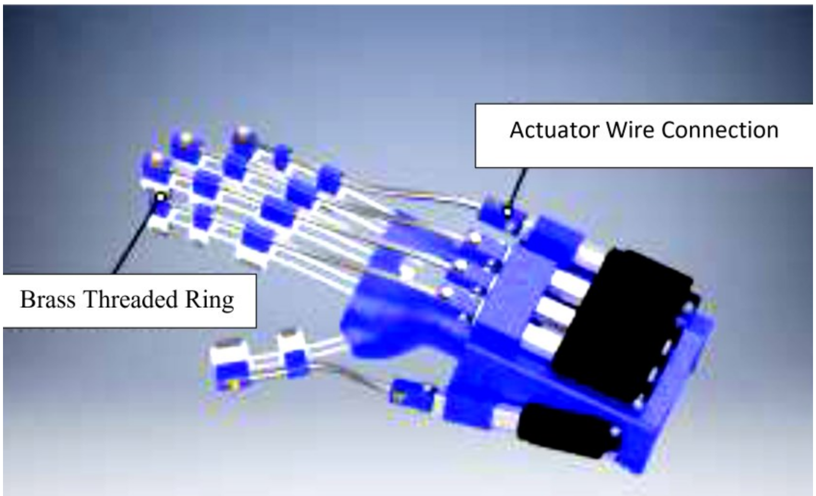

(b)

Figure 6-15. (a) Developed design concept based on the QFD process. (b)

Figure 6-14 (C) shows the developed virtual environment to analyze and quantify hand motion data [183]. The proposed concept provides a cost-effective method of quantitative evaluation for the digital rehabilitation. It is a systematic and comprehensive method for designers to address both customers and technical requirements, which leads to improved efficiency and reduced design cycle time. By this way, design information in different domains can be managed effectively in a design process. The case study shows that the generated concept satisfies all customer needs and improves limitations of the existing systems.

Cable-driven design concept [184] for the hand rehabilitation.

	DP 1	DP 211	DP 212	DP 213	DP 214	DP 22	DP 231	DP 232	DP 24	DP 25	DP 31
DP 1	X										
DP 211		X									
DP 212			X								
DP 213		X	X	X							
DP 214					X						
DP 22		X				X					
DP 231		X					X				
DP 232		X						X			
DP 24	X					X	X	X	X		
DP 25	X					X	X	X	X	X	
DP 31										X	X
DP 32											X

(a)

	DP 1	DP 211	DP 212	DP 213	DP 214	DP 22	DP 231	DP 232	DP 24	DP 25	DP 31
DP 1	X										
DP 211		X				X	X				
DP 212			X								
DP 213		X	X	X							
DP 214					X						
DP 22		X				X					
DP 231		X					X				
DP 232		X						X			
DP 24	X					X	X	X	X		
DP 25	X					X	X	X	X	X	
DP 31										X	X
DP 32											X

(b)

Figure 6-16 Derived DSM for (a) the proposed design concept, and (b) the soft actuator-driven design concept

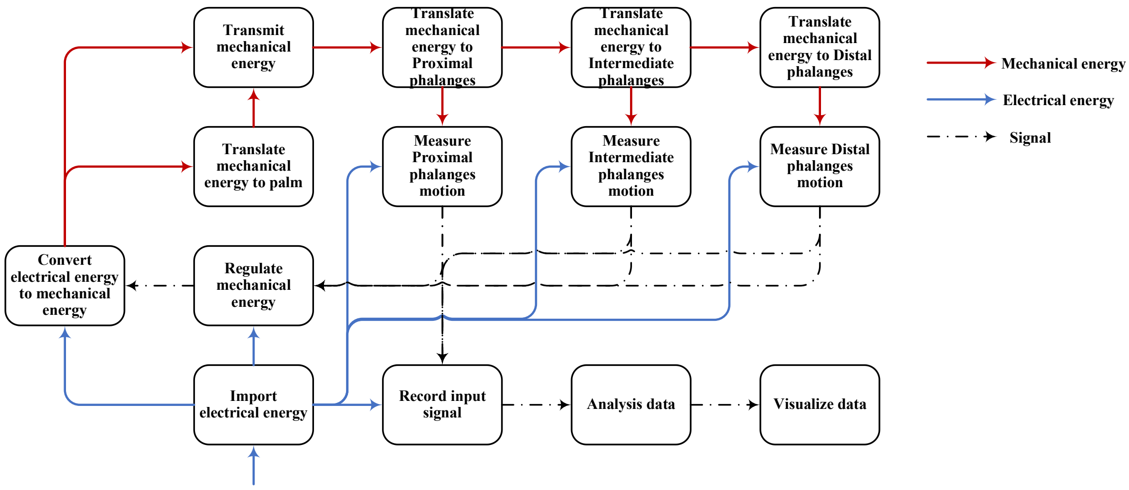

Figure 6-17 Functional model for design candidate 3.

6.4.3 Typical errors in the design concept generation

As conceptual design is an iterative process, it requires specific steps based on design criteria. There are some sources of errors that may lead to inefficient designs as follows.

No decoupling: This problem occurs in mapping the functional domain to physical domain when function requirements and their associated design parameters are known. The coupled design matrix will increase the cost of design changes and product maintenance [185]. Increasing the design range of design parameters can improve the solution, however, adjusting the design matrix is a more reliable option.

Wrong design parameter: Another typical error occurs during the concept generation when a design parameter selected to satisfy the related function requirement is incompatible with other design parameters in the system. For example, in the hand rehabilitation device design, an electromagnetic actuator can satisfy its functional requirement, but it is incompatible with a soft actuator-driven finger structure. A DSM analysis can be applied to prevent these incompatibilities and modify design matrix.

Non-matching system and design ranges: For some design concepts where system and design ranges of one or more design parameters are not completely matched with function requirements or customer requirements, the required performance may not be satisfied. Selecting a design parameter with a suitable design range can reduce this error.

6.5 Summary

Considering customer requirements in product conceptual design is a vital human-centric design process. Existing product design methods require considerable time to collect feedbacks from each design stage. In this chapter, a comprehensive method for the concept generation and evaluation is proposed based on benchmarks of existing solutions for different function requirements to work effectively in different domains and rank generated design concepts. The selected methods are integrated for their effectiveness and feasibility. A domain mapping matrix is built as one of the essences of the approach to map customer requirements into TMs and function requirements into design parameters. The approach can generate, evaluate and rank design concepts at the early stage of product development based on Axiomatic Design, DSM, and QFD. While the design matrix and DSM formation are applied to verify design concepts and find potential conflicts between design elements, QFD is used to determine the best design candidate that satisfies customer requirements. The Axiomatic Design, DSM and QFD are complementary for the decomposition, integration and mapping of design domains in the concept generation and evaluation. The value of the proposed method is that it considers the integration and evaluation of customer requirements, function requirements and product components. One of the advantages of the proposed approach is the qualitative and quantitative evaluation to analyze and rank design concepts. Integrating QFD, Axiomatic Design, and DSM provides a well-structured framework to consider all aspects of design, such as customer requirements, feasibility evaluation, and concept ranking, which leads to the design cycle reduction and desirable solutions. The linguistic QFD-MABAC concept ranking approach can benefit situations when uncertain data are considered in the design process.

The method is demonstrated in the design of a hand rehabilitation device, which shows that it can lead to better design strategies and improved design attributes based on customer requirements and alleviate unnecessary couplings between components. As shown in the case study, the generated design solutions can effectively address customer needs with desirable solutions. The generated concept of the hand rehabilitation device provides competitive advantages in portability, affordability, and non-contact measurement features. The proposed method simultaneously considers different aspects of product design such as customer, functional and physical domains. A weighting model will be developed to consider uncertain factors in the relationship matrix and model correlations of customer requirements. In the next chapter, the proposed approach will be integrated into a reinforcement learning environment for an automated method of product concept development to generate and evaluate design alternatives for large-scale design problems.

Chapter 7 Generative Product Concept Development and Evaluation using Multi-agent Reinforcement Learning

In this chapter, an automatic approach to use RL as an alternative of classical approaches is introduced to perform repetitive tasks in the product concept development. In this context, this work investigates the transferability, effort, and feasibility of RL in product development.

7.1 Deep reinforcement learning

The foundation of reinforcement learning is based on a Markov Decision Process (MDP) consisting of a group of parameters. RL is a type of machine learning that involves an agent learning to make decisions through interactions with an environment. RL offers several advantages over other traditional machine learning methods such as supervised learning and unsupervised learning. RL is well-suited for dynamic and complex environments where decisions must be made based on changing conditions. The agent learns through trial and error, adapting its behavior over time to achieve optimal outcomes. Unlike supervised learning, where labeled data are required, RL does not need explicit examples of correct actions. The agent learns from rewards and punishments received after each action, making it applicable in scenarios where obtaining labeled data are expensive or impractical. Also, RL agents can continuously learn and improve their strategies over time. They can adapt to new situations and update their policies to respond to changes in the environment, which is particularly useful in non-stationary or evolving systems. Moreover, RL methods inherently address the exploration-exploitation trade-off. The agent explores the environment to discover new strategies while also exploiting its current knowledge to maximize rewards. Striking the right balance between exploration and exploitation is critical to finding optimal solutions. RL algorithms can often be adapted to different tasks and domains with relatively minor adjustments. This makes RL versatile and capable of addressing a wide range of problems. Based on aforementioned advantages, RL is selected in this research to automate the design process. Figure 7-1 shows a typical workflow of deep reinforcement learning. The major elements of reinforcement learning are the environment and agent. At each step of interactions of the agent with the environment, a set of states is observed and evaluated to decide potential future actions. The agent receives a reward from the environment at every step. The goal of the agent is to maximize its cumulative reward. In the reinforcement learning process as shown in Figure 7-1 and Equation (7-1), A is a set of all possible actions in the action space, S denotes a set of all possible states. P refers to the probability of transition from s_t to s_{t+1} after taking action a in state s at time step t, and R represents the reward function allocating the immediate reward that the agent receives after the transition to next state s_{t+1}. $\gamma \in [0,1]$ is a Discount Factor that is applied in the calculation of the discounted expected return. In a reinforcement learning problem formulation, Q-learning can be used with a Deep Neural Network as a function approximator. Q values rate different actions at a state according to Learning Rate α and Discount Factor γ.

$$Q(s_t, a_t) \leftarrow Q(s_t, a_t) + \alpha[r_t + \gamma \max Q\,(s_{t+1}, a_t) - Q(s_t, a_t)] \tag{7-1}$$

With the recent advances in Deep Neural Networks (DNNs), high-dimensional representations (features) can be extracted to optimize reinforcement learning training algorithms and enhance decision-making capabilities. In deep reinforcement learning, DNNs extract various environment contents to generate the optimal policy. Policy-based and value-based approaches are two main approaches in deep reinforcement learning. Proximal Policy Optimization (PPO) is used in this research to estimate the policy as the function approximator. It is a model-free, online, and on-policy technique with either discrete or continuous action space which is suitable for most design applications. The PPO explores the design space by sampling actions based on the stochastic policy. The training process and initial condition derive the degree of randomness in the action selection. After passing defined steps, the policy gradually becomes progressively less random as the update rule assists the policy to exploit rewards that have been achieved. The proposed algorithm of PPO is as follows.

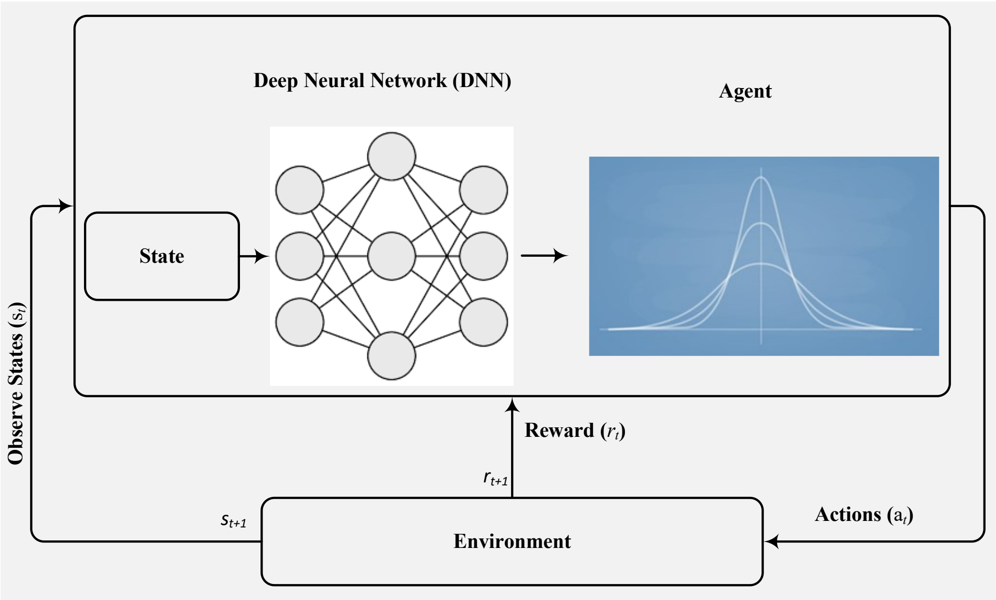

Figure 7-1 A framework of Deep reinforcement learning.

The algorithm of the PPO approach is shown in Table 7-1. If we define state observation as S_t, Action as A_t, next state as S_{t+1} then the reward achieved from S_t to S_{t+1} is R_{t+1}. At S_t, the agent calculates each action probability in the action space by $\pi(A|S_t;\theta)$ and randomly chooses action A_t according to the probability distribution. The detailed process in explained in the following steps.

Step 1: Construction of actor $\pi(A|S;\theta)$ with random parameter settings θ.

Step 2: Construction of critic $V(S;\phi)$ with random parameter settings ϕ.

Step 3: Performing N experiences in the following sequence:

$$S_{ts}, A_{ts}, R_{ts+1}, S_{ts+1}, \dots, S_{ts+N-1}, A_{ts+N-1}, R_{ts+N}, S_{ts+N} \tag{7-2}$$

where ts is the starting time step that is $ts = 1$ at the start of the training episode and $ts \leftarrow ts + N$ for each following set of N experiences in the same training episode.

Step 4: The advantage function is calculated for each episode step $t = t_{s+1}, t_{s+2}, \dots, t_{s+N}$. The return G_t is calculated based on the sum of rewards and discounted future rewards as follows.

$$G_t = \sum_{k=t}^{ts+N} (\gamma^{k-t} R_k) + b\gamma^{N-t+1} V(S_{ts+N};\varphi) \tag{7-3}$$

where, γ is a discount factor and b is equal to 0 if S_{ts+N} is a terminal state and 1 otherwise. Advantage function D_t is calculated as follows.

$$D_t = G_t - V(S_t; \varphi) \tag{7-4}$$

Step 5: Learning over different mini-batches of experiences from K epochs.

a. Randomly sampling a mini-batch set of size M from the current set of experience.

b. Critic parameters are updated by calculating loss L_{Critic} across all sampled data.

$$L_{Critic}(\varphi) = \frac{1}{M}\sum_{i=1}^{M}\left(G_i - V(S_i; \varphi)\right)^2 \tag{7-5}$$

c. Normalizing advantage values D_i according to recent data in the mini-batch.

$$\widehat{D_i} \leftarrow \frac{D_i - mean(D_i, D_2, \dots, D_M)}{std(D_i, D_2, \dots, D_M)} \tag{7-6}$$

d. Updating the actor parameters by calculating the actor loss function L_{Actor} across all sampled mini-batch data.

$$L_{Actor}(\theta) = \frac{1}{M}\sum_{i=1}^{M}\left(-min(r_i(\theta).D_i,\ \ c_i(\theta).D_i) + w\mathcal{H}_i\,(\theta, S_i)\right) \tag{7-7}$$

$$r_i(\theta) = \frac{\pi(A_i \mid S_i; \theta)}{\pi(A_i \mid S_i; \theta_{old})} \tag{7-8}$$

$$c_i(\theta) = max(min(r_i(\theta),\ \ 1+\varepsilon),\ \ 1-\varepsilon) \tag{7-9}$$

where G_i, D_i and ε are the return value, advantage function and clip factor, respectively. $\pi(A_i \mid S_i; \theta)$ is the probability of taking action A_i when in state S_i, given the updated policy parameters θ. $\pi(A_i \mid S_i; \theta_{old})$ is the probability of taking action A_i when in state S_i, given the previous policy parameters θ_{old} from before the current learning epoch. $\mathcal{H}_i(\theta)$ and w are the entropy loss and entropy loss weight factor, respectively.

Step 6: Iterating Steps 3 to 5 until the training episode reaches a terminal state.

The following section describes the design environment of the proposed approach.

Table 7-1 pseudocode of the Proximal Policy optimization (PPO) algorithm

Algorithm 7-1 Proximal Policy optimization (PPO) Algorithm

Input: Action space.

Output: Appropriate weights of the neural connections and trained agents.

Construct the actor $\pi(A|S;\theta)$ with random parameter settings θ.

Construct the critic $V(S;\phi)$ with random parameter settings ϕ.

for $episode = 1$, *terminal state* do

Produce N experiences

$S_{ts}, A_{ts}, R_{ts+1}, S_{ts+1}, \dots, S_{ts+N-1}, A_{ts+N-1}, R_{ts+N}, S_{ts+N}$

The return G_t is calculated

$G_t = \sum_{k=t}^{ts+N}(\gamma^{k-t}R_k) + b\gamma^{N-t+1}V(S_{ts+N};\varphi)$

The advantage function D_t is calculated

$D_t = G_t - V(S_t;\varphi)$

Learn over different mini-batches of experiences from K epochs.

Randomly sample a mini-batch set of size M

The critic parameters are updated by calculating the loss L_{Critic}

$L_{Critic}(\varphi) = \frac{1}{M}\sum_{i=1}^{M}\left(G_i - V(S_i;\varphi)\right)^2$

Normalizing advantage values D_i

Updating the actor parameters by calculating the actor loss function L_{Actor}

$L_{Actor}(\theta) = \frac{1}{M}\sum_{i=1}^{M}\left(-min(r_i(\theta).D_i,\ c_i(\theta).D_i) + w\mathcal{H}_i(\theta, S_i)\right)$

end for

Training episode reaches a terminal state

7.1.1 The environment

reinforcement learning agents are used to interactively communicate with the environment to form the optimal design concepts. Technically, since the agents are acting as the replacement of human designers, the environment should follow design rules during the product design. QFD and Axiomatic Design as main design approaches are used to model the environment. The QFD is applied to map customer requirements and their importance degrees to design components of a formed concept. Conversely, Axiomatic Design is used to check feasibility and design parameters compatibility of the design concept.

During the design process, a two-steps QFD can be applied in mapping customer requirements into TMs and design parameters [158]. In the reinforcement learning environment, in order to mimic the behavior of human designers, a few rules should be considered. The first rule is addressing customer needs as much as possible to obtain a competitive product. The second rule is checking the design validation and optimizing the structure of the design concept which is the voice of designers. Figure 3-1 in Chapter 3 shows a process of customer requirements being translated into TMs and design parameters in a two-steps QFD process. Customer requirements and associated weights d_m are inputs of this tool. The correlation matrix represents relations between different TMs. The output of each HOQ in a sequential QFD process is the relative weight which is decided based on information in the relationship matrix. The relationship matrix in HOQ is shown in Equation (3-4), where r_{mn} signifies relations between CR_m and TM_n. The absolute importance weight of each technical measure is calculated based on the relationship matrix and customer requirements weight as follows.

$$W_j = \frac{1}{n} \times \left[(r_{j1} \times d_1) + \ldots + (r_{jn} \times d_n) \right] \qquad , \forall\, i = 1, \ldots, n \tag{7-10}$$

where d_i signifies the weight of CR_i, and r_{ij} is the relation value between TM_j and CR_i. The effect of correlations between TMs can also be estimated using Khoo and Ho's formula [160] to decide the final importance weight of each technical measure as follows.

$$W_j^f = W_j + \frac{1}{n-1} \sum_{i=1, i \neq j}^{n} (W_j \times C_{ij}) \qquad , i, j = 1, \ldots, n \tag{7-11}$$

where C_{ij} denotes the correlation between TM_i and TM_j, $i \neq j$. After calculating W_j^f in HOQ 1, the same approach can be applied in HOQ 2 for the component deployment. The input of HOQ 2 is calculated W_j^f in the previous step. This sequential approach can relate different design parameters (or components) of a product to degrees of the customer satisfaction. Equation (3-9) uses information in the relationship matrix to connect design parameters and TMs, where p_{ij} signifies the relation of TM_i and DP_j. The advantage of this approach is its potential to evaluate the generated design concepts based on the customer satisfaction. However, it cannot fully validate design concepts in terms of the design parameters compatibility and efficiency. Therefore, in this research, Axiomatic Design is used to address these settings as a complementary design method. In the Axiomatic Design process, function requirements of the product are decomposed and mapped into related design parameters in a zigzag process. Technically, different solutions can be selected to satisfy a function requirement. For example, in designing a leaf blower, using a gas-powered engine, an electric motor or a hand operated mechanism are solutions to satisfy the required function. However, a challenge is how to integrate different components of a product to be compatible with each other and working efficiently. Moreover, in some design approaches such as design for maintenance, one of the goals is to reduce the coupling relations between components as much as possible. Coupling is a term to define the lack of independence in a design matrix. This matrix offers valuable data about relations of design elements. In the ideal design, function requirements are independent of each other, and the number of design parameters is equal to the number of function requirements. Once a design concept is formed, matrix analysis methods can be used to evaluate the design matrix. In Axiomatic Design, each function requirement is related to a group of design parameters. If we suppose function requirements as a vector with n elements and design parameters as a vector with m elements, a design matrix with n rows and m columns can be formed in Equation (3-12). The formed design matrix can be used for the quality assessment of generated concepts. In this chapter, the design approaches developed in previous chapters are used to advance the design environment of reinforcement learning agents.

7.1.2 The proposed algorithm

In searching solutions to meet design requirements, function requirements have different possibilities to meet CRs. Figure 7-2 shows a concept generation tree for a typical product. Each branch represents a possible design concept to satisfy requirements at function and sub-function requirements levels. However, evaluating all of the possibilities is hard for human designers as the large number of various factors should be considered. Therefore, in this work, human designers are replaced by design agents in the reinforcement learning design environment. Figure 7-3 shows the proposed multi-agent reinforcement learning system for the design space exploration. Details are discussed as follows.

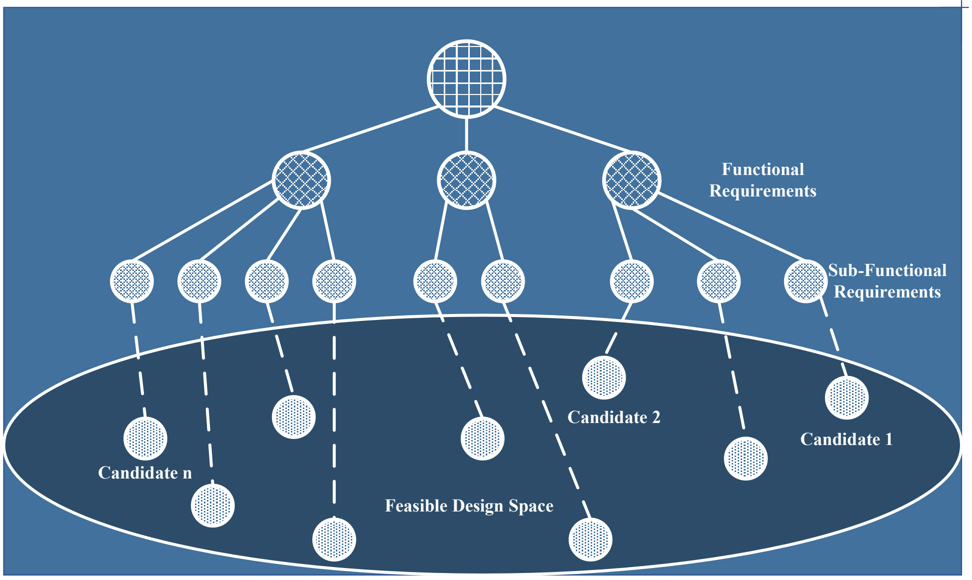

Figure 7-2 The concept generation tree for a typical product.

Step 1: The design process starts based on customer requirements and their associated weights. Two sequences of HOQ are used to map customer requirements into TMs and design components. A database of different components is used by reinforcement learning agents together with HOQ to meet design requirements.

Step 2: Using Axiomatic Design theory, customer requirements are mapped into a sept of function requirements. Also, function requirements form a set of design parameters (design components) in the zig zag process. For each FR, there is a set of design components to meet the FR in the database. The database is used by reinforcement learning agents to maximize customer requirements.

Step 3: The task of satisfying each function requirements is allocated to each agent in the multi- agent design process. During the design exploration phase, each agent iterates over possible solutions to improve the reward.

Step 4: The main reward function considers contributions of different agents during the design space exploration. Although each agent may select a best solution to satisfy customer requirements, however the selected component may not be compatible with solutions explored by other agents. Therefore, the reward function should consider not only the customer requirements satisfaction, but also verify the generated design concept.

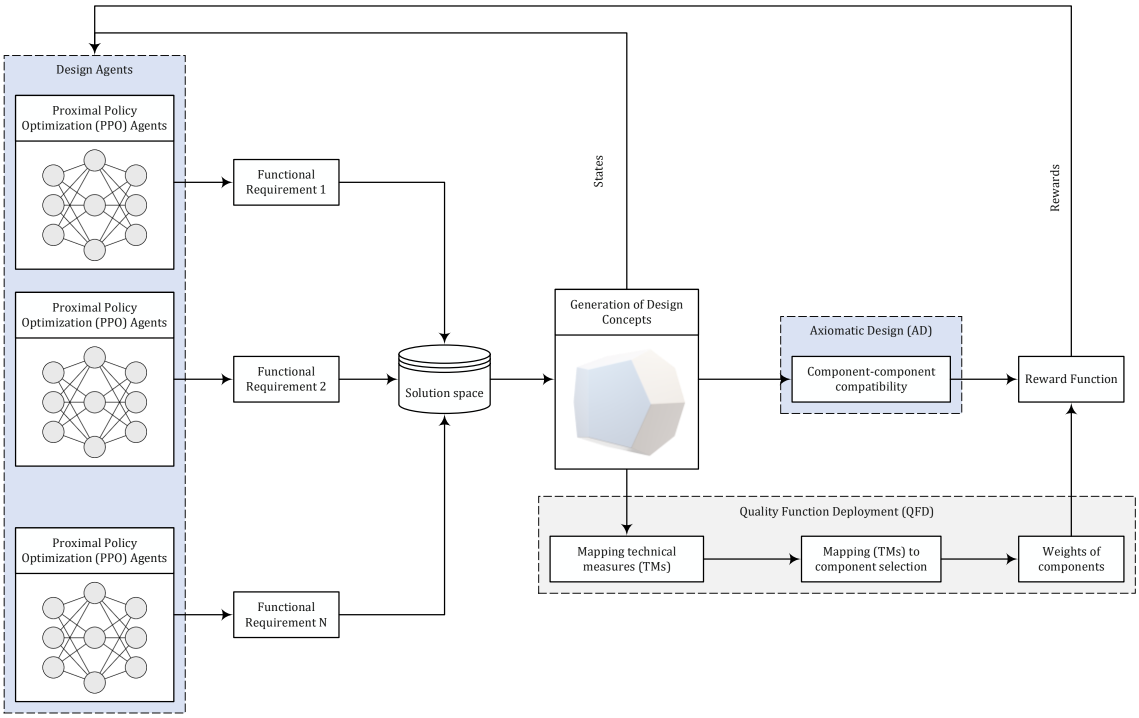

Figure 7-3 The proposed multi-agent reinforcement learning system for the design space exploration.

$$R_{CR}^{f} = \sum_{j=1}^{n}\sum_{k=1}^{p}\left(\left(\frac{\sum_{i=1}^{m} W_{CR_i} r_{ij}^{1}}{\sum_{j=1}^{n}\sum_{i=1}^{m} W_{CR_i} r_{ij}^{1}}\right)_j \times r_{jk}^{2}\right) + R_{AD} \quad , i = 1, \dots, m, j = 1, \dots, n, k = 1, \dots, p \tag{7-12}$$

where $m, n,$ and p are the number of customer requirements, number of TMs, and number of related design parameters to satisfy product functions, respectively. r_{ij}^{1} and r_{jk}^{2} are the values inside the relationship matrix in HOQs 1 and 2. Also W_{CR_i} is the weight of customer requirement i. The first term of the reward function equation tries to satisfy customer requirements as much as possible. However, this may not adequate as generated design concepts may not be feasible. Therefore, another term R_{AD} is added to the reward function to consider the design feasibility based on Axiomatic Design. R_{AD} is zero if the generated design is feasible, otherwise it can assign different negative values based on the component-component compatibility check and design matrix.

Step 5: Running the multiple agent design process until the reward function converges to the maximum value. In this research, the reinforcement learning design problem is solved based on two approaches. In the first approach, all design variables and constraints are handled by one super-agent. In the second approach, each agent acts as a designer for each sub-system (component). Exploration and exploitation are also important concepts in reinforcement learning. Exploration refers to the process of taking actions that the agent has not yet tried in order to learn more about the environment and potentially discover better strategies for maximizing the reward. This involves taking risks and trying out new actions, even if they may not immediately appear to be the most promising. Exploitation, on the other hand, involves taking actions that have already been tried and are known to be effective in maximizing the reward. This involves taking advantages of the knowledge and experience that the agent has already gained from the previous exploration. Finding the right balance between exploration and exploitation is crucial in reinforcement learning. If the agent only focuses on exploitation, it may miss better potential strategies that have not been discovered. On the other hand, if the agent only focuses on exploration, it may waste time and resources trying ineffective strategies and may not be able to achieve the optimal performance. The reward function in reinforcement learning serves as an objective function for the agent and maps the characteristics of the product to rewards. As such, it embodies the prior knowledge of the design tasks' objectives and products' requirements that must be fulfilled. To achieve this, individual reward functions are defined for each requirement, and the overall reward is computed as the weighted sum of these individual rewards. While it is theoretically possible to use discrete rewards for each characteristic, such as a reward of one point for every characteristic that fulfills the underlying requirement, shaping the rewards with a negative penalty for characteristics that do not meet the requirements can guide and accelerate the learning process. To apply reinforcement learning in design automation, product designers must first analyze the design tasks and identify the relevant design parameters that define the design states. In the following section, the proposed approach is implemented in designing a hand rehabilitation device to evaluate the effectiveness of the proposed approach shown in Figure 7-4.

7.2 Case study

The design problem of hand rehabilitation devices introduced in the previous chapter is solved using the proposed reinforcement learning approach.

7.2.1 Implementation

The proposed reinforcement learning method can function independently to automatically generate an optimal solution for a desired product based on available data and specified objectives. The method includes two basic components: (1) a knowledge base consisting of function requirements and solution options, and (2) a searching agent to navigate the design space and identify optimal solutions. The proposed method provides two input schemes as a general interface for required information: the parameter set and solution database. The parameter set defines the weight of customer requirements, and the solution database includes existing solutions for functions required and their relations to customer requirements. In this approach, a human designer will act as a supervisor to define the design space in terms of relevant conventional and intensified unit models, materials, logical rules, objectives, and state and action bounds. The searching agent will be a reinforcement learning agent with the ability to discover the action space and learn the design space to improve its search.

It is assumed that customer requirements and their weights are available for the design inputs. QFD is used to decide the first part of the reward function in Equation (7-12). The second part will be calculated based on the component-component compatibility of selected actions. Figure 5-2 in Chapter 5 shows HOQ 1 for the rehabilitation device analysis. In this HOQ, customer requirements are translated into TMs. A relationship matrix is used to represent their relations. The output of this phase is TMs weights used in HOQ 2 to decide the reward function. Figure 7-5 shows

HOQ 2 of the rehabilitation device. The decided weights of TMs are related to the selected design parameters (components) to meet customer requirements.

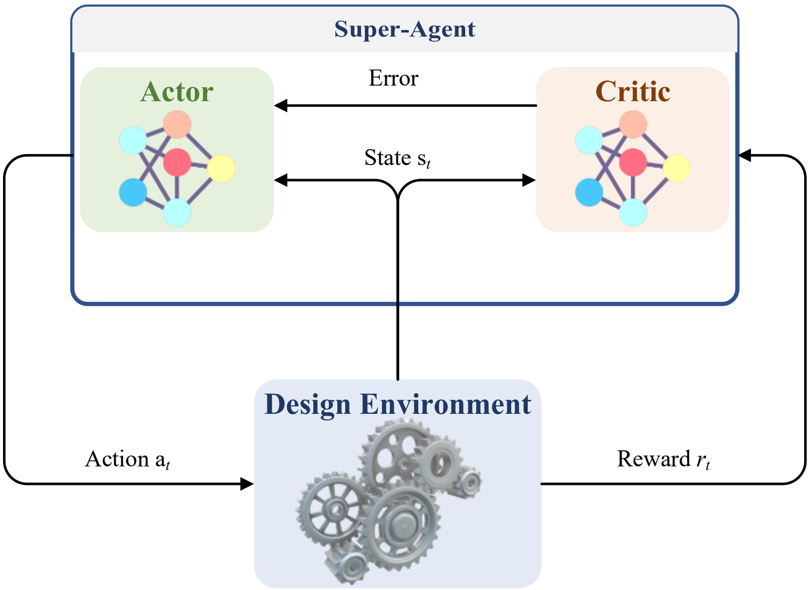

(a)

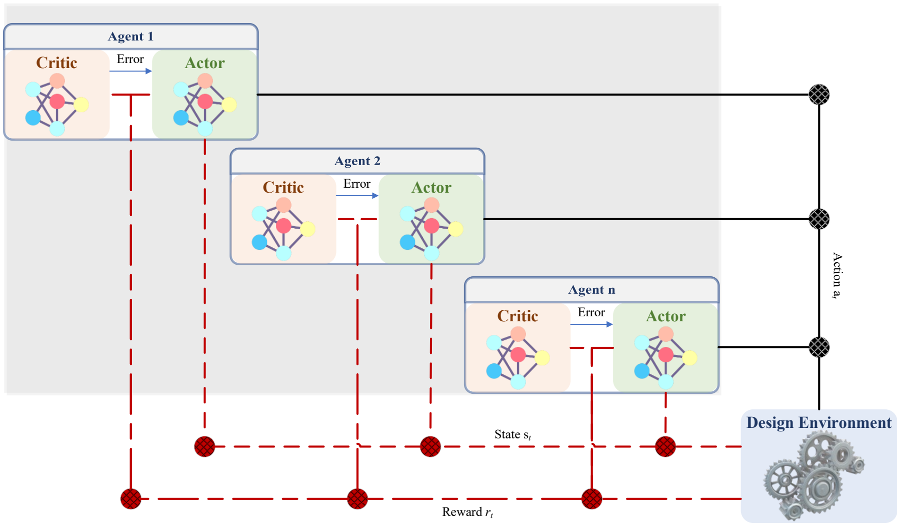

(b)

Figure 7-4 (a) Handling design variables using a super-agent. (b) A multi-agent framework for design space exploration.

The proposed multi-agent-based design approach is implemented in MATLAB Simulink to model interactions of agents with the environment. The parameter settings, actor-critic definition, and action space are defined in the MATLAB environment and linked with Simulink to model the design framework. All of the agent interactions with the design environment are performed in the Simulink environment. During each episode, the algorithm runs Microsoft Excel API, transfers selected actions, and reads calculated reward function and design states. Table 7-2 shows all action spaces for the case study of searching solutions of the hand rehabilitation device.

Row #	Weight Chart	Relative Weight	Maximum Relationship	Functional Requirements(Explicit and Implicit) / Technical Requirements	PLA	Direct Linkage	Wrist Palm Splint	Finger Splint PIP Joint	Finger Splint DIP Joint	Finger Structure 2	Assistive control system	Electromagnetic Actuator	Direct Energy	Leap Motion	EMG Recorder	Palm support cover	VR Headset
				Column #	1	2	3	4	5	6	7	8	9	10	11	12	13
				Direction of Improvement													
1		7%		Structure weight	0.225	0.175	0.025	0.025	0.025	0.125		0.175		0.125	0.075	0.025	
2		6%		Component size		0.1591	0.06818	0.0227	0.0227	0.1136		0.1136	0.0682	0.1136	0.1591		0.1591
3		10%		Component cost	0.1667	0.1296					0.0926	0.1667	0.0926	0.1667	0.0926		0.0926
4		6%		Actuator energy consumption							0.375	0.625					
5		9%		Adjustable Parts				0.1667	0.1667	0.0556		0.1667		0.2778		0.1667	
6		14%		Motion accuracy		0.1852				0.1111	0.2593	0.1852			0.2593		
7		7%		Degrees of freedom		0.2308				0.5385		0.2308					
8		11%		Tracking accuracy						0.2		0.3333		0.4667			
9		3%		Range of Motion (ROM)						0.0769	0.5385				0.3846		
10		5%		Motion velocities		0.1579				0.2632	0.2632	0.1579		0.1579			
11		5%		Applied force							0.2632	0.4737		0.2632			
12		2%		Material properties	0.4286	0.2381				0.3333							
13		6%		Component noise							0.25	0.75					
14		6%		Power energy density								0.25	0.75				
15		3%		Number of components						0.1154		0.2692		0.3462			0.2692
				Target													
				Max Relationship													
				Technical Importance Rating	0.039	0.0888	0.00605	0.018	0.018	0.1195	0.1261	0.2684	0.0593	0.1415	0.071	0.0165	0.0279
				Relative Weight	4%	9%	1%	2%	2%	12%	13%	27%	6%	14%	7%	2%	3%
				Weight Chart													

Figure 7-5 HOQ 2 for the rehabilitation device design.

There are in total nine different agents to select the best option for each design variable $(X_1, X_2, \ldots, X_9)$. In this design problem, the discrete action space for each agent is modeled using a coding system. For example, agent one decides Material Type (X1) from 5 different possible options. For each material type, a number is assigned $(1,2, \ldots, 5)$. In another example for Finger Structure (X3), agent three decides the best structure to satisfy customer requirements from 10 different possible options that are assigned as (1,2,…,10). When agents interact with the environment, assigned numbers by the agents form a nine-digit code that decides the structure of a generated design concept. Each letter of the code represents a related DP. For example, ith letter represents X_i. As another example, if the 7th letter is 2, it means that X7 is assigned as "Flex Sensor". In the Axiomatic Design process, design parameters (solutions) are mapped from different function requirements. Technically, there is a wide range of options to satisfy each function requirement. As a result, a design concept is formed when design parameters satisfy related function requirements. In traditional methods, human designers evaluate options for each function requirement to form design concepts. However, this process is very iterative and time-consuming. For example, Figure 6-10 in Chapter 6 shows different exoskeleton finger structures to satisfy function requirements for supporting hand movements. Each finger structure provides different advantages and drawbacks in terms of customer requirements. Also, some finger structures may not be compatible with all actuator types. Similarly, other design parameters should be decided to not only form a feasible product concept, but also satisfy customer requirements as much as possible. The proposed method can explore and learn different possibilities to automatically generate the design concept and satisfy customer requirements.

Table 7-2 Action spaces in searching solutions of a hand rehabilitation device

Material Type (X1)	Aluminum Alloy	Steel	PLA	Polycarbonate	Carbon Fiber	ABS				
Derive system (X2)	Elastic Joints	Pulley System	Cable-conduits	Linkage-slider	Direct Linkage					
Finger Structure (X3)	Type 1	Type 2	Type 3	Type 4	Type 5	Type 6	Type 7	Type 8	Type 9	Type 10
Control approach (X4)	Assistive-resistive	PID								
Actuator type (X5)	Electromagnetic	Hydraulic	Pneumatic							
Power source (X6)	Lithium-polymer battery	Lithium-ion battery	Direct Energy							
Motion Detection (X7)	Vision-based sensor	Flex Sensor	Gyro Sensor							
Command Signal (X8)	Brain Activity	EMG Recorder								
Display type (X9)	VR module	2D display								

7.2.2 Solution search and result

The case study design problem is solved using the proposed approaches as shown in Figure 7-4. The first approach uses a super-agent to handle all discrete design variables ($X_1, X_2, \dots, X_9$). In this case, the action space is vast and consists of 64800 different actions. Figure 7-6 (a) shows results for the single super-agent training and exploration. The red area shows the infeasible design space, meaning that design points that are located in this area either contain incompatible components or fail to satisfy all customer requirements. When the network is provided with an excessive number of state inputs to choose from a large number of possible actions, it increases the complexity of the problem to search the optimal solution.

To make the large-scale design problem manageable, it is essential to reduce their dimensions and complexity to avoid the curse of dimensionality. One way to achieve this is to decompose an entire design space into decentralized parts and search solutions using multiple agents. These individual agents can be trained to optimize specific parameters and deployed based on the situation. By breaking down the complexity for agents, significant improvements in scalability can be achieved. Figure 7-6 (b) shows results for the multi-agent training and exploration with the centralized execution. In this case, selecting different components for each function requirement is allocated to each agent. Table 7-2 shows the action space for this case study. There are in total nine different agents with the PPO algorithm used in the multi-agent problem. The environment is reset at the beginning of each episode using an initial value during the system training. If there is no intended starting point, such as in the case of a basic product variant, the initial value will be randomly sampled from the action space, allowing the agent to take the same number of actions in both directions of the design space. The reward function and training parameters reflect the design constraints and objectives, enabling the agent to explore all possible areas of the solution space while also preventing it from exceeding suitable design solutions. Each modification is defined as a step, which corresponds to an action selected from the action space for every parameter of the state.

(a)

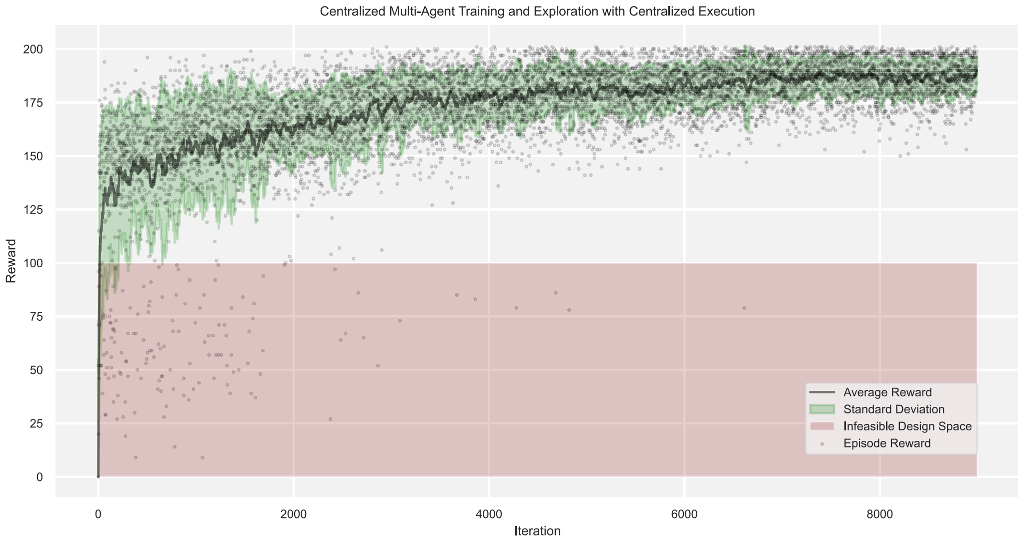

(b)

Figure 7-6. Training results of the proposed algorithm. (a) Single super-agent training and exploration. (b) Centralized multi-agent training and exploration with the centralized execution.

As shown in Figure 7-6, the number of infeasible design points in the multi-agent training approach is significantly less than using a single super-agent. It means that comparing with a single super-agent, in case of the collaborative multi-agent training, the multi-agents are able to recognize and explore the design space efficiently. Apart from the challenges mentioned, there is also a concern that the single agent algorithm may only optimize locally [186], which could lead to the creation of small-scale control loops that are optimized based on intrinsic factors and rely on the local information, while ignoring broader interdependencies. Additionally, a suboptimal problem-solving strategy may arise from the insufficient exploration of the state and action space, which can result in the selection of suboptimal actions and lack of guarantee of optimality [187]. Moreover, using multiple agents for design tasks leads to a reduction of iterations, which is more efficient compared to using a single super-agent. Also, Figure 7-6 shows a standard deviation of the generated solutions for both approaches. The dispersion of feasible design points is much higher in case of using a single super-agent for training and exploration. However, in the case of centralized multi-agent training and exploration, the near optimal design points are much closer to each other, meaning that the algorithm is able to converge and generate design concepts efficiently.

In order to build an optimal policy, the agent faces the dilemma of exploring new states while maximizing its overall reward at the same time. This is called Exploration vs Exploitation trade-off. To balance both, a best overall strategy is the short-term sacrifices. Therefore, the agent should collect enough information to make the best overall decision in the process. However, it is challenging for the single super-agent to collect enough experience to take optimal design decisions. Also, to ensure the effective design automation in reinforcement learning, it is important to consider the entire design space. If too much emphasis is placed on exploitation at the early process, it may lead to overlooking potentially excellent design solutions and ultimately prevent the learning of a successful policy. In addition to the fundamental algorithmic settings, choosing appropriate hyperparameters is also crucial. The discount factor influences the importance of immediate and long-term rewards. The learning rate affects the trade-off between the learning speed and stability. Other algorithmic and neural network parameters in deep reinforcement learning also significantly impact the overall performance. It is therefore essential to consider the optimal design of the state/action space and reward structure, as their proper alignment can result in the optimal system behavior and facilitate the search for optimal control strategies.

After training the multi-agent framework, the trained agents are able to generate feasible design concepts, satisfy customer requirements as much as possible and make optimal design decisions in similar design problems. In this case study, one of the stop criteria for training reaches the average reward to 180. At this level, most of generated concepts are near optimal and have some advantages. If designers, as supervisors in the training process, increase stop criteria to values around 200, the obtained solutions are more optimal. When the training stops, the agents are able to automatically generate product concepts based on the obtained experience. The output of each agent's decision is shown in a form of digit that can be decoded to a form shown in Table 7-2. A design concept is a form of decoded decisions of a group of agents. For example, Table 7-3 shows one of the best generated hand rehabilitation concepts based on the proposed approach. The reward value of this concept is around 198. Figure 7-7 shows two common hand rehabilitation devices in the market. Comparing with the existing solutions, the generated concept has its special advantages. For example, the device structure is more compact and portable. Also, the suggested configuration uses one vision-based sensor to track all finger joints simultaneously. By using this approach costly flex and gyro sensors can be eliminated from the structure leading to a reduction in design complexity and production cost. Moreover, the device structure is adjustable for users to be able to attach the device to their hands with palm and finger splits. As it uses light weight commercially affordable additive manufacturing materials, the device weight and cost can be reduced. During a rehabilitation treatment, it is important to display and visualize quantified motion data. The generated concept displays the hand treatment data captured by the vision-based sensor using a virtual reality module which is suitable for patients to interact with the device. Figure 7-7 (a) shows a device concept with pneumatic actuators that require external components and air tubes that consume more energy and increase the system weight. Also, it doesn't have a complete tracking system for measuring the range of motions of finger joints. Another concept of the linkage mechanism with electromagnetic actuators is shown in Figure 7-7 (b). This concept uses Microsoft Kinect for body skeletal tracking with the imitation to track finger joints. If we decompose design concepts shown in Figure 7-7 (a) and (b) into major components and use the approach shown in Equation (7-12) to find the reward value, it would be 149 and 181 respectively. However, the customer satisfaction is 198 for the proposed solution which uses a slider mechanism to mimic the range of motions of human hands.

Table 7-3 The proposed design solution

Material Type (X1)	Derive system (X2)	Finger Structure (X3)	Control approach (X4)	Actuator type (X5)	Power source (X6)	Motion Detection (X7)	Command Signal (X8)	Display type (X9)
ABS	Linkage-slider	Type 9	Assistive-resistive	Electromagnetic	Lithium-polymer battery	Vision-based sensor	EMG Recorder	VR module

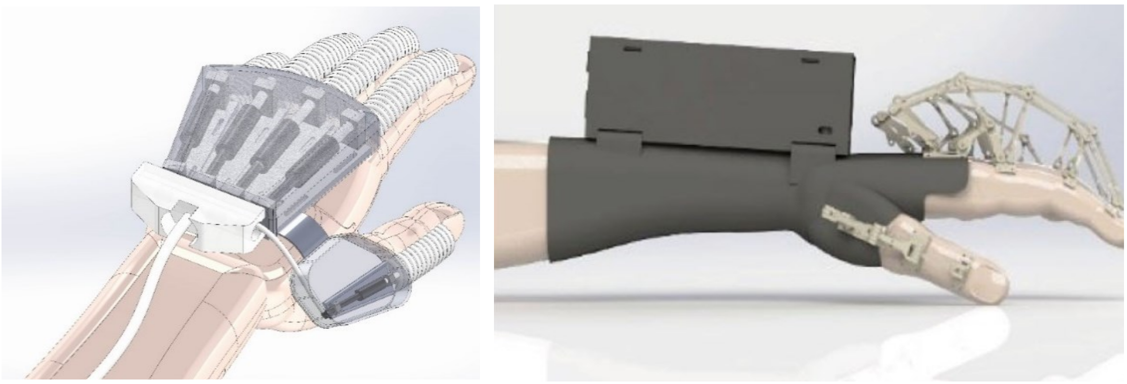

(a) Soft actuator based concept [23]　　　(b) Linkage driven concept [188]

Figure 7-7 Examples of hand rehabilitation device concepts in literature.

The presented method fills the gap of existing design approaches by using a reinforcement learning method to expedite the design process and improve the design exploration. In the concept generation process, reinforcement learning agents are able to interact with the design environment to optimize design concepts. In comparison with optimization methods, the proposed approach provides advantages of transfer learning using machine learning techniques for the model to leverage knowledge learned from one task and apply it to a new task. The idea behind the transfer learning is that there are often underlying patterns and structures that are shared across tasks although specific details of a task are different [189]. By leveraging knowledge learned from a pre-trained model, the new model can learn these shared patterns quickly with less data.

Conceptual design typically involves exploring a large space of design possibilities and selecting the most promising option based on a set of criteria, such as cost, performance, and feasibility. reinforcement learning can be used to automate some aspects of this process by training agents to explore the design space and select promising options based on rewards. However, there are some challenges to using reinforcement learning in the conceptual design. One of the challenges is defining an appropriate reward function to capture design criteria. This can be difficult as the criteria for a good design are often complex and may be difficult to quantify. Additionally, the design space for many problems may be very large, making it difficult for reinforcement learning agents to explore all possible options. The presented work proposes a multi-agent approach to handle complex design tasks and defines a reward function to achieve the optimal design concept. Comparing with the existing approaches, the proposed method has the following advantages.

❖ Since the design process is handled by design agents, in comparison with traditional approaches that are manually handled by designers, the entire design space can be explored efficiently and quickly.

❖ After the training process, agents have experience and knowledge to form product concepts. The knowledge can be enhanced by participating in different design problems. The trained agents can be transferred to other design problems to perform specific design tasks.

❖ By allocating each design task to a specific agent, large scale design problems can be decomposed into different sub-problems that can be handled by trained agents. This collaborative design approach can reduce the design cycle time and cost.

7.3 Summary

This chapter proposes a multi-agent reinforcement learning method in which several agents work and learn together in a shared environment. All agents work in cooperative environments with the same objective.

QFD and Axiomatic Design are applied in the learning environment for reinforcement learning agents to generate and evaluate design concepts. The proposed method performs the domain mapping for customer satisfactions, concept generation and evaluation in a large proportion of repetitive tasks during product development. To the best of author's knowledge, this work is the first attempt to explore the application of reinforcement learning in domain mapping of product design to generate and evaluate design concepts based on customer requirements. The novelty of this research lies in the integrated design framework for a learning environment and collaborative multi-agent architecture to enable the design automation. The proposed method can be used in product concept development to improve functionality, efficiency, and user experience of the design process. The case study demonstrates that the method is a generative conceptual design approach in the design space exploration. By learning from past product data and optimizing the design process, the reinforcement learning method can improve the efficiency of the product design, remove incompatible design and improve the design quality. Overall, the proposed method has the potential to improve different aspects in product design from user experience to process efficiency. However, it is important to note that implementing reinforcement learning in product design requires a deep understanding of the technology and expertise in machine learning.

The primary obstacles in this research involve creating a multi-agent learning technique that mimics the collaborative design process, functions as an efficient optimization process, and enables agents to work on different variables of the problem. Furthermore, expanding this approach to support constraints and a mixture of integer and continuous variables presents a significant challenge. In order to improve adaptability of the agents to different scenarios, the future research will develop methods that enable agents to quickly adjust to new conditions. This includes not only fast re-training under changed circumstances, but also accelerating transfer of the adapted policy to the agent. One potential strategy to achieve this could use a permanently trained agent within a design framework, followed by a policy transfer. Another approach to increase generalizability and performance under changing conditions could involve combining deep reinforcement learning with traditional decision-making and task decomposition approaches. In addition to the aforementioned points, research efforts should also be directed to transfer learning into faster and more effective learning and performance of complex tasks by agents. In a multi-agent system, an individual agent could leverage experience gained by other agents and adapt better to unfamiliar situations. The development of such swarm intelligence could enhance the utilization of local and global information and enable a flexible response and adaptation of the product to unexpected events.

Chapter 8 Implementation of the Proposed Design Concept

In Chapters 6 and 7, a hand rehabilitation solution is proposed to improve the existing devices. Implementation of the proposed solution is presented in this chapter.

8.1 Virtual environment and hand motion analysis

A virtual environment (VE) is proposed as a part of the hand rehabilitation system. The system is designed to fit different hand sizes with features of the ease of use, ability to generate reports, and portability as shown in Figure 8-1 (a). The proposed system offers a real-time virtual environment for users to interact with objects such as grasping and manipulating targets to practice specific motor skills. The virtual environment uses Unity3D's built-in physics engine to model interactions of different objects when forces are applied to them. The real-time simulation applies rigid body dynamics and Newton's laws of the motion to detect collisions between objects when they are affected by gravity, forces, and torques. Users can select a specific finger or palm to measure and record motion parameters like angles, positions, and velocities (Figure 8-1 (b)). The system provides functions to capture hand joint motions, process data and display exercise protocols and virtual feedbacks for the hand rehabilitation. It contains three modules as follows. 1) Data input module: Data of the hand rehabilitation are captured and collected using a Leap Motion sensor. The hand is recognized by the sensor to detect finger joints and joint positions for each frame. Hand movements are captured and displayed for users to see the motion data and interactively track the motion in a 3D space. 2). Data analysis module: Real-time frame data are transferred to analysis codes written in C# language for de-noising and extracting motion parameters. 3). User interface module: Outputs are displayed in a virtual environment developed using the Unity engine. In the following sub-sections, details of the system are presented including hardware, hand skeletal model, and parameters of the trajectory of palm and fingertip movements.

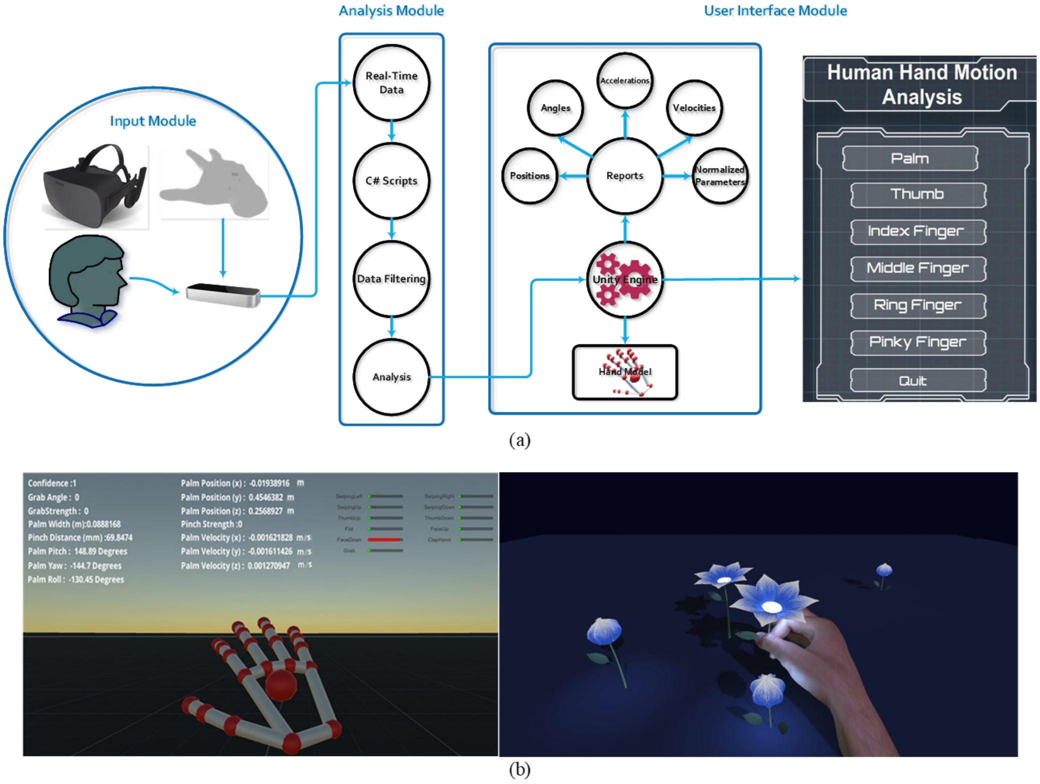

Figure 8-1 (a) Framework and modules of the proposed system. (b) Developed virtual environment of the hand motion analysis.

8.1.1 Data input module

The system is able to capture both hands of users in the working area simultaneously. Captured data by the Leap Motion sensor generate the 3D spatial and temporal information of hand joints. The Leap Motion is a small peripheral system for real-time motion capturing of hand and finger movements. It uses three infrared LEDs and two monochromatic IR cameras to capture hands and objects in a field of view of 150 degrees [190] with a range of approximately 25 to 600 millimeters in a hemispherical field [191]. For improving accuracy, the sensor is calibrated based on the application of hand movements. Figure 8-2 shows the calibration process of a user hand, the sensor field of view, observable hemispherical area, and captured image of the hand. The sensor detection accuracy of hand motions is approximately 0.7 millimeters [192], which provides enough precision for positioning human hands [193] and applications of rehabilitations [194].

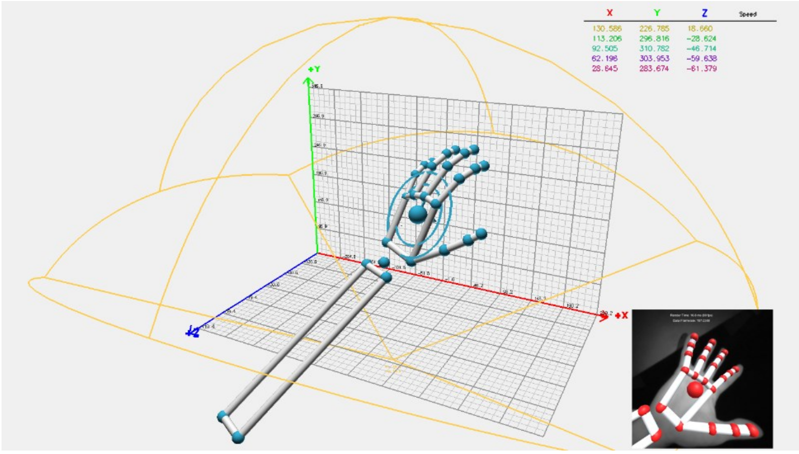

Figure 8-2 Calibration of Leap motion sensor in X,Y, and Z directions.

8.1.2 Data analysis module

A C# coded program processes the stream of frames from the sensor, and extracts data of hands such as the palm and fingertips. A data structure is then formed for each joint based on the 3D spatial and temporal information. For example, the tip position of fingers over time is defined as follows.

$$\rho = \varphi\langle(x, y, z), t\rangle \tag{8-1}$$

where φ is a function of temporal (t) and spatial data based on $x, y, and\ z$ axes in a Cartesian coordinate system. Data captured by the sensor are often variate with noise. In order to conduct the data analysis from raw data, a robust de-noising method is required. Wavelet Transform (WT) is applied for de-noising data with three consecutive steps including the signal decomposition, thresholding of coefficients and signal reconstruction [195]. The wavelet analysis is performed on the noisy signal up to a selected level N. The level of decomposition can be determined based on desired frequency band features. Thresholding of the detail coefficients from levels 1 to N is then implemented. The signal is finally synthesized by adjusted detail coefficients. For n noisy samples of a function f, a signal can be represented as follows.

$$y_i = f(t_i) + \varepsilon_i, \quad i = 1, \dots, n \tag{8-2}$$

where ε is the noise level and $f(t_i)$ is uncorrupted signal. The wavelet denoising procedure has three steps namely decomposition, thresholding, and reconstruction as shown in following three equations.

$$Z = W(y) \tag{8-3}$$

$$S = D(Z, \lambda) \tag{8-4}$$

$$\hat{f} = W^{-1}(S) \tag{8-5}$$

where W is a forward wavelet transform operator of signal y, D represents a denoising operator with threshold λ, and W^{-1} is an inverse wavelet transform operator respectively. We want to denoise y_i to generate $\hat{f}(t_i)$ as an approximation of $f(t_i)$. Figure 8-3 shows de-noised data for Z positions of Palm in a cartesian space based on different levels of decomposition. The wavelet transform uses db4 as a wavelet base function with frequency range of 32-64 Hz. The signal is subjected to a four-layers decomposition. As shown in the plot, the signal is smoothed compared to original data. The same position data can be captured and analyzed for all finger joints as well. Phalanges have 14 bones that comprise the bony core of fingers [196]. Each finger contains three phalanges, excluding the thumb which has two. Figure 8-4 illustrates the angle between finger joints based on position data captured by the sensor.

8.1.3 User interface module

The developed rehabilitation User Interface (UI) includes a main menu for users to choose functions based on treatment needs. User interface module supports the data analysis and system application via a data processor, Leap Motion sensor and computer screen. The user interface can be operated with Virtual Reality (VR) headsets using the Leap Motion sensor. Skeletal hands and user interface are presented through virtual environment linking movements according to the user performance via interactions with the visual feedback. The main menu in Figure 8-1 contains six parts including the hand Palm, Thumb, Index, Middle, Ring, and Pinky fingers. The motion data for wrist can be accessed using the palm tab in the developed user interface. Figure 8-5 shows a Palm model in the developed user interface for the hand motion analysis. The integration of these modules provides an easy-to-use environment for the data analysis of rehabilitation applications. The motion data can be saved during operations for the option to access them later.

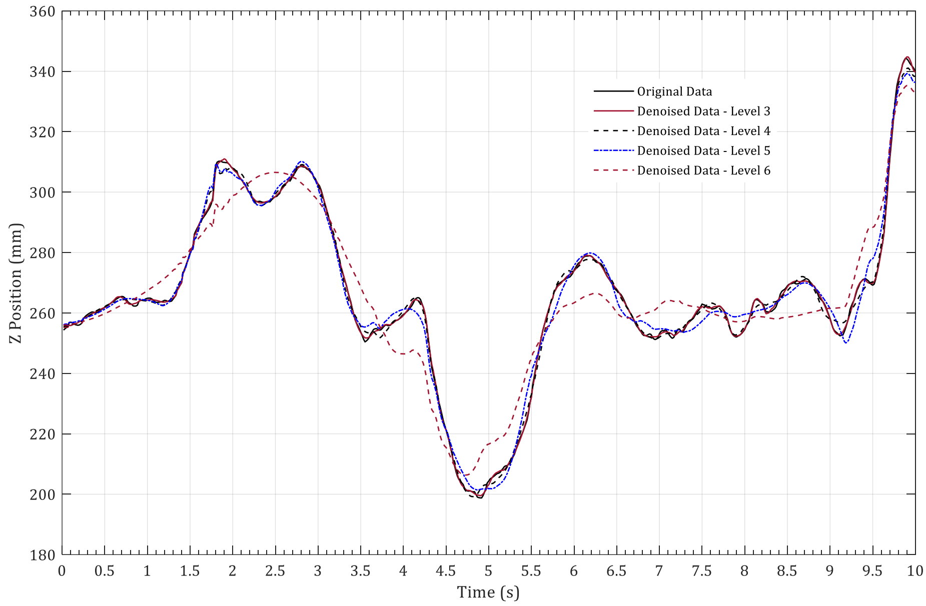

Figure 8-3 De-noised position data of palm in the cartesian space using wavelet transform with different levels.

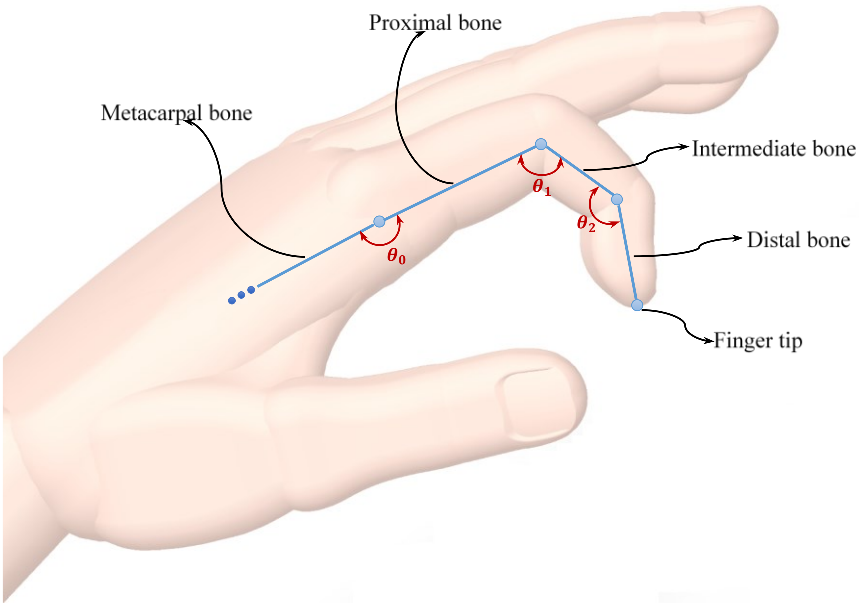

Figure 8-4 Angles between finger bones for a human hand based on captured data.

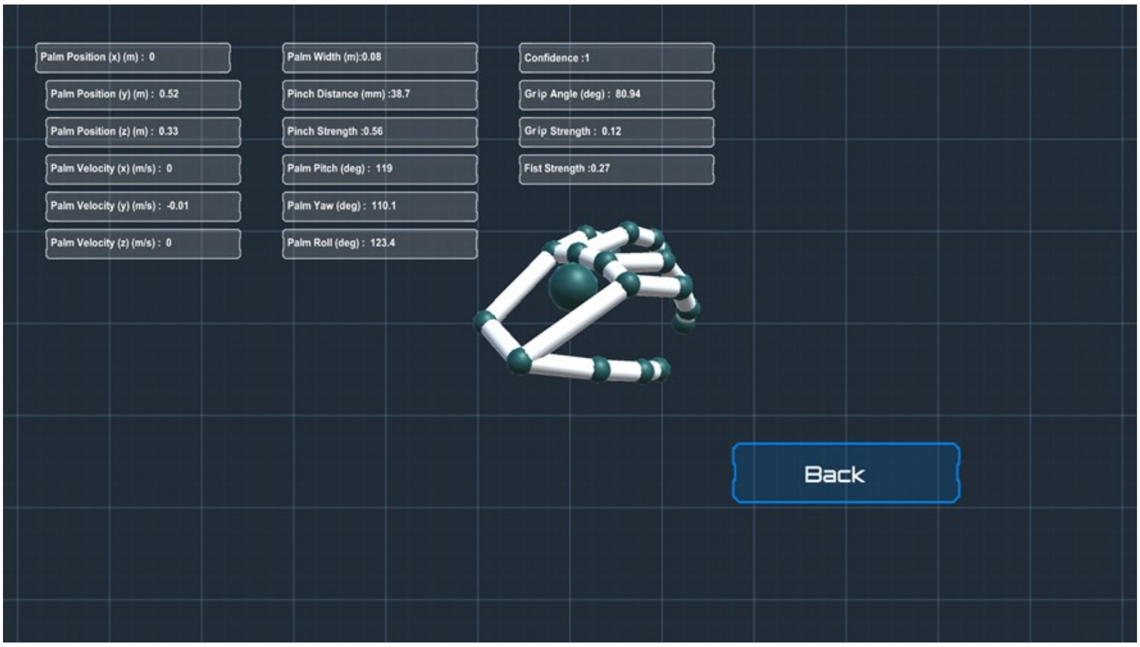

Figure 8-5 Developed user interface to visualize and analyze hand motion parameters.

8.2 Hand motion parameters

The developed system can measure joint positions of the user hand. Wrist and finger joint positions e.g. Metacarpophalangeal (MCP) and Proximal Interphalangeal (PIP) are used to calculate motion parameters like angles between the fingers and wrist. Motion data are stored in a data frame in a sequence of consecutive movements. A segmentation algorithm is developed to extract the motion data for each specific joint along the particular axis of interests. Captured hand data are defined as follows.

$$[P_1, \dots, P_n, \dots P_N] \in R^{3K \times N} \quad , 1 \leq n \leq N \tag{8-6}$$

where N is the total number of frames, K is the number of position points per frame ($K = 46$ for left and right hands).

$$P_n = \left[p_1^{v_n,1}, \dots, p_k^{v_n,k}, \dots, p_K^{v_n,K}\right] \in R^{3K} \quad , \quad 1 \leq k \leq K \tag{8-7}$$

$$p_k^{v_n,k} = (x_k^n, y_k^n, z_k^n) \in R^3 \tag{8-8}$$

where P_n characterizes a set of all K captured joints per frame n, $p_k^{v_n,k}$ is particularly the *kth* 3D coordinate joint position in frame n. A set of vectors for hand bones is defined as follows.

$$V = [v_1^n, v_2^n, \dots, v_l^n, \dots, v_L^n] \tag{8-9}$$

where L denotes the total number of hand bones in the analysis module. Joint positions corresponding to each hand are stored in a database during the rehabilitation. In Cartesian coordinates, the distance between joints p and q can be calculated using the Euclidean distance formula as follows.

$$d(p,q) = d(q,p) = \sqrt{(p_x - q_x)^2 + \left(p_y - q_y\right)^2 + (p_z - q_z)^2} \tag{8-10}$$

Velocity of the palm is estimated as an average velocity from all five finger tips as follows.

$$V_i^{palm} = \frac{v_i^{thumb} + v_i^{index} + v_i^{middle} + v_i^{ring} + v_i^{pinky}}{5} \tag{8-11}$$

where v_i^k denotes the velocity of the k^{th} finger tip between two consecutive frames. Hand position data can have different applications in rehabilitations. For example, a palm 3D position can be calculated by measuring the distance of the palm centre to the sensor origin. Figure 6 depicts a palm position and direction vectors of the palm velocity during a training process. By measuring joint positions and velocities of the hand, users can have a cost-effective tool for the data analysis. Available 3D position data of different joints can be applied to extract useful information like angular positions and velocities. The normal of a finger vector is represented as follows.

$$e_1 = \left[\|\vec{v}_{thumb}\|, \|\vec{v}_{index}\|, \dots, \left\|\vec{v}_{pinky}\right\|\right] \tag{8-12}$$

The angle between two fingers can be determined as follows.

$$\theta = arccos\left(\frac{\vec{u}.\vec{v}}{\|\vec{u}\|.\|\vec{v}\|}\right) \tag{8-13}$$

where θ is the angle between $\vec{u}$ and $\vec{v}$ that are 3D position vectors. Angles between vectors of adjacent fingers and hand normal are presented in following equations.

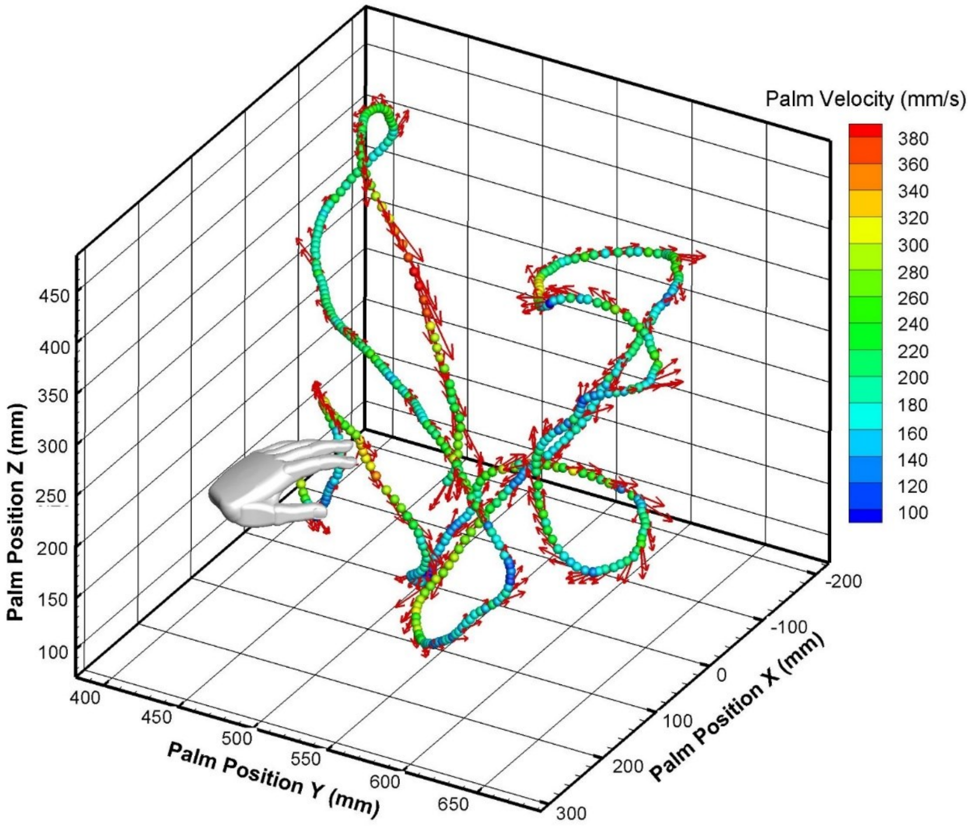

Figure 8-6 Tracking hand palm position in cartesian space and direction vectors of the palm velocity to display and record the details of hand motion.

$$e_2 = \begin{bmatrix} \langle \hat{v}_{thumb}, \hat{v}_{index} \rangle \\ \langle \hat{v}_{index}, \hat{v}_{middle} \rangle \\ \langle \hat{v}_{middle}, \hat{v}_{ring} \rangle \\ \langle \hat{v}_{ring}, \hat{v}_{little} \rangle \end{bmatrix} \tag{8-14}$$

$$e_3 = \begin{bmatrix} \langle \hat{v}_{thumb}, \hat{v}_{normal} \rangle \\ \langle \hat{v}_{index}, \hat{v}_{normal} \rangle \\ \langle \hat{v}_{middle}, \hat{v}_{normal} \rangle \\ \langle \hat{v}_{ring}, \hat{v}_{normal} \rangle \\ \langle \hat{v}_{little}, \hat{v}_{normal} \rangle \end{bmatrix} \tag{8-15}$$

where $\langle . \rangle$ is the dot product and $\|.\|$ signifies the norm of a vector. Obtained data can then be displayed and recorded based on treatment time and joint coordinates to accomplish required tasks in rehabilitations. For user interface operations, data frames are transferred into the Unity system. During the treatment, if the data frame matches one of the user inputs, an operation related to the command will be displayed on the user interface. Normalized Fist is a normalized value to quantify the measure of a fist hand pose. Angles between fingers and palm are used to find the normalized value. This parameter is zero for an open hand, and 1 for a fist hand pose to represent the closeness of fingers to each other. This parameter can be used to monitor the treatment progress. For instance, by comparing the normalized fist of an injured hand with a normal hand, some exercises can be prescribed to achieve treatment goals. Figure 8-7 shows a normalized fist of a user hand after following a predefined movement. To examine repeatability, hand measurements are tested for five times under same conditions.

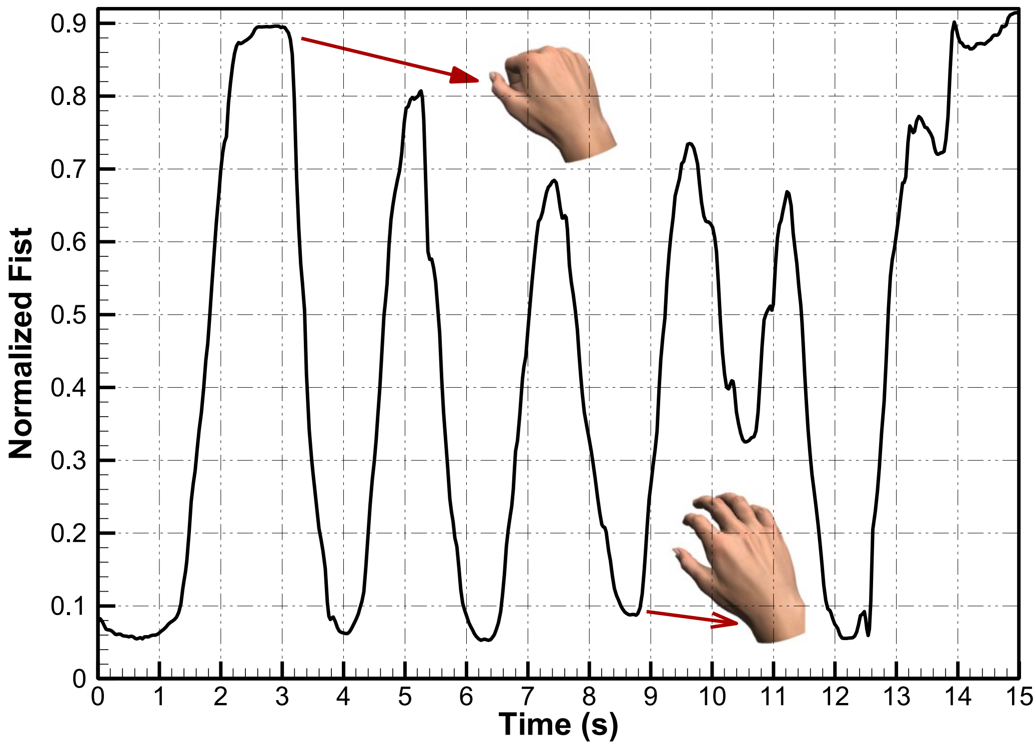

Figure 8-7 Normalized Fist of a user hand based on the angles between fingers and palm to measure the fist hand pose.

8.3 Discussion

The proposed system is examined in applications of the hand rehabilitation. Range of Motion (ROM) signifies an angle of the motion related to a specific axis. The angle is calculated at joints of fingers and wrist. The focus of the proposed system is the active ROM for users without using the external force in operations. The wrist recovery is one of the most common rehabilitation treatments [197]. During rehabilitations, patients usually follow instructions to regain the full ROM of their wrist [197]. The virtual environment together with the Leap Motion sensor provides an effective tool to measure the active ROM of fingers and wrist. By comparing measured ROM with the normal ROM of a healthy hand, users can evaluate their hand movements. The developed framework can accurately track, record and display the active ROM of the wrist of users. An example of the wrist ROM measured by the proposed system is shown in Figure 8-8. The active range of motion of the wrist is 0 to 85 degrees for flexion and 0 to 80 degrees for extension [198]. In the extension, the hand is raised up to bring the back of the hand closer to the upper side of the arm. In the flexion, the hand is moved from a palm down position to bring the palm adjacent to the arm underside.

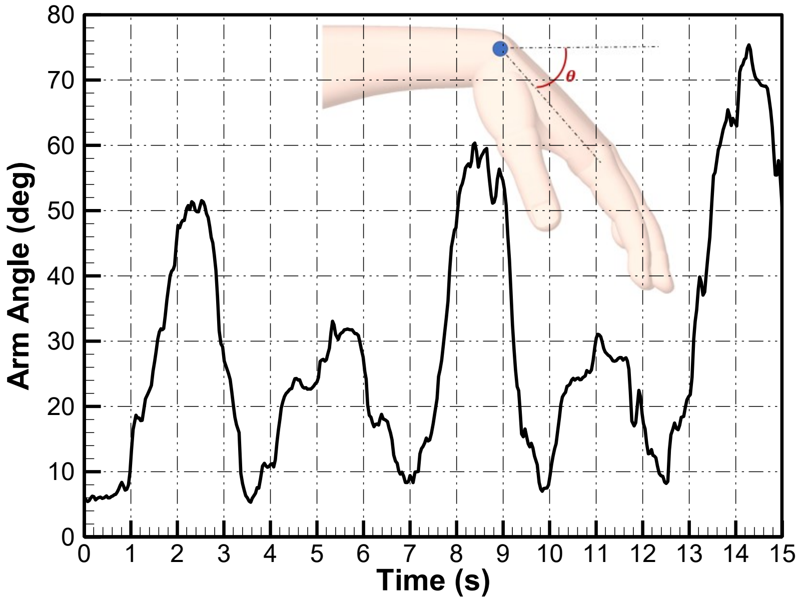

Figure 8-8 Example of the flexion and extension movements for achieving full range of motion of the wrist.

Based on widely used measurements like joint angles, and angular velocities of joints in the upper limb rehabilitation [199], the ROM is computed for the finger flexion-extension and abduction-adduction movements. The ROM of fingers during activities can show rigidity, one of the key measurements of the Parkinson's Disease (PD) [200]. Unlike PD patients, fingers can move in a certain rhythm throughout treatment for normal hands. A measure of rigidity is calculated using the time-based variation of joint positions during the treatment. For normal hands, the temporal evolution of joint angles is approximately periodic. In contrast, for individuals with difficulties in moving joints, it may not be periodic. The angular position of hand joints has a good measure to assess motion difficulties and improve treatment outcomes. For instance, an injured joint can lead to some difficulties in grasping or pinching objects for patients. By measuring the angle between hand joints, therapists can assess ROM of fingers in rehabilitations and monitor the treatment progress. An example of the joint angular data of a healthy hand for the thumb movement is shown in Figure 8-9. Variations in the joint angular velocity are approximated as differences in the joint angles between two consecutive frames in treatment. This parameter is a measure of the unbalanced activity if the value differs from the normal hand. The angular velocity of the thumb movement during a flexion-extension practice for a normal hand is calculated as shown in Figure 8-9 (b). As shown in this plot, the angular velocity of the joint follows some oscillations, however, de-noising data can suggest useful information for further analysis. Furthermore, joint angles and angular velocity data show the symmetry of motions. In the rehabilitation, the symmetry ratio is expressed by acceleration and deceleration times in one movement [201]. By determining angular velocities, a symmetry ratio can be calculated for normal and patient hands to analyze and quantify the outcome of PD treatments.

The proposed hand rehabilitation concept is fabricated and 3D-printed using ABS material. Figure 8-10 shows the first prototype of the device. It can be used for various rehabilitation treatments. The device uses 5 actuators to drive finger structures. It can be integrated with the developed virtual environment to track and record joint motion parameters. For more information about the developed device please refer to references [23, 202].

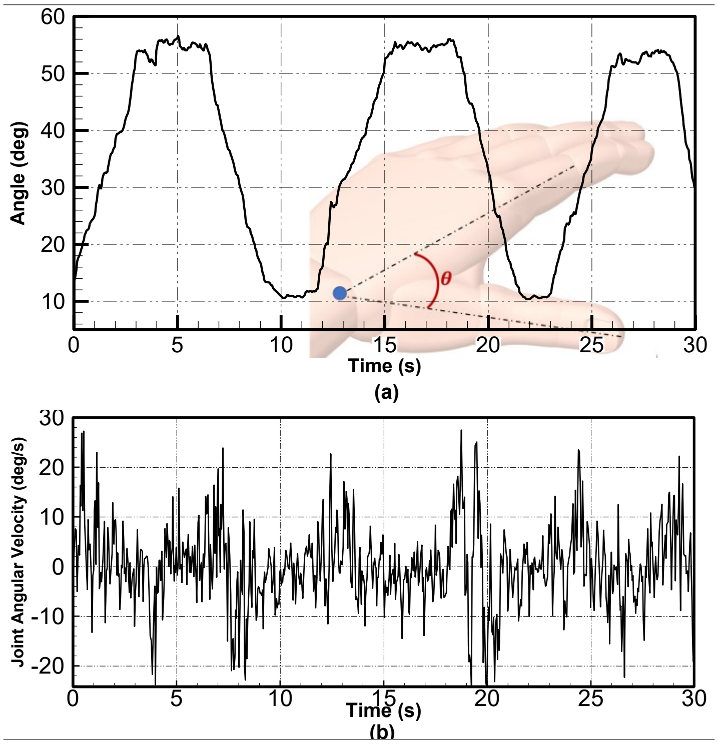

Figure 8-9 Measuring range of motion of hand joints. (a) Variation of finger joint angular data profiles during rotation of the thumb movement, (b) joint angular velocity data profiles during thumb flexion-extension movement for a normal hand.

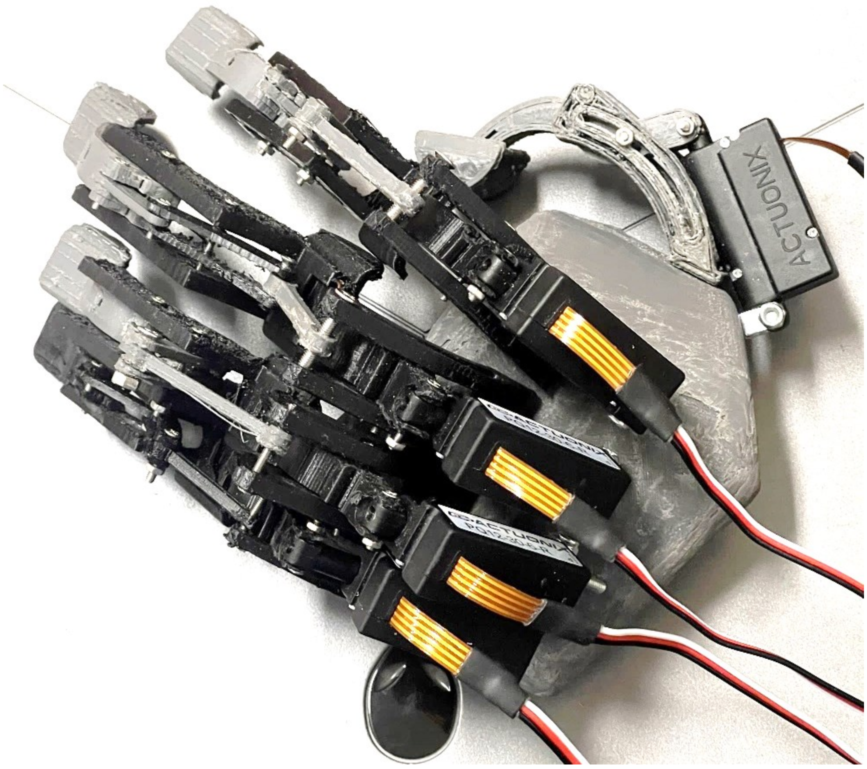

Figure 8-10 A prototype of the proposed device.

8.4 Summary

This chapter introduces a low-cost noncontact measurement system of the joint movement evaluation for hand rehabilitations. The developed system measures hand joint positions to calculate spatial temporal motion parameters of wrist and fingers. It requires the minimal human involvement to reduce errors in an interactive environment for analyzing and recording temporal data of different motion parameters of hands. The system uses data processing methods to analyze, record, and display exercise motion data of hand joints. The data can be displayed to users and assist their self-exercise. By assessing real-time data, hand movements can be evaluated to guide the exercising process. The introduced user interface supports the data process and trainings in rehabilitations to identify the order and difficulty of movements, and the treatment accuracy.

Chapter 9 Conclusion and Future Work

9.1 Research summary

In this thesis, different design approaches are developed to alleviate limitations of the existing methods for the product concept generation and evaluation. By applying the comprehensive approach developed in Chapter 6, designers can consider voice of customers and technical aspects simultaneously. Moreover, in Chapter Five, the quantitative analysis of traditional approaches with the proposed method shows that the proposed data processing in QFD provides more accurate results and better performance in terms of number of the pairwise comparison, total deviation, and consistency ratio. The case study of the hand rehabilitation device design proves that the proposed concept has superior advantages compared to the existing devices. The motion capture analysis shows that the tracking accuracy is appropriate for rehabilitation applications. The summary of the outcomes of this thesis are as follows:

The first research task introduces a method for analyzing the roof data of House of Quality (HOQ) to extract additional information of correlations between technical requirements based on the decision-making trial and evaluation laboratory, analytic network process, and quality function deployment. Comparing with the existing methods, the proposed method provides benefits of decision-making and time-saving for designers at early stages of the product design.

The second research task introduces two effective approaches based on Best-Worst Method and Full Consistency Method (FUCOM) to decide weights of TMs in the relationship matrix of HOQ. The novel integrated approach of FUCOM-QFD is developed for the rapid weight allocation in the relationship matrix. The proposed BWM-QFD and FUCOM-QFD approaches use a consistency ratio and the total deviation measure for reliable decision-making. The methods not only reduce the data collection, but also improve inconsistency problems. The vector-based pairwise comparison and consistency measure are two important features of the proposed approaches.

The third research task proposes an approach to generate and evaluate design concepts by integration of the extended Axiomatic Design, QFD and DSM. The domain mapping matrix is one of the essences of this approach to decide TMs, function requirements and design parameters based on customer requirements. The proposed approach provides a structured method to quantify, validate and qualify design concepts. A cases study of design of a hand rehabilitation device demonstrates effectiveness of the proposed method.

An automatic approach is introduced in research task four to apply reinforcement learning as an alternative solution of classical approaches to perform repetitive tasks in the product concept development and evaluation. A multi-agent reinforcement learning method is proposed to enable different agents working and learning together in a shared environment. The environment is formed for all agents to achieve the same objective collaboratively. A case study of designing a rehabilitation device is conducted to evaluate the effectiveness of the proposed approach. The solution shows the effectiveness of the proposed method with the time-saving advantage.

Finally in research task five, the proposed rehabilitation device concept is fabricated and validated. A low-cost system is developed to assist users and therapists to measure hand motions and analyze important data of hand joints. The system consists of modules of data capturing, data analysis, and user interface. Signal processing and wavelet de-noising methods are developed to improve accuracy of the data analysis. The proposed hand motion analysis approach is validated by a gold standard motion capturing system. The case study shows effectiveness of the proposed system.

9.2 Research contributions

1) Contributions to improve the correlation matrix in HOQ for product development are as follows.

- ❖ A systematic method is developed to decide TMs interactions and their influence on design solutions using information of the roof part in HOQ.

- ❖ Handling correlations in HOQ with DEAMETL is searched to evaluate relations between TMs and establish direct and indirect causal relationships and influence levels.
- ❖ DEMATEL-based analytic network process is proposed to efficiently model interrelations of TMs and reduce time-consuming pairwise comparisons.

2) Contributions to improve weighting solutions of relationship matrix are as follows.

- ❖ Accuracy and consistency are improved for normalized weights in the relationship matrix using optimization based on pairwise comparison vectors.
- ❖ A novel integrated approach of FUCOM-QFD is introduced for the rapid weight allocation in the relationship matrix.
- ❖ A vector-based pairwise comparison approach is implemented to significantly reduce the data collection in HOQ.
- ❖ A two-step QFD process is developed to map customer requirements, TMs, and design solutions to form design concepts based on customer requirements.

3) Contributions to product concept generation and evaluation are as follows.

- ❖ A domain mapping approach is proposed to translate customer requirements, functional requirements and design parameters into product attributes for analysis, synthesis and evaluation of design concepts.
- ❖ A decision support system is introduced based on the fuzzy-quality function deployment and multi-attributive border approximation area comparison (MABAC) to rank generated concepts.
- ❖ The integrated method is enabled by a holistic design approach to address the product's functional and non-functional requirements.
- ❖ A well-structured conceptual design process is empowered by technical feasibility evaluations using the design matrix and design structure matrix for the efficient design space exploration.

4) Contributions to reinforcement learning in generative product design are as follows.

- ❖ A scalable intelligent design architecture is proposed to use reinforcement learning for adaptable and optimum design decisions based on customer requirements.
- ❖ A multi-agent approach is developed to take the advantage of parallel design explorations for the collaborative design.
- ❖ A special reward function is formed to generate the optimal design concept.

5) Contributions made in the medical device design are as follows.

- ❖ A hand rehabilitation device is proposed to improve the existing devices.
- ❖ A graphical user interface is developed specifically for hand and finger rehabilitations to assist users track their treatments, record motion data, and support self-assessment of joint motions in rehabilitations.
- ❖ The proposed hand rehabilitation device is fabricated and prototyped.
- ❖ The virtual environment interface and hand motion analysis are validated to identify their accuracy for hand movements in rehabilitations.

9.3 Future work

The developed methods are demonstrated in the design of a hand rehabilitation device. The methods show effective design solutions and improved design attributes based on customer requirements and alleviate existing design limitations. As a general design approach, it can be extended to different industrial applications such as aerospace and manufacturing products where design complexities exist in the system required to simultaneously consider different aspects of customer, functional and physical domains.

Although the proposed approaches provide advantages for designers to generate, evaluate, and rank design concepts, there are some limitations. For example, in order to search the entire design space, there is a need of the database of multiples solutions to satisfy different functional requirements. Moreover, tuning training parameters to solve the design problem using the multi-agent approach is a challenging task. Therefore, it is suggested to develop adoptable agents to cover different design problems. The primary obstacles in this research involve creating a multi-agent learning technique that mimics the collaborative design process, functions an efficient optimization process, and enables agents to work on different variables of the problem. In order to improve adaptability of the agents to different scenarios, the future research will develop methods that enable agents to quickly adjust for new conditions. This includes not only fast re-training agents under changed circumstances, but also the accelerated transfer of the adapted policy to the agents. One potential strategy to achieve this could use a permanently trained agent within a design framework, followed by a policy transfer. Another approach to increase generalizability and performance under changing conditions could involve combining deep reinforcement learning with traditional decision-making and task decomposition approaches. In addition to the aforementioned points, research efforts should be directed to faster and more effective learning and performance of complex tasks by agents. In a multi-agent system, an individual agent could leverage experience gained by other agents and adapt better to unfamiliar situations. The development of such swarm intelligence could enhance the utilization of local and global information and enable a flexible response and adaptation of the product to unexpected events.

Papers published and submitted during this research

Following paper is related to contents of Chapter 4.

1. H. R. Fazeli and Q. Peng, Efficient Extraction of Information from Correlation Matrix for Product Design using an Integrated QFD-DEMATEL Method, *Computer-Aided Design & Applications,* vol. 18, no. 5, pp. 1131-1145, 2021.

Following paper is related to contents of Chapter 5.

2. H. R. Fazeli and Q. Peng, Integrated approaches of BWM-QFD and FUCOM-QFD for improving weighting solution of design matrix, *Journal of Intelligent Manufacturing,* 2021.

Following paper is related to contents of Chapter 6.

3. H. R. Fazeli and Q. Peng, Generation and evaluation of product concepts by integrating extended axiomatic design, quality function deployment and design structure matrix, *Advanced Engineering Informatics,* vol. 54, p. 101716, 2022.

Following paper is related to contents of Chapter 7.

4. H. R. Fazeli and Q. Peng, Generative Product Concept Development and Evaluation using Multi-Agent Reinforcement Learning *IEEE Transactions on Systems, Man, and Cybernetics Systems,* 2023. (under review)

Following papers is related to contents of Chapter 8.

5. H. R. Fazeli and Q. Peng, Estimation of spatial-temporal hand motion parameters in rehabilitation using a low-cost noncontact measurement system, *Medical Engineering & Physics,* vol. 90, pp. 43-53, 2021.

6. H. R. Fazeli, S. K. Venkatesh, and Q. Peng, A Virtual Environment for Hand Motion Analysis, *Procedia CIRP,* vol. 78, pp. 127-132, 2018.

References

1. Y. Mingshun, Y. Ting, L. Yanjie *et al.*, Rating the Customer Requirements based on DEMATEL and Entropy, *International Journal of Online Engineering,* vol. 9, 2013.

2. H. Zhang, X. Han, R. Li *et al.*, A new conceptual design method to support rapid and effective mapping from product design specification to concept design, *The International Journal of Advanced Manufacturing Technology,* vol. 87, no. 5, pp. 2375-2389, 2016/11/01, 2016.

3. G. Dieter, and L. Schmidt, *Engineering Design: Fifth Edition*: McGraw-Hill Higher Education, 2012.

4. S. Briceno, B. Laughlin, and D. N. Mavris, A Virtual Simulation Platform for the Design, Testing, and Verification of Unmanned Aerial Vehicle Designs, in 2014 Simulia Community Conference, Rhode Island (USA), 2014.

5. A. Jamnia, *Introduction to Product Design and Development for Engineers*: CRC Press, 2018.

6. V. Tiwari, P. K. Jain, and P. Tandon, Product design concept evaluation using rough sets and VIKOR method, *Advanced Engineering Informatics,* vol. 30, no. 1, pp. 16-25, 2016/01/01/, 2016.

7. M. K. Thompson, Improving the requirements process in Axiomatic Design Theory, *CIRP Annals,* vol. 62, no. 1, pp. 115-118, 2013/01/01/, 2013.

8. H. Bin, L. H. Feng, L. W. Zhen *et al.*, Automated Conceptual Design of Multiple Input and Multiple Output Mechanical Transmission System. pp. 78-82.

9. S. Devanathan, D. Ramanujan, W. Z. Bernstein *et al.*, Integration of Sustainability Into Early Design Through the Function Impact Matrix, *Journal of Mechanical Design,* vol. 132, no. 8, 2010.

10. Y. Kang, and D. Tang, Matrix-based computational conceptual design with ant colony optimisation, *Journal of Engineering Design,* vol. 24, no. 6, pp. 429-452, 2013/06/01, 2013.

11. D.-B. Luh, Y.-T. Ko, and C.-H. Ma, A structural matrix-based modelling for designing product variety, *Journal of Engineering Design,* vol. 22, no. 1, pp. 1-29, 2011/01/01, 2011.

12. D. George, R. Renu, and G. Mocko, Concept Generation Through Morphological and Options Matrices, *ICoRD'13.* pp. 199-210.

13. P. Kumar, and P. Tandon, A paradigm for customer-driven product design approach using extended axiomatic design, *Journal of Intelligent Manufacturing,* vol. 30, no. 2, pp. 589-603, 2019/02/01, 2019.

14. K. Sivasamy, C. Arumugam, S. R. Devadasan *et al.*, Advanced models of quality function deployment: a literature review, *Quality & Quantity,* vol. 50, no. 3, pp. 1399-1414, 2016/05/01, 2016.

15. N. Ozlem Erdil, and O. M. Arani, Quality function deployment: more than a design tool, *International Journal of Quality and Service Sciences,* vol. 11, no. 2, pp. 142-166, 2019.

16. D. Maritan, *Practical Manual of Quality Function Deployment*, Switzerland Springer International Publishing, 2014.

17. H. Raharjo, On normalizing the relationship matrix in quality function deployment, *International Journal of Quality & Reliability Management,* vol. 30, no. 6, pp. 647-661, 2013.

18. Z. Iqbal, N. P. Grigg, K. Govindaraju *et al.*, A distance-based methodology for increased extraction of information from the roof matrices in QFD studies, *International Journal of Production Research,* vol. 54, no. 11, pp. 3277-3293, 2016/06/02, 2016.

19. L.-H. Chen, and C.-N. Chen, Normalisation models for prioritising design requirements for quality function deployment processes, *International Journal of Production Research,* vol. 52, no. 2, pp. 299-313, 2014/01/17, 2014.

20. L.-H. Chen, and C.-N. Chen, A QFD-Based Mathematical Model for New Product Development Considering the Target Market Segment, *Journal of Applied Mathematics,* vol. 2014, pp. 594150, 2014/12/01, 2014.

21. I. van de Poel, Methodological problems in QFD and directions for future development, *Research in Engineering Design,* vol. 18, no. 1, pp. 21-36, 2007/05/01, 2007.

22. D. M. Camelo, and E. Mulet, A multi-relational and interactive model for supporting the design process in the conceptual phase, *Automation in Construction,* vol. 19, no. 7, pp. 964-974, 2010/11/01/, 2010.

23. H. R. Fazeli, and Q. Peng, Generation and evaluation of product concepts by integrating extended axiomatic design, quality function deployment and design structure matrix, *Advanced Engineering Informatics,* vol. 54, pp. 101716, 2022/10/01/, 2022.

24. I. Grubišić, H. Skala Kavanagh, and S. Grazio, Novel approaches in hand rehabilitation, *Periodicum biologorum,* vol. 117, no. 1, pp. 139-145, 2015.

25. F. Akasaka, Y. Nemoto, K. Kimita *et al.*, Development of a knowledge-based design support system for Product-Service Systems, *Computers in Industry,* vol. 63, no. 4, pp. 309-318, 2012/05/01/, 2012.

26. J.-C. Cong, C.-H. Chen, P. Zheng *et al.*, A holistic relook at engineering design methodologies for smart product-service systems development, *Journal of Cleaner Production,* vol. 272, pp. 122737, 2020/11/01/, 2020.

27. M. Tamhankar, and M. I. Campbell, An Intelligent and Efficient Tree Search Algorithm for Computer-Aided Component Selection. pp. 69-78.

28. Y.-G. Ghim, Experience matrix: A structured concept development method for the industrial design practice in new product development, *The Design Journal,* vol. 25, no. 2, pp. 205-224, 2022/03/04, 2022.

29. M. Leary, and C. Burvill, Enhancing the Quality Function Deployment Conceptual Design Tool, *Journal of Mechanical Design,* vol. 129, no. 7, pp. 701-708, 2007.

30. P. Palominos, L. E. Quezada, and M. A. Gonzalez, Incorporating the voice of the client in establishing the flexibility requirement in a production system, *International Journal of Production Economics,* vol. 211, pp. 34-43, 2019/05/01/, 2019.

31. C.-H. Lee, C.-H. Chen, and Y.-C. Lee, Customer requirement-driven design method and computer-aided design system for supporting service innovation conceptualization handling, *Advanced Engineering Informatics,* vol. 45, pp. 101117, 2020/08/01/, 2020.

32. O. A. Shvetsova, S. C. Park, and J. H. Lee, Application of Quality Function Deployment for Product Design Concept Selection, *Applied Sciences,* vol. 11, no. 6, pp. 2681, 2021.

33. A. Karasan, E. Ilbahar, S. Cebi *et al.*, Customer-oriented product design using an integrated neutrosophic AHP & DEMATEL & QFD methodology, *Applied Soft Computing,* vol. 118, pp. 108445, 2022/03/01/, 2022.

34. L.-Y. Zhai, L.-P. Khoo, and Z.-W. Zhong, A rough set based QFD approach to the management of imprecise design information in product development, *Advanced Engineering Informatics,* vol. 23, no. 2, pp. 222-228, 2009/04/01/, 2009.

35. J. Fan, S. Yu, J. Chu *et al.*, Research on multi-objective decision-making under cloud platform based on quality function deployment and uncertain linguistic variables, *Advanced Engineering Informatics,* vol. 42, pp. 100932, 2019/10/01/, 2019.

36. J. A. Carnevalli, P. A. C. Miguel, and F. A. Calarge, Axiomatic design application for minimising the difficulties of QFD usage, *International Journal of Production Economics,* vol. 125, no. 1, pp. 1-12, 2010/05/01/, 2010.

37. O. Kulak, S. Cebi, and C. Kahraman, Applications of axiomatic design principles: A literature review, *Expert Systems with Applications,* vol. 37, no. 9, pp. 6705-6717, 2010/09/01/, 2010.

38. S.-G. Kim, Axiomatic Design, *CIRP Encyclopedia of Production Engineering*, L. Laperrière and G. Reinhart, eds., pp. 72-76, Berlin, Heidelberg: Springer Berlin Heidelberg, 2014.

39. R. Xiao, and X. Cheng, Attribute Importance Determination of the Customer Needs for Product Family Based on Axiomatic Design and Conjoint Analysis, *Advances in Mechanical Design.* pp. 2341-2355.

40. Q. Liu, J. Chen, Y. Wu *et al.*, Linguistic Z-numbers and cloud model weighted ranking technology and its application in concept evaluation of information axiom, *The Journal of Supercomputing,* vol. 78, no. 5, pp. 6061-6089, 2022/04/01, 2022.

41. M. A. Mabrok, M. Efatmaneshnik, and M. J. Ryan, Integrating Nonfunctional Requirements Into Axiomatic Design Methodology, *IEEE Systems Journal,* vol. 11, no. 4, pp. 2204-2214, 2017.

42. D. Tang, G. Zhang, and S. Dai, Design as integration of axiomatic design and design structure matrix, *Robotics and Computer-Integrated Manufacturing,* vol. 25, no. 3, pp. 610-619, 2009/06/01/, 2009.

43. A. Mollajan, and S. H. Iranmanesh, Modularisation of system architecture to improve system recoverability: a unique application of design structure matrix, *Journal of Engineering Design,* vol. 32, no. 12, pp. 703-750, 2021/12/02, 2021.

44. A. H. Tilstra, C. C. Seepersad, and K. L. Wood, A high-definition design structure matrix (HDDSM) for the quantitative assessment of product architecture, *Journal of Engineering Design,* vol. 23, no. 10-11, pp. 767-789, 2012/11/01, 2012.

45. Q. Liu, K. Wang, Y. Li *et al.*, A novel function-structure concept network construction and analysis method for a smart product design system, *Advanced Engineering Informatics,* vol. 51, pp. 101502, 2022/01/01/, 2022.

46. C. He, Z.-k. Li, S. Wang *et al.*, A systematic data-mining-based methodology for product family design and product configuration, *Advanced Engineering Informatics,* vol. 48, pp. 101302, 2021/04/01/, 2021.

47. Z. Li, and D. Cao, Conceptual Design of Compliant Mechanism Based on Port Ontology, *Advances in Mechanical Engineering,* vol. 5, pp. 401492, 2013.

48. W. Z. Bernstein, D. Ramanujan, S. Devanathan *et al.*, Function Impact Matrix for Sustainable Concept Generation: A Designer's Perspective. pp. 377-383.

49. J. Cong, C.-H. Chen, and P. Zheng, Design entropy theory: A new design methodology for smart PSS development, *Advanced Engineering Informatics,* vol. 45, pp. 101124, 2020/08/01/, 2020.

50. J. J. Shah, S. M. Smith, and N. Vargas-Hernandez, Metrics for measuring ideation effectiveness, *Design Studies,* vol. 24, no. 2, pp. 111-134, 2003/03/01/, 2003.

51. T. Kurtoglu, M. I. Campbell, and J. S. Linsey, An experimental study on the effects of a computational design tool on concept generation, *Design Studies,* vol. 30, no. 6, pp. 676-703, 2009/11/01/, 2009.

52. G.-N. Zhu, J. Hu, J. Qi *et al.*, An integrated AHP and VIKOR for design concept evaluation based on rough number, *Advanced Engineering Informatics,* vol. 29, no. 3, pp. 408-418, 2015/08/01/, 2015.

53. J. Qi, J. Hu, H. Huang *et al.*, New customer-oriented design concept evaluation by using improved Z-number-based multi-criteria decision-making method, *Advanced Engineering Informatics,* vol. 53, pp. 101683, 2022/08/01/, 2022.

54. T. Caporaso, S. Grazioso, G. Di Gironimo *et al.*, Design of Wearables for Biosignal Acquisition: A User Centered Approach for Concept Generation and Selection, *Design Tools and Methods in Industrial Engineering II.* pp. 818-826.

55. W. Song, X. Ming, and Z. Wu, An integrated rough number-based approach to design concept evaluation under subjective environments, *Journal of Engineering Design,* vol. 24, no. 5, pp. 320-341, 2013/05/01, 2013.

56. Z. Ayağ, and R. G. özdemr, An analytic network process-based approach to concept evaluation in a new product development environment, *Journal of Engineering Design,* vol. 18, no. 3, pp. 209-226, 2007/06/01, 2007.

57. Y. Liu, Y. Han, J. Zhou *et al.*, Establishing the relationship matrix in QFD based on fuzzy regression models with optimized h values, *Soft Computing,* vol. 22, no. 17, pp. 5603-5615, 2018/09/01, 2018.

58. Y. Shi, Q. Peng, and J. Zhang, An Objective Weighting Method of Function Requirements for Product Design Using Information Entropy, *Computer-Aided Design and Applications,* vol. 17, no. 5, pp. 966-978, 2019.

59. F. Kutlu Gündoğdu, and C. Kahraman, A novel spherical fuzzy QFD method and its application to the linear delta robot technology development, *Engineering Applications of Artificial Intelligence,* vol. 87, pp. 103348, 2020/01/01/, 2020.

60. S. Li, D. Tang, and Q. Wang, Rating engineering characteristics in open design using a probabilistic language method based on fuzzy QFD, *Computers & Industrial Engineering,* vol. 135, pp. 348-358, 2019/09/01/, 2019.

61. S. Avikal, R. Singh, and R. Rashmi, QFD and Fuzzy Kano model based approach for classification of aesthetic attributes of SUV car profile, *Journal of Intelligent Manufacturing,* vol. 31, no. 2, pp. 271-284, 2020/02/01, 2020.

62. M. Yazdani, P. Chatterjee, and A. Ebadi Torkayesh, An Integrated AHP-QFD-Based Compromise Ranking Model for Sustainable Supplier Selection, *Handbook of Research on Interdisciplinary Approaches to Decision Making for Sustainable Supply Chains*, pp. 32-54, Hershey, PA, USA: IGI Global, 2020.

63. B. Song, Q. Peng, J. Zhang *et al.*, A Fuzzy Number based Hierarchy Analytic Method and Application in Improvement of Rehabilitation Devices, *Computer-Aided Design and Applications,* vol. 16, no. 2, pp. 369-381, 2019.

64. F. Zhang, M. Yang, and W. Liu, Using integrated quality function deployment and theory of innovation problem solving approach for ergonomic product design, *Computers & Industrial Engineering,* vol. 76, pp. 60-74, 2014/10/01/, 2014.

65. H. Zheng, H. Zhang, and F. Zhang, An innovative design of energy-saving products based on QFD/TRIZ/DEA integration. pp. 831-834.

66. J. Sharma, and A. Rawani, Ranking engineering characteristics in Quality Function Deployment by factoring-in the roof values, *International Journal of Productivity and Quality Management,* vol. 3, no. 2, pp. 223-240, 2008.

67. F. Chavoshi, and A. Shahin, Does correlation matrix influence prioritisation of the results of house of quality? The case of a manufacturing company, *International Journal of Productivity and Quality Management,* vol. 21, no. 2, pp. 174-186, 2017.

68. A. Shahin, E. Bagheri Iraj, and H. Vaez Shahrestani, Developing House of Quality by integrating top roof and side roof matrices and service TRIZ with a case study in banking services, *The TQM Journal,* vol. 28, no. 4, pp. 597-612, 2016.

69. A. K. Gupta, and B. A. Modi, Selection of Sustainable Technology for VOC Abatement in an Industry: An Integrated AHP–QFD Approach, *Journal of The Institution of Engineers (India): Series A,* vol. 99, no. 3, pp. 565-578, 2018/09/01, 2018.

70. D. K. Pal, B. Ravi, and L. S. Bhargava, Rapid tooling route selection for metal casting using QFD–ANP methodology, *International Journal of Computer Integrated Manufacturing,* vol. 20, no. 4, pp. 338-354, 2007/06/01, 2007.

71. Z. Ayağ, An integrated approach to concept evaluation in a new product development, *Journal of Intelligent Manufacturing,* vol. 27, no. 5, pp. 991-1005, 2016/10/01, 2016.

72. S. Moslem, M. Gul, D. Farooq *et al.*, An Integrated Approach of Best-Worst Method (BWM) and Triangular Fuzzy Sets for Evaluating Driver Behavior Factors Related to Road Safety, *Mathematics,* vol. 8, no. 3, pp. 414, 2020.

73. M. W. Herman, and W. W. Koczkodaj, A Monte Carlo study of pairwise comparison, *Information Processing Letters,* vol. 57, no. 1, pp. 25-29, 1996/01/15/, 1996.

74. J. Rezaei, Best-worst multi-criteria decision-making method: Some properties and a linear model, *Omega,* vol. 64, pp. 126-130, 2016/10/01/, 2016.

75. D. Pamučar, Ž. Stević, and S. Sremac, A New Model for Determining Weight Coefficients of Criteria in MCDM Models: Full Consistency Method (FUCOM), *Symmetry,* vol. 10, no. 9, pp. 393, 2018.

76. H. Raharjo, On normalizing the relationship matrix in quality function deployment, *International Journal of Quality & Reliability Management,* vol. 30, no. 6, pp. 647-661, 2013.

77. J. Huang, X.-Y. You, H.-C. Liu *et al.*, New approach for quality function deployment based on proportional hesitant fuzzy linguistic term sets and prospect theory, *International Journal of Production Research,* vol. 57, no. 5, pp. 1283-1299, 2019/03/04, 2019.

78. A. Shahin, and S. Akasheh, Classifying customer requirements using Kano model and Kano map: the case of hospital services, *International Journal of Productivity and Quality Management,* vol. 21, no. 4, pp. 500-515, 2017.

79. E. Dace, A. Stibe, and L. Timma, A holistic approach to manage environmental quality by using the Kano model and social cognitive theory, *Corporate Social Responsibility and Environmental Management,* vol. 27, no. 2, pp. 430-443, 2020.

80. A. Chaudha, R. Jain, A. R. Singh *et al.*, Integration of Kano's Model into quality function deployment (QFD), *The International Journal of Advanced Manufacturing Technology,* vol. 53, no. 5, pp. 689-698, 2011/03/01, 2011.

81. F. Feizi, A. Karbalaei-Ramezanali, and H. Tusi, Mineral Potential Mapping Via TOPSIS with Hybrid AHP–Shannon Entropy Weighting of Evidence: A Case Study for Porphyry-Cu, Farmahin

Area, Markazi Province, Iran, *Natural Resources Research,* vol. 26, no. 4, pp. 553-570, 2017/10/01, 2017.

82. K. Jenab, H. Pourmohammadi, and M. Sarfaraz, An i-AHP&QFD warranty model, *Benchmarking: An International Journal,* vol. 21, no. 6, pp. 884-902, 2014.

83. C. Ucler, Brainstorming the cryoplane layout by using the iterative AHP-QFD-AHP approach, *Aviation,* vol. 21, no. 2, pp. 55-63, 2017.

84. K. Venkata Subbaiah, K. Yeshwanth Sai, and C. Suresh, QFD–ANP Approach for the Conceptual Design of Research Vessels: A Case Study, *Journal of The Institution of Engineers (India): Series C,* vol. 97, no. 4, pp. 539-546, 2016/10/01, 2016.

85. Y. Fu, M. Li, H. Luo *et al.*, Industrial robot selection using stochastic multicriteria acceptability analysis for group decision making, *Robotics and Autonomous Systems,* vol. 122, pp. 103304, 2019/12/01/, 2019.

86. D.-k. Chen, Y.-q. Wang, N. Jin *et al.*, The Application of QFD and Information Entropy in Improved Design for the Manned Capsule. pp. 371-379.

87. H.-Y. Wu, and H.-Y. Lin, A hybrid approach to develop an analytical model for enhancing the service quality of e-learning, *Computers & Education,* vol. 58, no. 4, pp. 1318-1338, 2012/05/01/, 2012.

88. H. Zhao, L. Yao, G. Mei *et al.*, A Fuzzy Comprehensive Evaluation Method Based on AHP and Entropy for a Landslide Susceptibility Map, *Entropy,* vol. 19, no. 8, pp. 396, 2017.

89. Z. Ding, M. Zhu, Z. Wu *et al.*, Combining AHP-Entropy Approach with GIS for Construction Waste Landfill Selection—A Case Study of Shenzhen, *International Journal of Environmental Research and Public Health,* vol. 15, no. 10, pp. 2254, 2018.

90. N. Mou, C. Wang, T. Yang *et al.*, Evaluation of Development Potential of Ports in the Yangtze River Delta Using FAHP-Entropy Model, *Sustainability,* vol. 12, no. 2, pp. 493, 2020.

91. M. Yazdani, C. Kahraman, P. Zarate *et al.*, A fuzzy multi attribute decision framework with integration of QFD and grey relational analysis, *Expert Systems with Applications,* vol. 115, pp. 474-485, 2019/01/01/, 2019.

92. N. Haber, M. Fargnoli, and T. Sakao, Integrating QFD for product-service systems with the Kano model and fuzzy AHP, *Total Quality Management & Business Excellence,* vol. 31, no. 9-10, pp. 929-954, 2020/07/03, 2020.

93. M. Z. Mistarihi, R. A. Okour, and A. A. Mumani, An integration of a QFD model with Fuzzy-ANP approach for determining the importance weights for engineering characteristics of the proposed wheelchair design, *Applied Soft Computing,* vol. 90, pp. 106136, 2020/05/01/, 2020.

94. G. Tian, H. Zhang, M. Zhou *et al.*, AHP, Gray Correlation, and TOPSIS Combined Approach to Green Performance Evaluation of Design Alternatives, *IEEE Transactions on Systems, Man, and Cybernetics: Systems,* vol. 48, no. 7, pp. 1093-1105, 2018.

95. X. Mi, M. Tang, H. Liao *et al.*, The state-of-the-art survey on integrations and applications of the best worst method in decision making: Why, what, what for and what's next?, *Omega,* vol. 87, pp. 205-225, 2019/09/01/, 2019.

96. A. Olewnik, and K. Lewis, Limitations of the House of Quality to provide quantitative design information, *International Journal of Quality & Reliability Management,* vol. 25, no. 2, pp. 125-146, 2008.

97. F. Franceschini, *Advanced Quality Function Deployment*: CRC Press, 2016.

98. H. Raharjo, A. C. Brombacher, and M. Xie, Dealing with subjectivity in early product design phase: A systematic approach to exploit Quality Function Deployment potentials, *Computers & Industrial Engineering,* vol. 55, no. 1, pp. 253-278, 2008/08/01/, 2008.

99. J. Rezaei, Best-worst multi-criteria decision-making method, *Omega,* vol. 53, pp. 49-57, 2015/06/01/, 2015.

100. S. Karapetrovic, and E. S. Rosenbloom, A quality control approach to consistency paradoxes in AHP, *European Journal of Operational Research,* vol. 119, no. 3, pp. 704-718, 1999/12/16/, 1999.

101. A. Tiwari, V. Oduguwa, and R. Roy, Rolling System Design Using Evolutionary Sequential Process Optimization, *IEEE Transactions on Evolutionary Computation,* vol. 12, no. 2, pp. 196-202, 2008.

102. C. Krahe, A. Bräunche, A. Jacob *et al.*, Deep Learning for Automated Product Design, *Procedia CIRP,* vol. 91, pp. 3-8, 2020/01/01/, 2020.

103. E. Rigger, K. Shea, and T. Stankovic, Task categorisation for identification of design automation opportunities, *Journal of Engineering Design,* vol. 29, no. 3, pp. 131-159, 2018/03/04, 2018.

104. P. Burggräf, J. Wagner, and T. Weißer, Knowledge-based problem solving in physical product development—A methodological review, *Expert Systems with Applications: X,* vol. 5, pp. 100025, 2020/04/01/, 2020.

105. X. Fei, J. Branke, and N. Gülpınar, New Sampling Strategies When Searching for Robust Solutions, *IEEE Transactions on Evolutionary Computation,* vol. 23, no. 2, pp. 273-287, 2019.

106. Y. Yu, T. Hur, J. Jung *et al.*, Deep learning for determining a near-optimal topological design without any iteration, *Structural and Multidisciplinary Optimization,* vol. 59, no. 3, pp. 787-799, 2019/03/01, 2019.

107. M. H. Rahman, C. Xie, and Z. Sha, A Deep Learning Based Approach to Predict Sequential Design Decisions.

108. X. Du, and F. Zhu, A new data-driven design methodology for mechanical systems with high dimensional design variables, *Advances in Engineering Software,* vol. 117, pp. 18-28, 2018/03/01/, 2018.

109. X. Lu, S. Menzel, K. Tang *et al.*, Cooperative Co-Evolution-Based Design Optimization: A Concurrent Engineering Perspective, *IEEE Transactions on Evolutionary Computation,* vol. 22, no. 2, pp. 173-188, 2018.

110. D. Hulse, K. Tumer, C. Hoyle *et al.*, Modeling multidisciplinary design with multiagent learning, *Artificial Intelligence for Engineering Design, Analysis and Manufacturing,* vol. 33, no. 1, pp. 85-99, 2018.

111. W. J. C. Verhagen, P. Bermell-Garcia, R. E. C. van Dijk *et al.*, A critical review of Knowledge-Based Engineering: An identification of research challenges, *Advanced Engineering Informatics,* vol. 26, no. 1, pp. 5-15, 2012/01/01/, 2012.

112. Z. Pirmoradi, G. G. Wang, and T. W. Simpson, *A Review of Recent Literature in Product Family Design and Platform-Based Product Development*, New York, NY: Springer New York, 2014.

113. I. As, S. Pal, and P. Basu, Artificial intelligence in architecture: Generating conceptual design via deep learning, *International Journal of Architectural Computing,* vol. 16, no. 4, pp. 306-327, 2018.

114. S. W. Kang, and C. S. Tucker, Automated Concept Generation Based on Function-Form Synthesis.

115. Y. Pan, A. Burnap, J. Hartley *et al.*, Deep Design: Product Aesthetics for Heterogeneous Markets, in Proceedings of the 23rd ACM SIGKDD International Conference on Knowledge Discovery and Data Mining, Halifax, NS, Canada, 2017, pp. 1961–1970.

116. B. Li, Y. Wang, K. Wang *et al.*, Application of CNN Deep Learning in Product Design Evaluation, *Advanced Manufacturing and Automation VIII.* pp. 517-526.

117. I. J. Goodfellow, J. Pouget-Abadie, M. Mirza *et al.*, Generative adversarial networks, *arXiv preprint arXiv:1406.2661*, 2014.

118. A. Burnap, Y. Liu, Y. Pan *et al.*, Estimating and Exploring the Product Form Design Space Using Deep Generative Models.

119. M. Andries, A. Dehban, and J. Santos-Victor, Automatic Generation of Object Shapes With Desired Affordances Using Voxelgrid Representation, *Frontiers in Neurorobotics,* vol. 14, no. 22, 2020-May-14, 2020.

120. X. Y. Lee, A. Balu, D. Stoecklein *et al.*, A Case Study of Deep Reinforcement Learning for Engineering Design: Application to Microfluidic Devices for Flow Sculpting, *Journal of Mechanical Design,* vol. 141, no. 11, 2019.

121. H. Cui, O. Turan, and P. Sayer, Learning-based ship design optimization approach, *Computer-Aided Design,* vol. 44, no. 3, pp. 186-195, 2012/03/01/, 2012.

122. J. P. Wang, Y. K. Shi, W. S. Zhang *et al.*, Multitask Policy Adversarial Learning for Human-Level Control With Large State Spaces, *IEEE Transactions on Industrial Informatics,* vol. 15, no. 4, pp. 2395-2404, 2019.

123. X. Cai, H. Qiu, L. Gao *et al.*, Metamodeling for high dimensional design problems by multi-fidelity simulations, *Structural and Multidisciplinary Optimization,* vol. 56, no. 1, pp. 151-166, 2017/07/01, 2017.

124. D. Hulse, K. Tumer, C. Hoyle *et al.*, Modeling Collaboration in Parameter Design Using Multiagent Learning, *Design Computing and Cognition '18.* pp. 577-593.

125. J. Choi, M. Hyun, and N. Kwak, Task-oriented Design through Deep Reinforcement Learning, *arXiv preprint arXiv:1903.05271*, 2019.

126. M. Sarmad, H. J. Lee, and Y. M. Kim, RL-GAN-Net: A Reinforcement Learning Agent Controlled GAN Network for Real-Time Point Cloud Shape Completion. pp. 5891-5900.

127. J. P. S. Chhabra, and G. P. Warn, A method for model selection using reinforcement learning when viewing design as a sequential decision process, *Structural and Multidisciplinary Optimization,* vol. 59, no. 5, pp. 1521-1542, 2019/05/01, 2019.

128. J. Pandremenos, and G. Chryssolouris, A neural network approach for the development of modular product architectures, *International Journal of Computer Integrated Manufacturing,* vol. 24, no. 10, pp. 879-887, 2011/09/01, 2011.

129. M. Panzer, and B. Bender, Deep reinforcement learning in production systems: a systematic literature review, *International Journal of Production Research,* vol. 60, no. 13, pp. 4316-4341, 2022/07/03, 2022.

130. H.-n. Wang, N. Liu, Y.-y. Zhang *et al.*, Deep reinforcement learning: a survey, *Frontiers of Information Technology & Electronic Engineering,* vol. 21, no. 12, pp. 1726-1744, 2020/12/01, 2020.

131. M. Naeem, S. T. H. Rizvi, and A. Coronato, A Gentle Introduction to Reinforcement Learning and its Application in Different Fields, *IEEE Access,* vol. 8, pp. 209320-209344, 2020.

132. J.-H. Lee, and H.-J. Kim, Reinforcement learning for robotic flow shop scheduling with processing time variations, *International Journal of Production Research,* vol. 60, no. 7, pp. 2346-2368, 2022/04/03, 2022.

133. L. Regenwetter, A. H. Nobari, and F. Ahmed, Deep Generative Models in Engineering Design: A Review, *Journal of Mechanical Design,* vol. 144, no. 7, 2022.

134. A. Raina, L. Puentes, J. Cagan *et al.*, Goal-Directed Design Agents: Integrating Visual Imitation With One-Step Lookahead Optimization for Generative Design, *Journal of Mechanical Design,* vol. 143, no. 12, 2021.

135. M. E. Ororbia, and G. P. Warn, Design Synthesis Through a Markov Decision Process and Reinforcement Learning Framework, *Journal of Computing and Information Science in Engineering,* vol. 22, no. 2, 2021.

136. J. Rabault, M. Kuchta, A. Jensen *et al.*, Artificial neural networks trained through deep reinforcement learning discover control strategies for active flow control, *Journal of Fluid Mechanics,* vol. 865, pp. 281-302, 2019.

137. J. Rabault, and A. Kuhnle, Accelerating deep reinforcement learning strategies of flow control through a multi-environment approach, *Physics of Fluids,* vol. 31, no. 9, pp. 094105, 2019.

138. H. Tang, J. Rabault, A. Kuhnle *et al.*, Robust active flow control over a range of Reynolds numbers using an artificial neural network trained through deep reinforcement learning, *Physics of Fluids,* vol. 32, no. 5, pp. 053605, 2020.

139. W. Liu, R. Wang, T. Zhang *et al.*, Hybridization of evolutionary algorithm and deep reinforcement learning for multi-objective orienteering optimization, *IEEE Transactions on Evolutionary Computation*, pp. 1-1, 2022.

140. K. Hayashi, and M. Ohsaki, Reinforcement Learning and Graph Embedding for Binary Truss Topology Optimization Under Stress and Displacement Constraints, *Frontiers in Built Environment,* vol. 6, 2020-April-30, 2020.

141. N. F. Soria Zurita, M. K. Colby, I. Y. Tumer *et al.*, Design of Complex Engineered Systems Using Multi-Agent Coordination, *Journal of Computing and Information Science in Engineering,* vol. 18, no. 1, 2017.

142. S.-G. Kim, S. M. Yoon, M. Yang *et al.*, AI for design: Virtual design assistant, *CIRP Annals,* vol. 68, no. 1, pp. 141-144, 2019/01/01/, 2019.

143. E. Rauch, and D. T. Matt, Artificial Intelligence in Design: A Look into the Future of Axiomatic Design, *Design Engineering and Science*, N. P. Suh, M. Cavique and J. T. Foley, eds., pp. 585-603, Cham: Springer International Publishing, 2021.

144. M. Ruiz-Montiel, J. Boned, J. Gavilanes *et al.*, Design with shape grammars and reinforcement learning, *Advanced Engineering Informatics,* vol. 27, no. 2, pp. 230-245, 2013/04/01/, 2013.

145. L. Mandow, J.-L. Pérez-de-la-Cruz, A. B. Rodríguez-Gavilán *et al.*, Architectural planning with shape grammars and reinforcement learning: Habitability and energy efficiency, *Engineering Applications of Artificial Intelligence,* vol. 96, pp. 103909, 2020/11/01/, 2020.

146. C. Li, P. Zheng, Y. Yin *et al.*, Deep reinforcement learning in smart manufacturing: A review and prospects, *CIRP Journal of Manufacturing Science and Technology,* vol. 40, pp. 75-101, 2023/02/01/, 2023.

147. V. Samsonov, K. Ben Hicham, and T. Meisen, Reinforcement Learning in Manufacturing Control: Baselines, challenges and ways forward, *Engineering Applications of Artificial Intelligence,* vol. 112, pp. 104868, 2022/06/01/, 2022.

148. K. Xia, C. Sacco, M. Kirkpatrick *et al.*, A digital twin to train deep reinforcement learning agent for smart manufacturing plants: Environment, interfaces and intelligence, *Journal of Manufacturing Systems,* vol. 58, pp. 210-230, 2021/01/01/, 2021.

149. C.-F. Chien, and Y.-B. Lan, Agent-based approach integrating deep reinforcement learning and hybrid genetic algorithm for dynamic scheduling for Industry 3.5 smart production, *Computers & Industrial Engineering,* vol. 162, pp. 107782, 2021/12/01/, 2021.

150. Y. Liu, M. Yang, and Z. Guo, Reinforcement learning based optimal decision making towards product lifecycle sustainability, *International Journal of Computer Integrated Manufacturing,* vol. 35, no. 10-11, pp. 1269-1296, 2022/11/02, 2022.

151. X. Zhao, C. Li, Y. Tang *et al.*, Reinforcement Learning-Based Selective Disassembly Sequence Planning for the End-of-Life Products With Structure Uncertainty, *IEEE Robotics and Automation Letters,* vol. 6, no. 4, pp. 7807-7814, 2021.

152. A. M. Farid, and L. Ribeiro, An Axiomatic Design of a Multiagent Reconfigurable Mechatronic System Architecture, *IEEE Transactions on Industrial Informatics,* vol. 11, no. 5, pp. 1142-1155, 2015.

153. P. Zheng, L. Xia, C. Li *et al.*, Towards Self-X cognitive manufacturing network: An industrial knowledge graph-based multi-agent reinforcement learning approach, *Journal of Manufacturing Systems,* vol. 61, pp. 16-26, 2021/10/01/, 2021.

154. T. Brito, J. Queiroz, L. Piardi *et al.*, A Machine Learning Approach for Collaborative Robot Smart Manufacturing Inspection for Quality Control Systems, *Procedia Manufacturing,* vol. 51, pp. 11-18, 2020/01/01/, 2020.

155. X. G. Luo, C. K. Kwong, J. F. Tang *et al.*, QFD-Based Product Planning With Consumer Choice Analysis, *IEEE Transactions on Systems, Man, and Cybernetics: Systems,* vol. 45, no. 3, pp. 454-461, 2015.

156. M. M. H. Chowdhury, and M. A. Quaddus, A multi-phased QFD based optimization approach to sustainable service design, *International Journal of Production Economics,* vol. 171, pp. 165-178, 2016/01/01/, 2016.

157. G. S. Wasserman, ON HOW TO PRIORITIZE DESIGN REQUIREMENTS DURING THE QFD PLANNING PROCESS, *IIE Transactions,* vol. 25, no. 3, pp. 59-65, 1993/05/01, 1993.

158. H. R. Fazeli, and Q. Peng, Integrated approaches of BWM-QFD and FUCOM-QFD for improving weighting solution of design matrix, *Journal of Intelligent Manufacturing*, 2021/09/29, 2021.

159. Z.-Q. Wang, Z.-S. Chen, H. Garg *et al.*, An integrated quality-function-deployment and stochastic-dominance-based decision-making approach for prioritizing product concept alternatives, *Complex & Intelligent Systems,* vol. 8, no. 3, pp. 2541-2556, 2022/06/01, 2022.

160. L. P. Khoo, and N. C. Ho, Framework of a fuzzy quality function deployment system, *International Journal of Production Research,* vol. 34, no. 2, pp. 299-311, 1996/02/01, 1996.

161. J. Delaram, and O. Fatahi Valilai, An architectural view to computer integrated manufacturing systems based on Axiomatic Design Theory, *Computers in Industry,* vol. 100, pp. 96-114, 2018/09/01/, 2018.

162. S. Wang, Z. Li, C. He *et al.*, An Integrated Method for Modular Design Based on Auto-Generated Multi-Attribute DSM and Improved Genetic Algorithm, *Symmetry,* vol. 14, no. 1, pp. 48, 2022.

163. S. D. Eppinger, and T. R. Browning, *Design Structure Matrix Methods and Applications*: MIT Press, 2012.

164. S.-L. Si, X.-Y. You, H.-C. Liu *et al.*, DEMATEL technique: A systematic review of the state-of-the-art literature on methodologies and applications, *Mathematical Problems in Engineering,* vol. 2018, 2018.

165. A. Mentes, H. Akyildiz, and I. H. Helvacioglu, A Grey Based Dematel Technıque for Rısk Assessment of Cargo Shıps.

166. A. Shahin, E. Bagheri Iraj, and H. Vaez Shahrestani, Developing the C-shaped QFD 3D Matrix for service applications with a case study in banking services, *International Journal of Quality & Reliability Management,* vol. 35, no. 1, pp. 109-125, 2018.

167. D. Vujanović, V. Momčilović, N. Bojović *et al.*, Evaluation of vehicle fleet maintenance management indicators by application of DEMATEL and ANP, *Expert Systems with Applications,* vol. 39, no. 12, pp. 10552-10563, 2012/09/15/, 2012.

168. J. L. Yang, and G.-H. Tzeng, An integrated MCDM technique combined with DEMATEL for a novel cluster-weighted with ANP method, *Expert Systems with Applications,* vol. 38, no. 3, pp. 1417-1424, 2011/03/01/, 2011.

169. S. Kheybari, F. M. Rezaie, and H. Farazmand, Analytic network process: An overview of applications, *Applied Mathematics and Computation,* vol. 367, pp. 124780, 2020/02/15/, 2020.

170. A. Elnady, W. B. Mortenson, and C. Menon, Perceptions of Existing Wearable Robotic Devices for Upper Extremity and Suggestions for Their Development: Findings From Therapists and People With Stroke, *JMIR rehabilitation and assistive technologies,* vol. 5, no. 1, pp. e12-e12, 2018.

171. Q. A. Boser, M. R. Dawson, J. S. Schofield *et al.*, Defining the design requirements for an assistive powered hand exoskeleton, *bioRxiv*, 2018.

172. M. Suarez-Escobar, J. A. Gallego-Sanchez, and E. Rendon-Velez, Mechanisms for linkage-driven underactuated hand exoskeletons: conceptual design including anatomical and mechanical specifications, *International Journal on Interactive Design and Manufacturing (IJIDeM),* vol. 11, no. 1, pp. 55-75, 2017/02/01, 2017.

173. F. Aggogeri, T. Mikolajczyk, and J. O'Kane, Robotics for rehabilitation of hand movement in stroke survivors, *Advances in Mechanical Engineering,* vol. 11, no. 4, pp. 1–14, 2019.

174. J. Rezaei, W. S. van Roekel, and L. Tavasszy, Measuring the relative importance of the logistics performance index indicators using Best Worst Method, *Transport Policy,* vol. 68, pp. 158-169, 2018/09/30/, 2018.

175. Q. Dong, and D. E. Whitney, Designing a Requirement Driven Product Development Process. pp. 11-20.

176. D. Pamučar, and G. Ćirović, The selection of transport and handling resources in logistics centers using Multi-Attributive Border Approximation area Comparison (MABAC), *Expert Systems with Applications,* vol. 42, no. 6, pp. 3016-3028, 2015/04/15/, 2015.

177. E. B. Brokaw, I. Black, R. J. Holley *et al.*, Hand Spring Operated Movement Enhancer (HandSOME): A Portable, Passive Hand Exoskeleton for Stroke Rehabilitation, *IEEE Transactions on Neural Systems and Rehabilitation Engineering,* vol. 19, no. 4, pp. 391-399, 2011.

178. F. Aggogeri, T. Mikolajczyk, and J. O'Kane, Robotics for rehabilitation of hand movement in stroke survivors, *Advances in Mechanical Engineering,* vol. 11, no. 4, pp. 1687814019841921, 2019/04/01, 2019.

179. P. Heo, G. M. Gu, S.-j. Lee *et al.*, Current hand exoskeleton technologies for rehabilitation and assistive engineering, *International Journal of Precision Engineering and Manufacturing,* vol. 13, no. 5, pp. 807-824, 2012/05/01, 2012.

180. J. Iqbal, H. Khan, N. G. Tsagarakis *et al.*, A novel exoskeleton robotic system for hand rehabilitation – Conceptualization to prototyping, *Biocybernetics and Biomedical Engineering,* vol. 34, no. 2, pp. 79-89, 2014/01/01/, 2014.

181. E. D. Oña, R. Cano-de la Cuerda, P. Sánchez-Herrera *et al.*, A Review of Robotics in Neurorehabilitation: Towards an Automated Process for Upper Limb, *Journal of Healthcare Engineering,* vol. 2018, pp. 9758939, 2018/04/01, 2018.

182. J. Huang, X. Tu, and J. He, Design and Evaluation of the RUPERT Wearable Upper Extremity Exoskeleton Robot for Clinical and In-Home Therapies, *IEEE Transactions on Systems, Man, and Cybernetics: Systems,* vol. 46, no. 7, pp. 926-935, 2016.

183. H. R. Fazeli, and Q. Peng, Estimation of Spatial-Temporal Hand Motion Parameters in Rehabilitation Using a Low-cost Noncontact Measurement System, *Medical Engineering & Physics*, 2021/02/23/, 2021.

184. A. Grandi, A. Prakash Karthikeyan, E. Vieira Vaz Junior *et al.*, Exoskeleton for Post-Stroke Hand Rehabilitation, *CAD'21 Proceeding*.

185. A. M. Farid, and N. P. Suh, *Axiomatic Design in Large Systems: Complex Products, Buildings and Manufacturing Systems*: Springer International Publishing, 2016.

186. M.-A. Dittrich, and S. Fohlmeister, Cooperative multi-agent system for production control using reinforcement learning, *CIRP Annals,* vol. 69, no. 1, pp. 389-392, 2020/01/01/, 2020.

187. S. Spielberg, A. Tulsyan, N. P. Lawrence *et al.*, Toward self-driving processes: A deep reinforcement learning approach to control, *AIChE Journal,* vol. 65, no. 10, pp. e16689, 2019.

188. Y. Bouteraa, I. B. Abdallah, and A. M. Elmogy, Training of Hand Rehabilitation Using Low Cost Exoskeleton and Vision-Based Game Interface, *Journal of Intelligent & Robotic Systems,* vol. 96, no. 1, pp. 31-47, 2019/10/01, 2019.

189. Y. Hou, Y. S. Ong, L. Feng *et al.*, An Evolutionary Transfer Reinforcement Learning Framework for Multiagent Systems, *IEEE Transactions on Evolutionary Computation,* vol. 21, no. 4, pp. 601-615, 2017.

190. L. O. R. Nájera, M. L. Sánchez, J. G. G. Serna *et al.*, Recognition of Mexican Sign Language through the Leap Motion Controller, in Proceedings of the International Conference on Scientific Computing (CSC), 2016, pp. 147.

191. B. Liu, S. Masuko, and J. Tanaka, Interactive Point System Supporting Point Classification and Spatial Visualization, *Human Interface and the Management of Information. Interaction, Visualization, and Analytics.* pp. 78-89.

192. P. Fuchs, VR Headsets *Virtual Reality Headsets - A Theoretical and Pragmatic Approach*: CRC Press, 2017.

193. F. Weichert, D. Bachmann, B. Rudak *et al.*, Analysis of the accuracy and robustness of the leap motion controller, *Sensors,* vol. 13, no. 5, pp. 6380-6393, 2013.

194. P. Chophuk, S. Chumpen, S. Tungjitkusolmun *et al.*, Hand postures for evaluating trigger finger using leap motion controller. pp. 1-4.

195. H. M. Tun, W. K. Moe, and Z. M. Naing, Analysis on ECG Data Compression Using Wavelet Transform Technique, *International Journal of Psychological and Brain Sciences,* vol. 2, no. 6, pp. 127, 2017.

196. A. Kumar, T. S. Mundra, and A. Kumar, Anatomy of Hand, *Encyclopedia of Biometrics*, S. Z. Li and A. Jain, eds., pp. 28-35, Boston, MA: Springer US, 2009.

197. K. K. Ang, C. Guan, K. S. Phua *et al.*, Brain-computer interface-based robotic end effector system for wrist and hand rehabilitation: results of a three-armed randomized controlled trial for chronic stroke, *Frontiers in Neuroengineering,* vol. 7, no. 30, 2014-July-29, 2014.

198. P. Page, and T. S. Ellenbecker, Specific training, *The Scientific and Clinical Application of Elastic Resistance*: Human Kinetics, 2003.

199. S. Spasojević, T. V. Ilić, S. Milanović *et al.*, Combined vision and wearable sensors-based system for movement analysis in rehabilitation, *Methods of information in medicine,* vol. 56, no. 02, pp. 95-111, 2017.

200. J. Jankovic, Parkinson’s disease: clinical features and diagnosis, *Journal of Neurology, Neurosurgery & Psychiatry,* vol. 79, no. 4, pp. 368-376, 2008.

201. S. Spasojević, T. V. Ilić, S. Milanović *et al.*, Combined Vision and Wearable Sensors-based System for Movement Analysis in Rehabilitation, *Methods Inf Med,* vol. 56, no. 02, pp. 95-111, 2017.

202. H. R. Fazeli, and Q. Peng, Estimation of spatial-temporal hand motion parameters in rehabilitation using a low-cost noncontact measurement system, *Medical Engineering & Physics,* vol. 90, pp. 43-53, 2021/04/01/, 2021.